2019-04-19

Elucidating the Roles of Novel Genes in MHC-I Presentation

Barry Kriegsman
University of Massachusetts Medical School

ELUCIDATING THE ROLES OF NOVEL GENES IN MHC-I PRESENTATION

A Dissertation Presented

By

Barry Alan Kriegsman

Submitted to the Faculty of the

University of Massachusetts Graduate School of Biomedical Sciences, Worcester

in partial fulfillment of the requirements for the degree of

DOCTOR OF PHILOSOPHY

April 19, 2019

Department of Pathology

ELUCIDATING THE ROLES OF NOVEL GENES IN MHC-I PRESENTATION

A Dissertation Presented

By

Barry Alan Kriegsman

This work was undertaken in the Graduate School of Biomedical Sciences

Immunology & Microbiology Program and MD/PhD Program

Under the mentorship of

Kenneth L. Rock, M.D., Thesis Advisor

Samuel M. Behar, M.D./Ph.D., Member of Committee

Leslie J. Berg, Ph.D., Member of Committee

Michael A. Brehm, Ph.D., Member of Committee

Michael B. Brenner, M.D., External Member of Committee

Lawrence J. Stern, Ph.D., Chair of Committee

Mary Ellen Lane, Ph.D.

Dean of the Graduate School of Biomedical Sciences

April 19, 2019

Acknowledgements

First and foremost, I would like to thank my thesis advisor, Ken Rock. Ken has been an outstanding role model for me, both as a scientist and a mentor. His ability to communicate science with others is unparalleled and, by following in his footsteps, I have made huge strides in my own presentation skills. Ken has always been approachable and reachable, and I truly appreciate the support he's provided to help me overcome challenges in the lab and in my personal life. I would also like to thank the members of my DEC, Larry Stern, Leslie Berg, Sam Behar, Mike Brehm, and Michael Brenner, for all of their helpful discussions over the years and for taking the time to review and discuss this dissertation with me.

Next, I would like to thank some members of the Rock Lab who have been part of this journey with me. Greg Orlowski, thanks for your magnetic personality and M.D./Ph.D.-related advice. Elena Merino-Rodriguez, thanks for showing me the ropes when I first started and all of your efforts to encourage lab socialization. Jiann-Jyh Lai, thanks for all of your help, especially regarding my mouse experiments. Jeff Colbert (a.k.a., the "cloning guru"), thanks for all of your experimental help and advice along the way; you've been an outstanding mentor and friend. Freidrich Cruz, thanks for always being willing to lend an ear and a helping hand; I don't know what the lab will do without you when you leave. Karthik Dhatchinamoorthy, thanks for assisting me on days where my multi-tasking became a little too much to handle and I wish you luck as you further advance this project. Joan Veinot, thanks for all of your administrative support

but, more importantly, for your great sense of humor. Sharlene Hubbard, thanks for all of your help with our animal husbandry. Lastly, I owe a great deal of thanks to Janice BelleIsle. Janice, the lab would not be nearly the same (or as lively) without you. Thanks for all of your help with the screen, cloning, mouse studies, and cell staining. I could not have done this without you.

I would also like to recognize some of my other UMass colleagues who have helped along the way. First, I'd like to give a big thanks to Pranitha Vangala for her collaboration and bioinformatics work, particularly on the RNA-seq for this project. Abraham Brass and Paul Meraner, thanks for your help in setting up and analyzing the HeLa screen. Benjamin Chen, thanks for tracking down and processing the clinical biopsy specimens. Mike Brehm and Dale Greiner, thanks for your support and assistance with the *in vivo* tumor studies. Kate Fitzgerald, thanks for all of your thoughtful discussions about what next steps we could take. I would also like to thank Mike Gallagher for his advice and reagent sharing for the RNA-seq. Priya Devarajan, thank you for all of your guidance and troubleshooting support with the cytotoxicity assays. I'd also like to thank three members of my M.D./Ph.D. class, Zachary Milstone, Asia Matthew-Onabanjo and Jim Strassner, who have helped with their time and reagents. Additionally, I would like to thank Mollie Jurewicz for her friendly discussions both at UMass and at the dog park; I look forward to celebrating your defense very soon.

Lastly, I would like to thank all of my friends, family, and Valli for your love and encouragement throughout this journey. I could not have done it without you.

Abstract

The major histocompatibility complex class I (MHC-I) antigen presentation pathway is necessary for the immune system to be able to detect, control, and eliminate cancers. MHC-I binds oligopeptides derived from cellular proteins and presents them on the cell surface to $CD8^+$ T cells. Consequently, the $CD8^+$ T cells can monitor whether any cells are making abnormal proteins and, if so, can destroy those cells. Because MHC-I presentation is not essential for cell viability, immune selection pressure often leads to cancers that are MHC-I low as they can better evade $CD8^+$ T cell recognition. It is, therefore, important to fully understand the mechanisms of MHC-I presentation as this will identify new ways to target and exploit the pathway for cancer therapeutics. Although several components of the MHC-I pathway have already been characterized, some knowledge gaps remain. Unbiased forward genetic screens from our lab identified some novel gene candidates, such as IRF2, which positively regulate MHC-I presentation. In this dissertation, I will reveal which antigen presentation pathway genes are transcriptionally controlled by IRF2 and contribute to the MHC-I presentation deficiency observed in cells lacking IRF2 and I will also show that IRF2 negatively regulates PD-L1 expression. By influencing both MHC-I antigen presentation and PD-L1 expression in this manner, cancers lacking IRF2 (of which there are many) are both harder to see and more difficult to eliminate.

Table of Contents

List of Tables

List of Figures

List of Abbreviations

APC = Antigen presenting cell
β2m = Beta2-microglobulin
CTLA-4 = Cytotoxic T-lymphocyte-associated antigen 4
CFSE = Carboxyfluorescein succinimidyl ester
ER = Endoplasmic reticulum
ERAP1 = Endoplasmic reticulum aminopeptidase 1
HLA = Human leukocyte antigen
HSP = Heat-shock protein; subclasses Hsp40, Hsp70, and Hsp90
IFN = Interferon; type I (IFNα or IFNβ) or type II (IFNγ)
IRF = Interferon regulatory factor; members IRF1, IRF2, …, IRF9
ISRE = Interferon-stimulated response element
KO = Knockout
MFI = Mean fluorescence intensity; geometric MFI (GMFI)
MHC = Major Histocompatibility Complex; class I (MHC-I) and class II (MHC-II)
NLRC5 = NOD-like receptor family CARD domain containing 5
NOX2 = NAPDH oxidase 2
NSCLC = Non-small cell lung cancer
OVA = Ovalbumin
P2C = Phagosome-to-cytosol
PD-1 = Programmed death protein 1
PD-L1 = Programmed death-ligand 1
PLC = Peptide-loading complex
RLUs = Relative luciferase units
qPCR = Quantitative polymerase chain reaction
S8L/SIINFEKL = H2-K^b epitope derived from ovalbumin ($OVA_{257-264}$)
sgRNA = Short guide RNA
TAP = Transporter associated with antigen processing; subunits 1 (TAP1) and 2 (TAP2)
TCR = T cell receptor
WT = Wild-type

List of Publications

Kriegsman BA, Vangala P, Chen BJ, Meraner P, Brass AL, Garber M, Rock KL. Frequent loss of IRF2 in cancers leads to immune evasion through increased PD-L1 and decreased MHC-I antigen presentation. *Manuscript under review.*

Cruz FM, Colbert JD, Merino E, **Kriegsman BA**, Rock KL. The Biology and Underlying Mechanisms of Cross-Presentation of Exogenous Antigens on MHC I Molecules. *Annu Rev Immunol.* 2017 Apr 26; 35:149-176. doi: 10.1146/annurev-immunol-041015-055254.

Kriegsman BA, Hanna BG. Metformin-Associated Lactic Acidosis in a Patient with Normal Renal Function. *Clin Diabetes.* 2015 Oct; 33(4): 193-194. doi: 10.2337/diaclin.33.4.193.

Wang S, Mata-Fink J, **Kriegsman B**, Hanson M, Irvine DJ, Eisen HN, Burton DR, Wittrup KD, Kardar M, Chakraborty AK. Manipulating the Selection Forces during Affinity Maturation to Generate Cross-Reactive HIV Antibodies. *Cell.* 2015 Feb 12; 160(4): 785-797. doi: 10.1016/j.cell.2015.01.027.

Mata-Fink J, **Kriegsman B**, Yu HX, Zhu H, Hanson MC, Irvine DJ, Wittrup KD. Rapid conformational epitope mapping of anti-gp120 antibodies with a designed mutant panel displayed on yeast. *J Mol Biol.* 2013 Jan 23; 425(2): 444-56. doi: 10.1016/j.jmb.2012.11.010.

Lopes J, Piazza A, Bermejo R, **Kriegsman B**, Colosio A, Teulade-Fichou MP, Foiani M, Nicolas A. G-quadruplex-induced instability during leading-strand replication. *EMBO J.* 2011 Aug 26; 30(19): 4033-46. doi: 10.1038/emboj.2011.316.

Chapter I: Introduction

Chapter I: Introduction

Overview of MHC-I presentation

$CD8^+$ T cells rely on the major histocompatibility complex class I (MHC-I) presentation pathway to monitor and maintain the body's health. This difficult task is achievable because all nucleated cells naturally generate and display peptides derived from cellular proteins on MHC-I on their cell surface [1]. Under normal physiological conditions, all of the peptides presented by a cell's MHC-I are from autologous proteins. In contrast, if a cell is infected with a virus or expresses mutant genes (e.g., in cancer), it will display foreign peptides. When an activated $CD8^+$ T cell recognizes these foreign peptide-MHC-I complexes, it can eliminate the abnormal cell.

$CD8^+$ T cell activation often requires cross-priming, which can occur thanks to some help from professional antigen-presenting cells (APCs), namely dendritic cells (DCs) and macrophages [2-4]. These DCs sample the extracellular milieu, process antigens, and display peptide fragments on MHC-I in a process called "cross-presentation" [5]. This allows the DCs, which do not have to be infected or tumorigenic themselves, to initiate an immune response against the transformed cells from which the antigens were sampled. When a naïve $CD8^+$ T cell is stimulated by peptide-MHC-I (signal 1) and other co-stimulation (signal 2), it will become activated [6]. (In contrast, if a naïve $CD8^+$ T cell is only stimulated by signal 1 but not signal 2, it may be tolerized instead of activated.) Effector $CD8^+$ T

cells then circulate in the periphery until they find their target cells, which express peptide-MHC-I through a process called “classical MHC I presentation.” If the T cell receptor of the effector $CD8^+$ T cell is specific for the peptide-MHC-I presented, it can kill that target cell, primarily by releasing the cytotoxins perforin and granzyme onto the target, ultimately leading to cell apoptosis.

Most of this dissertation will focus on the classical MHC I pathway rather than cross-presentation but since there are many similarities between these two pathways, it is important to understand how they work. Classical MHC I presentation – the MHC-I presentation of peptides derived from endogenously synthesized proteins either of self or foreign origin – can occur because intracellular proteins do not last forever. When a protein reaches the end of its lifetime, it is conjugated with ubiquitin and then sentenced to the proteasome for degradation, which cleaves the protein into oligopeptides [7]. Although the majority of these oligopeptides are then trimmed by cytosolic peptidases into amino acids, a fraction of the oligopeptides are translocated into the endoplasmic reticulum (ER) by the transporter associated with antigen processing (TAP), which contains two subunits – TAP1 and TAP2 [8]. Some of these peptides require further N-terminal trimming by an ER aminopeptidase (ERAP) in order to be the right length (usually 8 or 9 amino acids) for loading onto MHC-I [9, 10]. After newly synthesized MHC-I heavy chain associates with the chaperone calnexin [11], it dimerizes with a β2-microglobulin (β2m) light chain and this MHC-I heterodimer then associates with the TAP heterodimer via a

transmembrane glycoprotein, tapasin [12]. Other members of the MHC-I peptide loading complex (PLC) include the chaperone calreticulin [11], which binds an N-linked glycan on the MHC-I heavy chain, and the oxidoreductase ERp57, which non-covalently associates with calreticulin and links to tapasin through disulfide bridges [13, 14]. Studies have shown that cells lacking any one of these PLC components experience deficits in MHC-I presentation [15-17]. This is because all members of the PLC are necessary to ensure that nascent MHC-I stably bind to mature peptides such that the resultant peptide-MHC-I complexes trafficked through the secretory pathway to the plasma membrane will have prolonged expression on the cell surface.

The two major mechanisms by which DCs cross-present peptides are the phagosome-to-cytosol (P2C) pathway and the vacuolar pathway. Antigens internalized by phagocytosis, macropinocytosis, or receptor-mediated endocytosis can be cross-presented efficiently, as compared to those taken up by fluid-phase pinocytosis [18-21]. In the P2C pathway, these antigens escape from the phagosome into the cytosol and then either follow the same aforementioned path as the endogenously synthesized antigens in classical MHC-I presentation or, after being hydrolyzed by the proteasome, get translocated back into the endocytic compartment where they can be trimmed by a different aminopeptidase (insulin-regulated aminopeptidase; IRAP) and loaded onto open MHC-I molecules which were recruited there from the cell surface or ER [22]. In the vacuolar pathway, internalized antigen does not gain access to

the cytosol. Instead, it remains in the endocytic compartment where it is cleaved by proteases (primarily cathepsins), further trimmed by IRAP, and then loaded onto open MHC-I in the endosome before being presented at the cell surface [23].

Although many components of these MHC-I pathways have already been identified, several unanswered questions remain. These include but are not limited to: (1) how the different components of the MHC-I pathway are transcriptionally regulated under basal versus inflammatory conditions; and (2) how antigen escapes the endocytic compartment in the P2C pathway and the involvement of chaperones in this process. In the following two sections, I will briefly review what is known about each of these topics and where additional research may help to fill some of these knowledge gaps.

Transcriptional control of MHC-I presentation

While still not well-characterized, most investigation into the transcriptional regulation of the MHC-I pathway has been done by looking into the transcriptional activation of the MHC-I genes themselves. Several conserved regulatory promoter elements have been identified within the MHC-I promoter, namely the enhancer A, the interferon-stimulated response element (ISRE), and the SXY-module. Enhancer A binding by NF-κB and ISRE binding by interferon regulatory factors 1 and 8 (IRF1 and IRF8) induce MHC-I transcription after stimulation with TNFα or IFN (type I and type II), respectively [24, 25]. In contrast,

NLRC5, which itself does not bind the SXY-module but rather forms an MHC-I enhanceosome (together with the RFX complex, NFY complex, and ATF1/CREB) at that site, appears to regulate MHC-I transcription under basal conditions [26-30]. NLRC5 also targets other MHC-I pathway genes, such as β2m, TAP1, and an immunoproteasome subunit LMP2 (Psmb9), and SXY-modules have been identified in each of these promoters [26, 31]. However, the transcriptional control of other MHC-I components, such as TAP2 and tapasin, under steady-state conditions has not yet been characterized [32]. Additionally, while much of the machinery of the MHC-I pathway is interferon-inducible [33] and ISREs have been found within the promoters of many of these genes [34], the exact mechanisms by which different IRFs may regulate each of these components under basal versus interferon-stimulated conditions has not been fully resolved. Furthermore, there exist specific regulatory mechanisms for controlling cross-presentation. It was recently shown that the transcription factor TFEB acts as a molecular switch to inhibit cross-presentation and enhance MHC-II presentation [35]. This balance imposed by TFEB appears to be caused by its ability to induce phagosomal acidification and increase proteolysis, both of which are reduced in efficient cross-presenting cells [23, 36]. Although mRNA expression for several cathepsins was strongly upregulated by TFEB expression, TAP2 mRNA was unaffected [35]. Thus, this transcription factor also could not provide an answer as to what controls TAP2 transcription. As part of my thesis research, I investigated the role of another transcription factor, IRF2, on the

MHC-I pathway; its involvement in regulating several genes necessary for MHC-I presentation, including TAP2, will be discussed in greater depth in Chapter III.

Antigen escape in P2C cross-presentation and roles of chaperones

It remains unclear how exactly antigen gets transferred from the endocytic compartment to the cytosol in P2C cross-presentation. Two ideas which have been proposed are phagosomal disruption or an ER-associated degradation (ERAD)-like mechanism. In phagosomal disruption, ingested particles destabilize the phagosomal membrane, thereby allowing the contents to reach the cytosol [37]. This mechanism could explain how ingested enzymes transferred to the cytosol remain enzymatically active and how large non-protein molecules, such as internalized dextrans, can also access the cytosol [18, 22]. In support of this theory, loss of the enzyme NOX2, which creates reactive oxygen species that can destabilize the phagosome, impairs cross-presentation [38]. However, it is also possible that the loss of NOX2 inhibits cross-presentation by way of enhanced phagosome acidification [38]. The ERAD-like mechanism where abnormal intraluminal proteins are tagged with ubiquitin and sent back into the cytosol for proteasomal degradation is supported by evidence that a number of ER proteins are also present in the phagosome [39, 40]. ERAD involves the cytosolic p97 ATPase and possibly several translocon channels including Sec61 and Derlin1 [41-43]. Studies have shown that silencing p97, Sec61, or a ubiquitin-conjugating enzyme involved in ERAD decreases cross-presentation

[44, 45]. However, inhibiting or reducing the expression of Sec61, which is necessary for translocating MHC-I and other important antigen presentation molecules into the ER, could simply explain the observed reductions in cross-presentation; it is therefore unclear whether Sec61 actually serves as a retrotranslocon for this pathway. Moreover, another study found that silencing Derlin1 did not inhibit cross-presentation [46], further muddying the waters. Additionally, heat-shock protein (HSP) chaperones, such as Hsp90, have also been implicated in this P2C transfer [47]. More broadly, it has been of interest to elucidate the roles of HSPs in antigen presentation given the known critical roles of other chaperones (e.g., calnexin, calreticulin) in this pathway. Given the numerous roles of Hsp70 in the cell, including regulation of protein folding, stabilization, trafficking and degradation, it is likely that Hsp70 influences antigen presentation. In fact, Hsp70 has been implicated in cross-presentation of antigens derived from infected or cancerous parenchymal cells [48, 49]. Hsp70 is released from necrotic (but not apoptotic) cells [50], and uptake of Hsp70-antigenic peptide complexes by APCs occurs through the CD91 receptor [51-53]. After Hsp70-chaperoned peptides are internalized by APCs, peptide processing and presentation occur using components of the classical MHC-I pathway [51]. Additionally, Hsp70 has also been suggested to play a role in the classical MHC-I pathway. Not only does Hsp70 associate with MHC epitope precursors [54, 55], but inhibition of Hsp70 has been shown to downregulate MHC-I expression on the cell surface [56]. Yet, currently the mechanisms by which Hsp70 and its

associated co-chaperones may facilitate classical MHC-I presentation are not well understood. For this reason, I decided to investigate the involvement of a family of Hsp70 co-factors (DnaJs or Hsp40s) on MHC-I presentation, which will be discussed further in Chapter V.

MHC-I and immune evasion

Given that MHC-I presentation equips the immune system with such a robust surveillance power, it is remarkable that some intracellular organisms and cancer cells manage to proliferate despite the odds stacked against them. As it turns out, many microbes and tumor cells, through a variety of evolutionary and immune selection pressures, are able to manipulate components of the MHC-I pathway so as to downregulate MHC-I presentation, thereby making it more difficult for the $CD8^+$ T cells to see them.

Viruses have co-evolved with their hosts over time and, along the way, have acquired several different escape mechanisms involving the MHC-I pathway. For example, Epstein-Barr virus (EBV) encodes for the protein EBNA1, which avoids proteasomal processing due to the long repetitive stretches of glycine and alanine residues it contains [57]. Mechanistically, it has been suggested that the 19S regulatory proteasome subunit cannot properly recognize and unfold these glycine and alanine repeats [58, 59]. There are also viral proteins which inhibit TAP-mediated peptide translocation. These include ICP47 of herpes simplex virus, US6 of human cytomegalovirus (HCMV), BNLF2a of EBV, and UL49.5 of

bovine herpesvirus [60-63]. This TAP inhibition prevents virus-derived peptides from accessing the ER and being loaded onto MHC-I. Other viral proteins, such as US3 of HCMV and E3-19K of adenovirus, specifically target tapasin [64, 65]. Additionally, some viral proteins (e.g., US2, US11, and mK3) induce ERAD of MHC-I by orienting members of the PLC in such a way that the MHC-I tail gets polyubiquitylated and retro-translocated into the cytosol where it can then be degraded by the proteasome [66-68].

Discovering that viruses can manipulate the MHC-I pathway to promote their own survival should not make it surprising that tumor cells exposed to immune selection pressure can also downregulate MHC-I presentation. In fact, studies have shown that after immunoediting, tumors which were predominantly MHC-I positive can become MHC-I deficient [69-71]. Furthermore, cancers with mutations or decreased expression in β2m, TAP, and other necessary MHC-I pathway components have been identified [72-74].

One way in which the immune system combats chronic MHC-I downregulation in tumors or virus-infected cells is through the activity of natural killer (NK) cells. These NK cells preferentially kill cells via “missing-self recognition” [75]. The NKG2D ligands, MHC-I-related sequences A and B (MICA/B), are typically not expressed on healthy cells [76]. However, in settings where surface MHC-I is absent, such as infection or transformation, MICA/B are upregulated, sending a “kill me” signal to NK cells through their NKG2D receptor [77, 78]. Interestingly, Kaposi’s sarcoma-associated herpesvirus (KSHV)

expresses the proteins kK3 and kK5, which can downregulate both MHC-I and MICA/B, thus preventing elimination of the infected cell by $CD8^+$ T cells or NK cells [79, 80].

The fact that so many different mechanisms exist for evading immune detection by manipulating the MHC-I pathway and its associated molecules should highlight the importance in studying these networks to better understand how microbes and cancers escape immune recognition. Accordingly, the interplay between host recognition of self vs. non-self will be revisited in a later section on immune checkpoint.

Interferon regulatory factor (IRF) family

Interferons (IFNs) are cytokines released by host cells which trigger anti-viral immune responses. There are three main classes of IFNs: type I (e.g., IFNα and IFNβ); type II (IFNγ); and type III (IFNλ). Type I and type III IFNs can be expressed by a variety of cell types whereas type II IFN is primarily expressed by T cells and NK cells [81]. Although these different types of IFNs have diverse biological activities, they all bind to receptors on the target cell(s) and initiate anti-viral responses. When the type I and type II receptors, IFNAR and IFNGR, bind their ligands, they activate signal transducer and activator of transcription (Stat) complexes, a family of transcription factors [82]. IFNAR signaling starts with activation of the tyrosine kinases Tyk2 and Jak1, which then phosphorylate Stat1 and Stat2, which then both associate with IRF9 to form a heterotrimeric complex

called ISGF3, which translocates into the nucleus and transcribes specific target genes. IFNGR signaling starts by activating Jak1 and Jak2, which then phosphorylate a Stat1 dimer, thereby enabling its translocation to the nucleus to activate target genes.

In order for these interferons to be useful to the host, they should be turned on when necessary and turned off in an unstimulated state. Therefore, interferon production requires regulation. The interferon-regulatory factor (IRF) family member, IRF1, was first identified as an activator of IFNβ expression [83]. Since then, a total of nine IRFs have been identified, which each have unique responsibilities within the cell. Here, I will briefly review the various functions of these IRFs, focusing primarily on IRF1 and IRF2, which were closely examined in the context of my thesis research.

After finding that IRF1 positively regulates IFNβ expression, another structurally similar transcription factor, IRF2, was identified and found to repress IRF1-induced activation of IFNβ [84]. Site-directed mutagenesis revealed the conserved IRF DNA-binding domain (DBD) as a ~120 amino acid region containing five tryptophan repeats within the N-terminus, which forms a helix-turn-helix domain and recognizes a DNA consensus sequence termed the interferon-stimulated response element (ISRE; $^{A}/_{G}\,NGAAANNGAAACT$) [82, 85]. Outside of the amino terminus, IRF1 and IRF2 only share about 25% homology and the C-termini of these two transcription factors differ significantly, with IRF1's being predominantly acidic and serine-threonine residues and IRF2's being rich

in basic residues [84]. Because the unique C-terminus of IRF1 includes its transcriptional activation domain, it is not surprising that IRF1 and IRF2 can have different effects on their target genes. However, despite the early IRF literature which favored an antagonistic relationship between IRF1 and IRF2 wherein the IRF1 activator would always compete with the IRF2 repressor for the same ISRE, more recent discoveries have revealed that IRF2 can also act as an activator. Its ability to activate some genes, such as VCAM-1, histone H4, and TLR3 [86-88], appears to be due to proteolytic cleavage of the IRF2 C-terminus (which contains a repression domain) following infection, which consequently converts IRF2 into either a strong repressor or an activator [89-92]. IRF1 and IRF2 can also be post-translationally serine-phosphorylated by protein kinase A, protein kinase C, and casein kinase II [93].

IRF1 and IRF2 have some shared and some different effects on cell function, development, and growth. Among the genes activated by IRF1 are those important for anti-viral (IFNβ, guanylate-binding proteins/GBPs) and anti-bacterial (iNOS) responses, apoptosis (caspase 1), and MHC antigen presentation (class II trans-activator/CIITA, TAP1, LMP2) [85]. The genes targeted by IRF2 are not as well defined, but IRF2 is generally thought to reduce type I IFN responses by competing with IRF1 and IRF9 [85]. Both IRF1 and IRF2 are required for NK cell development and for promoting Th1 differentiation and suppressing Th2 differentiation [94-97]. Additionally, IRF1 is necessary for $CD8^+$ T cell differentiation whereas IRF2 helps differentiate $CD4^+$ DCs [98, 99]. In addition to

its pro-apoptotic role via caspase 1 activation, IRF1 can arrest cell growth after DNA damage [100, 101]. These functions, plus its ability to suppress lysyl oxidase [102], which is often upregulated in hypoxic tumors, has caused some to ascribe a tumor suppressor-like role to IRF1. In contrast, one report found that IRF2 overexpression causes oncogenic transformation *in vitro* (which could be reverted by IRF1 overexpression) [103], although the mechanisms by which this occurred are unknown and these findings have not been reproduced. On the other end of the spectrum, IRF1 appears to promote autoimmunity as mice lacking IRF1 show a lower incidence of collagen-induced arthritis and experimental allergic encephalomyelitis whereas a loss of IRF2 results in a $CD8^+$ T cell-mediated, psoriasis-like skin disease [104, 105].

The other human IRFs, IRF3-9, contribute to host immunity in many ways. For example, IRF3 and IRF7 cooperate to induce type I IFN upon virus infection or TLR stimulation in the early and late stages, respectively [106-108]. IRF4, which is regulated by T cell receptor (TCR) signal strength, is important for $CD8^+$ T cell responses to acute viral infections and T helper cell fate determination [109, 110]. IRF5 positively regulates TLR-induced pro-inflammatory cytokine expression [111]. IRF6, which is constitutively expressed in the skin, helps differentiate keratinocytes [112]. IRF8 is important for $CD8\alpha^+$ DC differentiation and also binds the ISRE in the enhancer of MHC-I genes [113-115]. IRF9, as mentioned above, forms part of the heterotrimeric ISGF3 complex and activates type I IFN-induced genes [116].

Immune checkpoint

As mentioned earlier, the quality of the T cell priming response is dependent on signal 1 (TCR-MHC interaction) and signal 2 (co-stimulation). Although TCR recognition of peptide-MHC initiates a T cell response, the co-stimulatory and inhibitory molecules (i.e., immune checkpoints) present on the APC and T cell regulate this response so as to maintain self-tolerance. In addition to modulating MHC-I presentation, tumor cells can better escape elimination from the immune system by enhancing immune checkpoint, thereby allowing “tumor tolerance.” Cancer immunotherapies designed to relieve inhibition imposed on the T cell (i.e., checkpoint blockade) have been focused primarily on cytotoxic T-lymphocyte-associated antigen 4 (CTLA-4) and the interaction between programmed death protein 1 and its ligand (PD-1/PD-L1) [117]. Such antibodies targeting CTLA-4 and the PD-1/PD-L1 axis have demonstrated clinical efficacy in a variety of cancer types, including but not limited to melanoma, non-small cell lung cancer (NSCLC), colorectal carcinoma, lymphoma, and renal cell carcinoma [118].

CTLA-4 is expressed exclusively on T cells and counteracts CD28-mediated co-stimulation [117]. Because CTLA-4 and CD28 share the same ligands – CD80 and CD86 – but CTLA-4 has a higher affinity for them, it is thought that CTLA-4 outcompetes CD28 for ligand binding [119]. Interestingly, CTLA-4 can also remove these ligands from the APC surface through trans-endocytosis [120]. In addition, CTLA-4 prevents T cell activation via signaling pathways involving the

phosphatases SHP-2 and PP2A, which counteract the kinase activity downstream of TCR and CD28 [121, 122]. Although tumors do not preferentially express or inhibit CTLA-4, anti-CTLA-4 therapeutics (e.g., ipilimumab for metastatic melanoma) can elicit potent anti-tumor responses [123, 124].

In contrast with CTLA-4 which is important at the T cell priming stage, the PD-1/PD-L1 axis plays a greater role in the periphery where the activated T cells interact with normal cells and tumor cells. When T cells expressing PD-1 interact with their ligand (PD-L1), T cell activity is reduced (also thought to be SHP-2-mediated) [125]. This is a normal physiological response in tissues to prevent excess collateral damage in areas undergoing T cell attack. However, tumors can manipulate this response by upregulating PD-L1, which is strongly induced by IFNγ, to suppress T cell-mediated elimination. Interestingly, PD-1 is not only expressed on T cells, but also on NK cells and B cells [126, 127], which is significant because tumor cells expressing low surface MHC-I and high PD-L1 could potentially avoid both T cell and NK cell-mediated elimination. So far, anti-PD-1 therapeutics (e.g., pembrolizumab for melanoma and NSCLC) have also experienced some clinical success [128]. However, not all patients are sensitive to checkpoint blockade. Because checkpoint blockade is extremely expensive and can have serious side effects, there is a need for good biomarkers to identify those patients that would be more likely to benefit from this type of therapy. Currently, tumors are screened for PD-L1 status as high PD-L1 expression is correlated with better responses to anti-PD-1 treatment [129, 130] but this is still

far from perfect since PD-L1 positivity neither guarantees nor excludes a clinical response to anti-PD-1 [131]. Some patients possessing tumors with microsatellite instability or a high mutational burden can also benefit from checkpoint blockade [132]. However, due to the evolving mutational landscape of such tumors, some tumors acquire resistance to checkpoint inhibitors by downregulating MHC-I presentation machinery [133-135].

Scope of thesis

The primary objective of my thesis was to identify and characterize a novel component of the MHC-I pathway. Through an unbiased forward-genetic screen in HeLa H1 cells, I identified several interesting gene “hits” that could positively regulate classical MHC-I presentation. From this list, I dedicated most of my time to studying an interferon regulatory factor, IRF2, that had not been previously recognized to positively regulate this pathway. In chapters III and IV, I will describe our results showing that IRF2 both transcriptionally activates key components of the MHC-I pathway and represses PD-L1 expression. I will also highlight how a loss of IRF2 leads to immune evasion and the implications of our findings for cancer progression and immunotherapy. Additionally, I spent time investigating genes from our lab’s cross-presentation screen. In chapter V, I will document my preliminary studies on a couple co-chaperones identified in this screen and their effects on MHC-I presentation.

Chapter II: Materials and Methods

Chapter II: Materials and Methods

Cells

DC3.2 is a J2 virus-immortalized dendritic cell line [4]. A particular DC3.2 clone (with Renilla luciferase) was used for all experiments as this clone has very strong cross-presentation and MHC class II presentation, as compared to other clones. RF33.70 is a T cell hybridoma that recognizes the ovalbumin (OVA) peptide $OVA_{257-264}$ in the context of H2-K^b [136]. MF2.2D9 is a T cell hybridoma that recognizes $OVA_{258-276}$ in the context of I-A^b [4]. RF33.70 and MF2.2D9 were transduced with lentivirus containing NFAT-luciferase by Freidrich Cruz. NIH-3T3 cells were stably transfected with the mouse H2-K^b molecule. HeLa H1 were kindly provided by Abraham Brass (UMass), A549 and MCF7 were kindly provided by Leslie Shaw (UMass), and the D53m and H50m mouse MCA-induced sarcoma lines were kindly provided by Robert Schreiber (Wash U, St. Louis). Dnajc10 MEFs [137] were kindly provided by Takao Iwawaki. The MCA-induced sarcoma lines were grown in R10 media and all other cell lines were grown in “HCM”: RPMI 1640 (Gibco) supplemented with 10% FBS (Hyclone), 1% NEAA (Gibco), 1% HEPES (Gibco), 1% Antibiotic-Antimycotic (Gibco), and 5 x 10^{-5} M 2-ME (Sigma). The MCF7 growth media was also supplemented with 10µg/mL insulin. Antibiotic selection for CRISPR-Cas9 knockout cells was done for two weeks in media containing 5µg/mL blasticidin (Invivogen). All cells were grown in a 10% CO_2 atmosphere at 37°C.

Plasmids

The LentiCRISPRv2 plus blasticidin selection plasmid [138, 139] was acquired from Addgene (83480) and, unmodified, is the same as the "no sgRNA" plasmid. The plasmids used to target mouse β2m, TAP1, TAP2, ERAP1, IRF2, IRF1 or to target human IRF2 were constructed by inserting the following sgRNA sequences, respectively, into the LentiCRISPRv2 plasmid as described below:

Mouse β2m: 5'-AGTATACTCACGCCACCCAC-3';

Mouse TAP1: 5'-ACTAATGGACTCGCACACGT-3';

Mouse TAP2: 5'-ATTACACGACCCGAATAGCG-3';

Mouse ERAP1: 5'-TGCAGCATCCAGAGCATAAT-3';

Mouse IRF2: 5'-TCCGAACGACCTTCCAAGAA-3';

Mouse IRF1: 5'-CTCATCCGCATTCGAGTGAT-3';

Human IRF2: 5'-TGCATGCGGCTAGACATGGG-3'.

Primer sets for cloning the sgRNAs above into the LentiCRISPRv2 plasmid are shown in Table 2.1. Construct cloning was done as follows: 100μM oligonucleotides from the primer sets were annealed and then diluted 1:50. 3μg of LentiCRISPRv2 plasmid was digested for 3hrs at 55°C with BsmBI (NEB) and removal of the 2kb filler sequence was confirmed by gel electrophoresis. The larger molecular weight band was gel extracted and quick ligated with the diluted annealed oligos according to the manufacturer's instructions (NEB). Stable competent *E. coli* (NEB) were then transformed with 2μL of the quick ligation product according to the manufacturer's instructions and grown overnight at 30°C

on LB+Ampicillin (100µg/mL) plates. Plasmids were isolated (Clontech) from individual colonies and sequenced (Genewiz) using the primer hU6-F: 5'-GAGGGCCTATTTCCCATGATT-3' to confirm proper insertion of the sgRNA into LentiCRISPRv2. In addition, sgRNAs were checked for high indel efficiencies in transduced cells by TIDE analysis [140].

Rescue plasmids used in Chapters III and IV were constructed by inserting mouse IRF2, TAP2, or ERAP1 cDNA or human IRF2 cDNA into the constitutive expression vector, pCDH-CMV (Addgene), with a modified multiple cloning site. Overlapping PCRs were run using the primers in Table 2.2 on either mouse cDNA from DC3.2 cells or human cDNA from HeLa H1 cells to create IRF2 cDNA sequences containing 6 synonymous mutations within the IRF2 sgRNA target site. The mouse IRF2 K78R sequence was constructed by further mutating A to G at nucleotide 233. The wild-type TAP2 and ERAP1 cDNA sequences were of C57BL/6 origin. All plasmids were sequenced to confirm correct sequences and reading frames.

Table 2.1. Primer sets for cloning LentiCRISPRv2 sgRNA constructs

	Forward	**Reverse**
Mouse β2m	5’-CACCG**AGTATACTCACGCCACCCAC**-3’	5’-AAAC**GTGGGTGGCGTGAGTATACT**C-3’
Mouse TAP1	5’-CACCG**ACTAATGGACTCGCACACGT**-3’	5’-AAAC**ACGTGTGCGAGTCCATTAGT**C-3’
Mouse TAP2	5’-CACCG**ATTACACGACCCGAATAGCG**-3’	5’-AAAC**CGCTATTCGGGTCGTGTAAT**C-3’
Mouse ERAP1	5’-CACCG**TGCAGCATCCAGAGCATAAT**-3’	5’-AAAC**ATTATGCTCTGGATGCTGCA**C-3’
Mouse IRF2	5’-CACCG**TCCGAACGACCTTCCAAGAA**-3’	5’-AAAC**TTCTTGGAAGGTCGTTCGGA**C-3’
Mouse IRF1	5’-CACCG**CTCATCCGCATTCGAGTGAT**-3’	5’-AAAC**ATCACTCGAATGCGGATGAG**C-3’
Human IRF2	5’-CACCG**TGCATGCGGCTAGACATGGG**-3’	5’-AAAC**CCCATGTCTAGCCGCATGCA**C-3’

Table 2.2. Primer sets for cloning IRF2 rescue/overexpression constructs

Primer name	**Sequence**
Human IRF2 AgeI fwd	5’-GACTACCGGTATGCCGGTGGAAAGGATGCGCATG-3’
Human IRF2 sgRNA mut rev	5’-GCCGTGCCTCGCTGCGTGCATCCAGGGGATCTGAAAAATCTTCTTTTCCTTG-3’
Human IRF2 sgRNA mut fwd	5’-GATGCACGCAGCGAGGCACGGCTGGGATGTGGAAAAAGATGCACCACTCTTTAGAAA-3’
Human IRF2 MluI rev	5’-GATCACGCGTTTAACAGCTCTTGACGCGGGCCTGG-3’
Mouse IRF2 AgeI fwd	5’-GATCACCGGTATGCCGGTGGAACGGATGCGAATG-3’
Mouse IRF2 sgRNA mut rev	5’-CCTTTTTTCGAGGGGCGCTCTGATAAGGGCAGCATCCGGTAGACTCTGAAGGCG-3’
Mouse IRF2 sgRNA mut fwd	5’-CTTATCAGAGCGCCCCTCGAAAAAAGGAAAGAAACCAAAGACAGAAAAAGAAGAGAG-3’
Mouse IRF2 MluI rev	5’-GATCACGCGTTTAACAGCTCTTGACACGGGCCTGG-3’

HeLa H1 CRISPR-Cas9 screen

HeLa H1 cells stably expressing Cas9 were transduced with lentiviral libraries that express short guide RNAs (sgRNAs) targeting 19,052 human genes, with six barcoded sgRNAs per gene. After four rounds of magnetic sorting on low MHC-I cells using the pan-HLA-A/B/C antibody W6/32, the sgRNA sequences from the surviving cells were identified via next generation sequencing (NGS). Gene candidates were ranked based on the number of unique gene candidates versus NGS reads.

Cell surface staining

Where indicated, mouse cells were blocked with 2.4G2 and stained for surface MHC class I levels with anti-K^b-APC (eBioscience, AF6-88.5.5.3), MHC class II levels with anti-I^A/I^E-PECy7 (BioLegend, M5/114.15.2), PD-L1 levels with anti-PD-L1-PE (BioLegend, 10F.9G2), or with isotype controls (eBioscience mouse IgG2a-APC eBM2a, eBioscience rat IgG2b κ-PE eB149) at 1:200 dilutions. Where indicated, human cells were stained for surface MHC class I levels with W6/32. W6/32 staining was performed either by two-step labeling with W6/32 hybridoma supernatant followed by 1:500 donkey-anti-mouse Alexa 647 (Life Technologies) or by one-step labeling with 1:200 FITC-conjugated W6/32 (eBioscience). Where indicated, human cells were stained for surface PD-L1 levels with 1:200 rabbit anti-PD-L1 (Abcam, 28-8), followed by 1:500 donkey-anti-rabbit Alexa 647 (Life Technologies). Normalized MFI was computed by dividing

the geometric MFI of each knockout cell line by the geometric MFI of the WT (no sgRNA) cell line.

T cell hybridoma Ag presentation

Cross-presentation and MHC class II presentation were measured by co-culturing DC3.2 lines in flat-bottom 96-well plates in the presence of the indicated concentrations of OVA-coated iron-oxide beads (Polysciences) and 5 x 10^4 RF33.70-Luc $CD8^+$ T cells or MF2.2D9-Luc $CD4^+$ T cells per well, respectively, for 16-18 hours. Then, One-Glo luciferase substrate (Promega) was added and luciferase activity quantified by an EnVision plate reader (Perkin Elmer). Rescue experiments were performed by adding the OVA-beads and RF33.70-Luc cells 48hrs post-transduction of the DC3.2 lines. Normalized $CD8^+$ T cell activation was calculated for rescue experiments by dividing the $CD8^+$ T cell activation (RLU of luciferase) at each point by the $CD8^+$ T cell activation of the DC3.2 no sgRNA line transduced with EV (no sgRNA, EV). Mapping experiments were done using DC3.2 and 3T3-K^b lines stably transduced with doxycycline-inducible non-secretable OVA or ubiquitin-SIINFEKL and adding the indicated concentrations of doxycycline to the cells for 2 hours prior to co-culturing them with the RF33.70-Luc $CD8^+$ T cells.

siRNA transfections

10^4 HEK293T or HeLa H1 cells were transfected with 10nM Silencer Select siRNA (Invitrogen) and 0.3µL Lipofectamine RNAiMAX (Invitrogen) per well in flat-bottom 96-well plates. Individual siRNAs used were negative control #1 (4390843) human β2m (s1854), human TAP1 (s13778), human IRF2 #1 (s7506), and human IRF2 #2 (s7504). After 72 hours, adherent cells were trypsinized, washed in PBS supplemented with 2% FBS, and stained with the surface MHC I pan-HLA-A/B/C antibody, W6/32. Normalized MFI was computed by dividing the geometric MFI of each experimental siRNA by the geometric MFI of the negative control siRNA. For experiments in Chapter V, 2 x 10^4 DC3.2 cells were transfected for 48 hours with 50nM siRNA pools or individual siRNAs (Dharmacon) targeting either mouse Dnajb4 or Dnajc10 or targeting β2m or I-Ab as controls. In some experiments, a non-targeting siRNA was also used as a negative control.

Minigene transfections

10^4 3T3-Kb cells were transfected with 100ng of various pTracer-CMV2 plasmids (Invitrogen) containing SIINFEKL precursors[141] and 0.4uL Lipofectamine 2000 (Invitrogen) in flat-bottom 96-well plates. After 72 hours, cells were stained with 25-D1.16 (specific for the combination of SIINFEKL and H-$2K^b$) [142], followed by donkey-anti-mouse Alexa 647 (Life Technologies) and analyzed by flow cytometry. Transfected cells were identified by GFP expression

and the MFI of 25-D1.16 staining was measured on the gated transfected cells. Transfection efficiency, based on GFP expression, ranged from 5-20%, depending on the vector. The normalized MFI for each experiment (with technical duplicates) was calculated by dividing the MFI of each knockout line by the MFI of the wild-type ("no sgRNA") line.

RNA-Seq

RNA was extracted using the RNeasy kit (Qiagen) after 2 hours of stimulating the DC3.2 lines with 5,000U/mL mouse IFNα, 2ng/mL mouse IFNγ, or media alone. A standard library preparation protocol was used with 50ng of total RNA as starting material. Libraries were checked for appropriate fragment size traces by Bioanalyzer (Agilent) and concentrations were determined to achieve similar sequencing depth per library. Libraries were run on NextSeq 500/550 high-output and mid-output kits (Illumina) and all libraries had at least 10^7 reads with single index paired-end sequencing. *Trimmomatic-0.32* [143] was used to remove 5' or 3' stretches of bases having an average quality of less than 20 in a window size of 10. Only reads longer than 36 bases were kept for further analysis. *RSEM* v1.2.28 [144] was used to estimate gene expression, with parameters *-p 4 --bowtie-e 70 --bowtie-chunkmbs 100 --strand-specific*. Gene quantification was run on the transcriptome (RefSeq v69 downloaded from UCSC Table Browser [145]. Genes with more than 15 TPM in any time point were considered expressed, and genes that did not achieve this threshold were removed from

further analysis. Batch effects were observed between samples from different replicates. We used the log transformed TPM normalized expression values as input to *ComBat* (package *sva* version 3.18.0) [146, 147] with default parameters and a model that specified different replicates as batches. Corrected TPM values were transformed back to read counts using the expected size of each transcript informed by *RSEM*. We only considered genes with at least 15 TPMs in at least one replicate at any time point. The expressed gene list was filtered to include only genes with homologs as defined by the previous step. We used the batch corrected counts per gene to identify differentially expressed genes by at least 2 fold between unstimulated cells (time 0) and 2 hours following stimulation with IFNα or IFNγ and whose change in expression was significant (p-adjusted < 0.05) according to the package *DESeq2* (v1.10.1) [148] in R (v3.5.1). Due to the large transcriptional changes observed in this system, we turned off the fold change shrinkage in *DESeq2* with *betaPrior=FALSE* and we added a pseudocount of 32 to all timepoints to avoid spurious large fold change estimates from lowly abundant genes.

Human lung specimens

27 non-small cell lung cancers were acquired from UMass Pathology archive of formalin-fixed and paraffin-embedded patient samples. PD-L1 expression was determined at the time of diagnosis by immunohistochemistry by a surgical

pathologist. RNA was extracted from the archival material and analyzed by qPCR (see below).

qPCR

RNA was extracted from cell lines using the RNeasy kit (Qiagen) or from formalin-fixed paraffin-embedded non-small cell lung cancers using the RNeasy FFPE kit (Qiagen) and reverse transcribed to cDNA using EcoDry pre-mix random hexamers (Clontech). 50ng cDNA were used per well (done in triplicate) with indicated TaqMan probes (Applied Biosystems), according to the manufacturer's instructions. The TaqMan probes used are listed in Table 2.3. mRNA expression levels in the IRF2-knockout DC3.2 were compared to those in the wild-type DC3.2 by first normalizing to the mRNA expression of β-actin (mouse) in each sample ($2^{\wedge-\Delta\Delta Ct}$). Statistical analysis was done using two-tailed unpaired t-tests from ≥ 3 independent experiments, comparing the expression of a given gene to that of H2-Ab1. Relative mRNA expression levels in each human lung tumor were measured by first normalizing to the mRNA expression of GAPDH (human) in each specimen ($2^{\wedge-\Delta Ct}$). Results are displayed after further normalization to one of the tumors. DC3.2 and 3T3-K^b lines knocked down for Dnajb4 or Dnajc10 were routinely screened for efficient knockdown in parallel to the described functional assays. For each gene examined, its relative mRNA expression in the knockdown cells was compared to that in negative control

siRNA-treated cells by first normalizing to the mRNA expression of β-actin (mouse) in each sample ($2^{\wedge-\Delta\Delta Ct}$).

Table 2.3. TaqMan probes for qPCR

Gene	Probe ID #
Mouse β-actin	4352933
Mouse β2m	Mm00437762_m1
Mouse H2-K1	Mm01612247_m1
Mouse H2-Ab1	Mm00439216_m1
Mouse Tap1	Mm00443188_m1
Mouse Tap2	Mm01277033_m1
Mouse Erap1	Mm00472842_m1
Mouse ERp57	Mm00433130_m1
Mouse Tapasin	Mm00493417_m1
Mouse Canx	Mm00500330_m1
Mouse Calr	Mm00482936_m1
Mouse Tapbpr	Mm00520408_m1
Mouse Irap	Mm00555903_m1
Mouse Psme1	Mm00650858_g1
Mouse Psme2	Mm01702833_g1
Mouse Psmb8	Mm00440207_m1
Mouse Psmb9	Mm00479004_m1
Mouse Psmb10	Mm00479052_g1
Mouse PD-L1	Mm03048248_m1
Human GAPDH	Hs02758991_g1
Human IRF2	Hs01082884_m1
Human TAP2	Hs00241060_m1
Human ERAP1	Hs00429970_m1
Mouse Dnajb4	Mm00508908_m1
Mouse Dnajc10	Mm00546461_m1

Chromatin immunoprecipitations

Chromatin immunoprecipitation (ChIP) generally followed the Thermo Fisher ChIP protocol. In short, 10^7 DC3.2-no sgRNA cells were stimulated for 2hrs with 2ng/mL IFNγ or media alone, harvested and fixed with 1% formaldehyde, quenched with glycine, and washed in cell lysis buffer then nuclear lysis buffer. Chromatin was sheared by sonication for 20min and fragment size (~300bp) was determined by gel electrophoresis. Immunoprecipitations of the sheared chromatin were done using 2µg of primary antibody – normal rabbit IgG (Santa Cruz sc-2027), rabbit anti-IRF1 (Abcam ab186384), or rabbit anti-IRF2 (Invitrogen B-80 H53L46) – by incubating for 1hr at RT then overnight at 4°C. The next day, 25uL of pre-washed Protein A/G beads (Pierce) were added to each of the samples and incubated at RT for 30min then 90min at 4°C. After washing sequentially with low-salt buffer, high-salt buffer, LiCl buffer, and TE buffer, the DNA was eluted from the beads. All immunoprecipitated samples were treated with RNase A (Qiagen) and Proteinase K (Qiagen) and then column purified (Clontech). ChIP-qPCR was performed in triplicate wells using SYBR Green (Bio Rad) and unique primer sets (Table 2.4) flanking the IRF1/2-binding site within the gene's promoter [34, 149, 150], according to the manufacturer's instructions. Data shown as mean + SEM of fold enrichment ($2^{\wedge-\Delta Ct}$) over the normal rabbit IgG control IP (N=2). Statistical analysis was done using ratio paired t-tests.

Table 2.4. Primer sets for ChIP-qPCR

Gene	Forward primer	Reverse primer
Mouse TAP2	5’-CAAATTGACAGGCGCCATCT-3’	5’-GCTTCTTCTCAAACTGGATCTCC-3’
Mouse ERAP1	5’-CTTAGGCTTGCTCTCTTTTAGCG-3’	5’-GACTCCTGCTCCCGATCCTC-3’
Mouse PD-L1	5’-CAAGAAAGCTAATGCAGGTTTCAC-3’	5’-CCTGCGGATGACTTTAGAGTC-3’

Western blotting

For IRF2 experiments (Chapters III and IV), whole cell lysates were prepared in RIPA buffer with protease inhibitor (Pierce), protein concentrations were determined by BCA assay (Pierce), and 10µg of denatured samples were run on 10% reducing gels (Genscript). After transfer, PVDF membranes (Millipore) were blocked with TBS-Tween 1x + 5% milk and then blotted with rabbit anti-IRF2 (Abcam ab124744) or rabbit anti-IRF1 (Abcam ab186384) in TBS-Tween 1x + 2% milk overnight at 4°C. The following day, membranes were washed 3x with TBS-Tween 1x, goat-anti-rabbit HRP (Millipore) was added for 1hr at RT, membranes were washed 3x, and HRP substrate (Millipore) was added. Following exposure, membranes were stripped (Millipore), blocked, and re-blotted with mouse anti-β-actin (Santa Cruz sc-47778) in TBS-Tween 1x + 2% milk overnight at 4°C. The following day, membranes were prepared as above except anti-mouse HRP (Pierce) was used instead.

For Dnajc10 experiments (Chapter V), the same protocol was used as above but with the following antibodies: mouse anti-Dnajc10 (Santa Cruz sc-100713), rabbit anti-BiP (Cell Signaling C50B12 and Abcam ab21685), mouse anti-β-actin (Santa Cruz sc-47778), rabbit anti-β2m (Abcam ab75853), rabbit anti-ERp57 (Cell Signaling G117), mouse anti-H2-K^b exon 8 (Spring Valley), rabbit anti-TAP1, and rabbit anti-calreticulin (Abcam ab2907).

In vitro cytotoxicity assays

OT-I $CD8^+$ T cells were pre-activated by co-culturing them for 4-5 days with irradiated, SIINFEKL-pulsed wild-type B-blasts in T cell media containing 30ng/mL IL-2. After this time, OT-I were checked for CD8 expression and upregulation of CD27 and CD44. WT or IRF2-null RMA cells were counted, sub-divided into respective tubes, SIINFEKL-pulsed at the indicated concentrations or kept un-pulsed, and CFSE-labeled as high (1μM) for cells pulsed with SIINFEKL and CFSE-labeled as low (0.1μM) for un-pulsed cells. Pulsed and un-pulsed cells were re-counted, mixed 1:1, and 10^5 cells total were plated per well in U-bottom 96-well plates. 5 x 10^4 OT-I were added to the respective wells and incubated at 37°C for 4hrs. Live RMA cells were gated by flow cytometry and CFSE levels analyzed. Specific killing was determined for each RMA line by calculating $100 \times [1 - \frac{\left(\frac{\%\,Targets}{\%\,Bystanders}\right)}{\frac{\%\,Control\,Targets}{\%\,Control\,Bystanders}}]$.

Dnajc10 construct cloning

To build the Dnajc10 constructs, Dnajc10 cDNA (as described below) was inserted into the doxycycline-inducible (pTRIPZ) or constitutive (pCDH) expression vectors. As controls, some experiments used empty vectors without a cDNA insert (EV) and others used vectors where enhanced green fluorescent protein cDNA had been inserted (EGFP). All Dnajc10 cDNA sequences were of C57BL/6 origin and contained 6 synonymous mutations within the Dnajc10

siRNA target site and an HA tag, which was inserted just upstream to the C-terminal KDEL motif because putting a tag downstream of KDEL causes the protein to be secreted rather than retained in the ER [151]. A point mutation at residue 63 (H63Q) of the J domain was created using a site-directed mutagenesis kit (Agilent). Point mutations within the thioredoxin-like motifs were generated either by site-directed mutagenesis or overlapping PCR. All plasmids were sequenced to confirm correct sequences and reading frames.

Immunoprecipitations

Dnajc10 was immunoprecipitated using Protein G Dynabeads (Life Technologies) that were BS_3-cross-linked (Pierce) to either mouse anti-Dnajc10 (Santa Cruz sc66.7) or rabbit anti-HA (Cell Signaling C29F4), according to the manufacturer's instructions. As control, beads were cross-linked to mouse or rabbit normal immune IgG (Santa Cruz), respectively. Cells were lysed in 1% digitonin, 20mM N-ethylmaleimide, and protease inhibitor (Pierce). Lysates were pre-cleared on normal immune IgG beads and some was stored as the "pre-clear" fraction. Then, lysates were divided onto the anti-Dnajc10 or normal immune IgG beads and incubated at RT for 20 minutes, after which time a "flow-through" fraction was collected. Bead-antibody-antigen complexes were then washed 3 times in PBS with 0.2% digitonin and a "wash 3" fraction was collected. Finally, protein "eluate" was captured from the beads using 50mM glycine, pH

2.8. All protein fractions were then denatured and run on reducing gels as above (Western blotting section) and blotted for the proteins of interest.

Dnajc10 *ex vivo* studies

Dnajc10$^{+/+}$ (WT) or Dnajc10$^{-/-}$ (KO) mice were acquired [137] and bred on a C57BL/6 background. Bone marrow and spleens were collected from male, 6-8-week-old WT and KO mice using a standard protocol. To generate bone marrow-derived dendritic cells (BMDCs), the bone marrow was cultured on tissue cultured-treated petri dishes for 7 days prior to harvesting the non-adherent differentiated BMDCs. During this time, the culture media (HCM) was supplemented with the cytokines GM-CSF and IL-4 on days 0, 1, and 4. BMDCs were confirmed to be >95% CD11b^{+}/CD11c^{+} by flow cytometry. For antigen presentation assays, 10^5 BMDCs were plated per well in flat-bottom 96-well plates and then OVA-beads and T cells were added, as described above. For flow cytometry analysis of MHC levels on BMDCs or splenocytes, cells were surface stained as described above.

Chapter III: IRF2 regulation of MHC-I presentation

Attributions and Copyright Information

The data described in Chapter III is part of a manuscript under review. Co-authors of this manuscript include Pranitha Vangala, Benjamin J. Chen, Paul Meraner, Abraham L. Brass, Manuel Garber, and Kenneth L. Rock. All experiments were performed by me (B.A.K.) and analyzed by B.A.K. and K.L.R. P.V. compiled and analyzed the RNA-seq data, which was also examined by M.G. A.L.B. and P.M. helped set up and analyze the HeLa screen. B.J.C. provided the clinical biopsy specimens used in the Chapter IV.

Chapter III: IRF2 regulation of MHC-I presentation

Introduction

The importance of adaptive immunity in preventing cancer was revealed through studies in which immunodeficient animals, such as those lacking IFNγ, perforin, or RAG-2, were found to have a marked increase in spontaneous and mutagen-induced tumors [152-154]. In addition, tumors derived from such immunodeficient animals grew when transplanted into other immunodeficient hosts but were rejected when placed into immunocompetent hosts [154-156], providing further evidence that the immune system recognized such tumors and could reject them. In contrast, many tumors arising in immunocompetent animals grew after being transplanted into immunocompetent hosts [154-156], thereby showing that cancers that arise and successfully progress in the face of the immune system have undergone immunoediting to escape from immune control. This immunoediting process is thought to be why many cancers express low levels of MHC-I [157]. The underlying molecular mechanisms responsible for these changes are poorly understood but have obvious potential impact on tumor progression and immunotherapy [135, 158].

As mentioned in Chapter I, the MHC-I presentation pathway is critical for immune recognition and elimination of tumors by $CD8^+$ T cells. In this process, a fraction of peptides that are generated by proteasomal degradation of cellular proteins are transported by the TAP transporter into the endoplasmic reticulum

(ER), wherein they can be further trimmed by the aminopeptidase, ERAP1 [8-10]. Subsequently, peptides of the correct length and sequence bind to MHC-I molecules and these complexes are then transported to the cell surface for display to $CD8^+$ T cells. This allows activated $CD8^+$ T cells to identify and kill cells that are presenting tumor-specific peptides (e.g., from mutant proteins) on their MHC-I [159].

We performed an unbiased, forward-genetic screen in human cervical carcinoma HeLa H1 cells to identify genes whose loss downregulated the MHC-I pathway. In this screen, the second strongest hit, second only to β2-microglobulin (the MHC-I light chain), was IRF2, an interferon regulatory transcription factor that had not been previously recognized to positively regulate this pathway. Here, I will describe the screen, the studies validating IRF2 as a positive regulator of MHC-I presentation in a variety of cell types, and the mechanisms by which IRF2 affects this pathway.

Results

HeLa H1 screen for novel regulators of classical MHC-I presentation

To identify genes positively regulating the classical MHC-I pathway, we performed a CRISPR-Cas9 screen in HeLa H1 cells. A lentiviral library expressing six barcoded sgRNAs targeting each gene of the human genome (~19,000 genes) was transduced at a low multiplicity of infection and then cells were immunoselected for MHC-I low variants. The rationale for this was that cells

will lose surface MHC-I levels if they have lesions anywhere in the MHC-I pathway, which includes the steps required for proteasomal processing and those involved in peptide transport, trimming, and loading onto MHC-I [15-17]. In this HeLa H1 screen, several known components of the MHC-I presentation pathway came up as very strong hits, including β2M, TAP1, TAP2, TAPBP (Tapasin), PDIA3 (ERp57), and the three RFX proteins that make up part of the enhanceosome complex with NLRC5 [32], RFXANK, RFXAP, and RFX5 (Fig. 3.1). Additionally, the second-most targeted gene was IRF2, with six out of six independent IRF2 sgRNAs hitting (Fig. 3.1), and this gene had not been previously recognized to positively regulate MHC-I presentation under basal conditions. As a result, we decided this gene warranted further investigation.

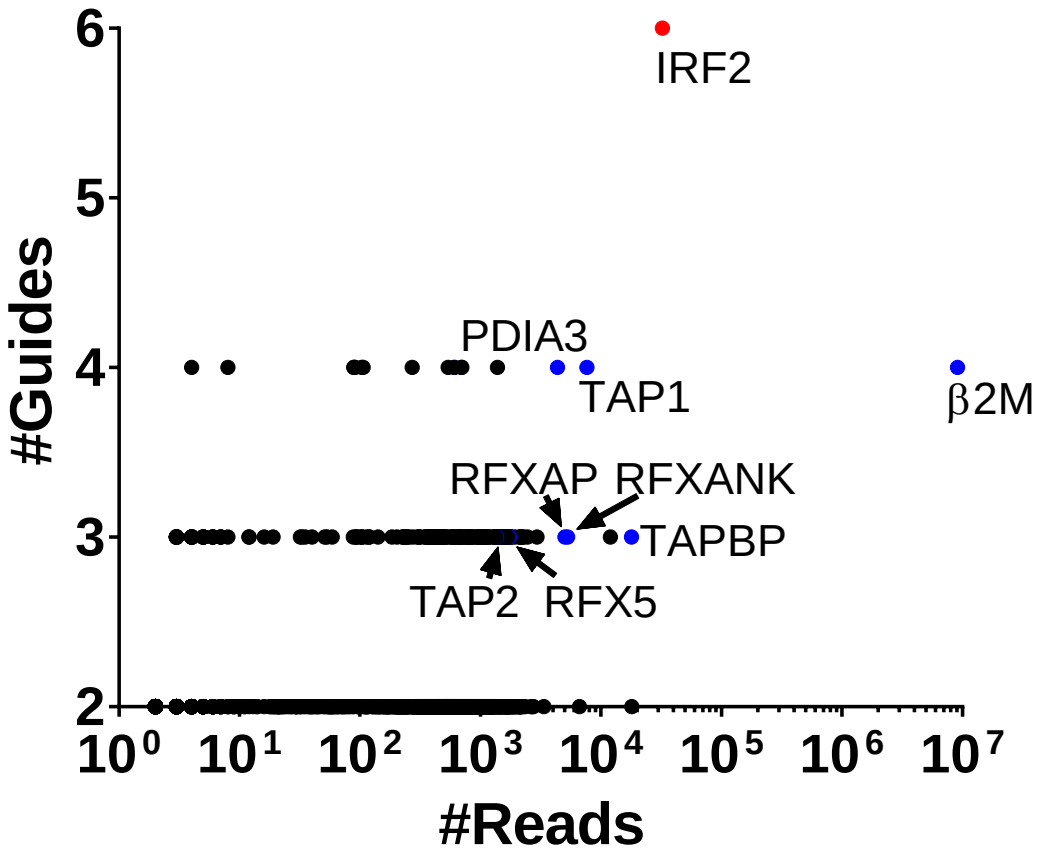

Figure 3.1. HeLa H1 CRISPR-Cas9 screen.

Scatterplot of top gene “hits” from the HeLa H1 CRISPR-Cas9 screen. Each gene was targeted by six independent sgRNAs. MHC-I low variants were immunoselected and barcoded sgRNAs were identified from this MHC-I low population. Gene candidates were ranked by their abundance in this MHC-I low population as shown by the number of independent guides targeting a given gene versus the number of total reads for all guides targeting that gene.

IRF2 positively regulates the MHC-I presentation pathway

To validate this hit, we tested whether IRF2 affects surface MHC-I levels in human cells by knocking out IRF2. HeLa H1 cells and HEK293T kidney cells were transduced with vectors expressing either Cas9 and a sgRNA targeting human IRF2 or Cas9 alone and surface MHC-I levels were checked by flow cytometry (Fig. 3.2a). The IRF2-knockout (IRF2-KO) HeLa H1 and HEK293T had significantly lower surface MHC-I levels than their wild-type (WT) controls (Fig. 3.2b). To further validate this finding with an independent technique, we silenced IRF2 expression with siRNAs and found that this also decreased surface MHC-I levels in HeLa H1 and HEK293T (Fig. 3.2c), confirming the phenotype. The magnitude of the decrease in MHC-I was similar to that observed when the expression of the TAP transporter was silenced. To determine whether IRF2 also affects surface MHC-I levels in mouse cells, we transduced NIH-3T3 fibroblasts stably transfected with H2-K^b (3T3-K^b) and DC3.2 dendritic cells [4] with vectors expressing either Cas9 and a sgRNA targeting mouse IRF2 or Cas9 alone. The IRF2-KO mouse fibroblasts and DC cells also had significantly reduced surface MHC-I levels (Fig. 3.2d). Loss of IRF2 expression was confirmed by western blot (Fig. 3.2e). DC3.2 cells also express MHC-II molecules and we found no change in surface MHC-II levels in the IRF2-KO cells (Fig. 3.2d), which demonstrates that IRF2 is selectively affecting the MHC-I pathway; further evidence supporting this conclusion will be described below.

To investigate the functional consequence of this reduction in MHC-I levels, we evaluated the importance of IRF2 for MHC-I cross-presentation (i.e., the presentation of peptides derived from exogenous antigen on MHC-I). The IRF2-KO DCs cross-presented more poorly than their WT controls (Fig. 3.2f), demonstrating that IRF2 positively regulates MHC-I antigen presentation. In the same experiments, MHC-II presentation was unaffected, again showing selectivity in IRF2 effects (Fig. 3.2g). Lastly, to confirm that IRF2 is responsible for these differences, we overexpressed IRF2 in the IRF2-KO DC3.2 line and found that it completely restored surface MHC-I levels (Fig. 3.2h) and the ability of these cells to cross-present antigen (Fig. 3.2i). Evidence that loss of IRF2 also compromises the presentation of endogenous cellular antigens will be described below.

To determine whether IRF2 was exerting its function as a transcription factor, we introduced a lysine to arginine point mutation at position 78 which prevents acetylation at this site and thereby prevents IRF2 from binding its DNA target sequences [160]. Overexpressing this mutant IRF2 did not restore function in the IRF2-KO DC3.2 cells (Fig. 3.2i). Therefore, IRF2 is necessary for optimal transcriptional regulation of MHC-I antigen presentation pathways.

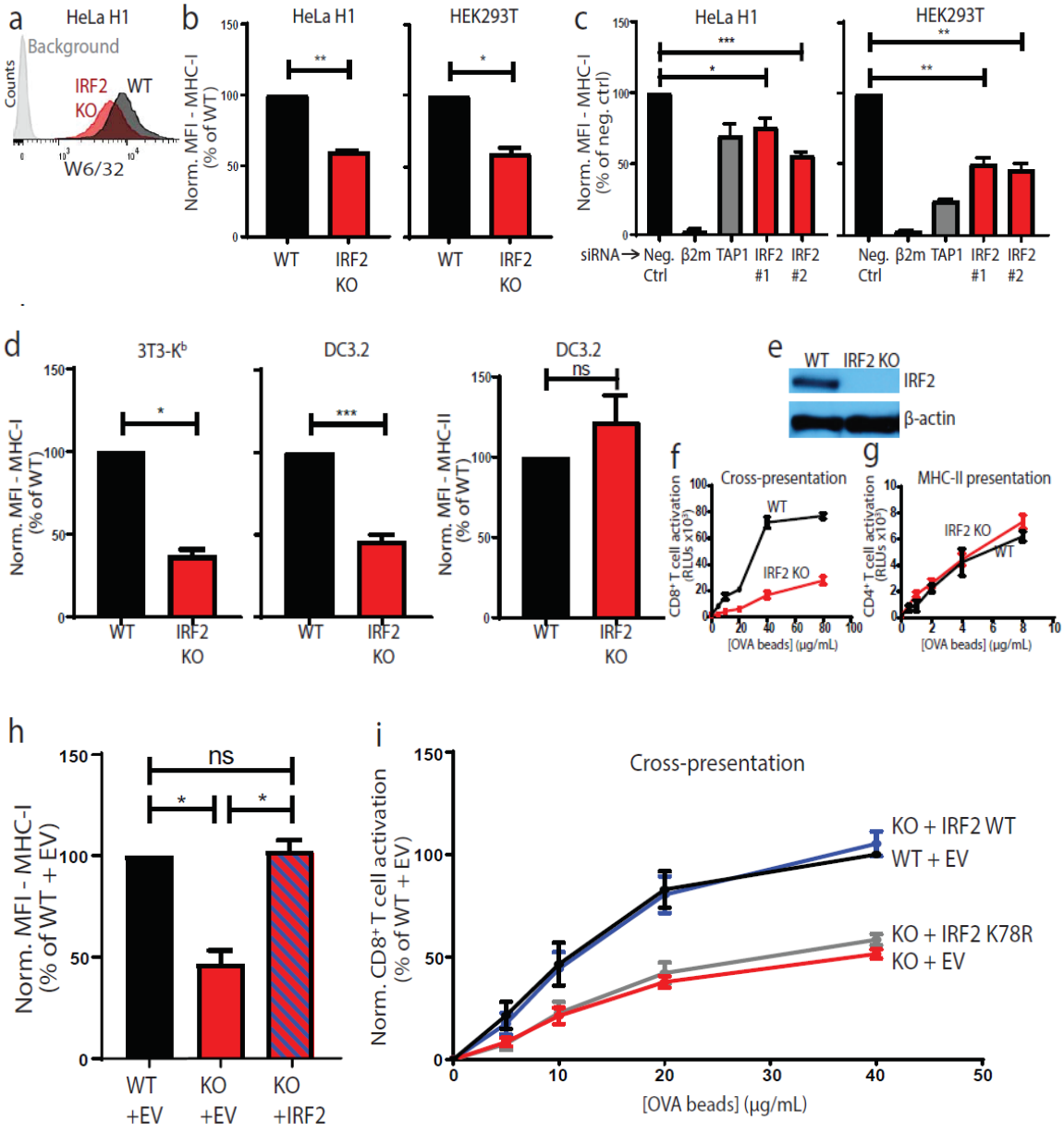

Figure 3.2. IRF2 positively regulates MHC-I presentation under basal conditions

Figure 3.2. IRF2 positively regulates MHC-I presentation under basal conditions

(a) Representative histograms of surface MHC I levels by W6/32 staining in HeLa H1 lines stably transduced with the LentiCRISPRv2 constructs; “IRF2 KO” (IRF2 sgRNA) or “WT” control (no sgRNA). Background is with secondary antibody staining only; (b) Normalized MFI of surface MHC I levels on HeLa H1 (left) or HEK293T (right) stable knockout lines; (c) normalized MFI of surface MHC I levels on HeLa H1 (left) or HEK293T (right) cells after 72hrs silencing with 10nM indicated siRNA; (d) Normalized MFI of surface MHC I levels by AF6 staining on 3T3-K^b stable knockout lines (left), surface MHC I levels on DC3.2 stable knockout lines (middle), or surface MHC II levels on DC3.2 stable knockout lines (right); (e) Representative Western blot in DC3.2 lines “IRF2 KO” (IRF2 sgRNA) or “WT” control (no sgRNA) for protein expression of IRF2 or β-actin as control; (f) Representative cross-presentation experiment of OVA-beads by DC3.2 lines to RF33.70-Luc $CD8^+$ T cell hybridoma; (g) Representative MHC-II presentation experiment of OVA-beads by DC3.2 lines to MF2.2D9-Luc $CD4^+$ T cell hybridoma; (h) Normalized MFI of surface MHC I levels on DC3.2 lines after transducing with pCDH expressing empty vector (EV) or wild-type IRF2 containing six synonymous mutations within the IRF2 sgRNA target site (IRF2); (i) Cross-presentation after transducing the DC3.2 lines with pCDH expressing empty vector (EV), wild-type IRF2 containing six synonymous mutations within the IRF2 sgRNA target site (IRF2 WT), or mutant IRF2 (IRF2 K78R) which also contains the same six synonymous mutations as IRF2 WT. (b, c, d, h, i) Bars represent mean + SEM (N≥3). Statistical analysis by two-tailed ratio paired t-tests; (f, g) Points represent mean ± SD of technical duplicates. *$p<0.05$, **$p<0.01$, ***$p<0.001$, ns=not significant

How does IRF2 regulate the MHC-I pathway?

Since IRF2 is functioning as a transcription factor, we next sought to determine what genes are regulated by IRF2 and could be responsible for producing the low MHC-I phenotype observed in the IRF2-KO cells. RNA-seq was performed on the wild-type and IRF2-KO DC3.2 lines (Fig. 3.3a, Table 3.1). Surprisingly, relatively few genes were differentially expressed by >2-fold (19 decreased and 33 increased). Of these 52 differentially expressed genes, we identified TAP2, ERAP1, and the immunoproteasome subunit PSME1 as potential contributors to the decreased MHC-I levels. To further confirm this result, we performed qPCR in these cell lines to check expression of all MHC-I pathway genes (Fig. 3.3b), which showed that the mRNA levels of TAP2, ERAP1, and PSME9 (another immunoproteasome subunit) were significantly downregulated in the IRF2-KO DC3.2; PSME1 levels were reduced but this decrease did not achieve statistical significance. Interestingly, the mRNA levels of the MHC heavy chain (H2-K1) and MHC light chain (β2m) were unaffected (Fig. 3.3b), indicating that IRF2 is not required for synthesis of the MHC-I heterodimer. ChIP-qPCR experiments confirmed that IRF2 regulates TAP2 and ERAP1 mRNA expression by directly binding to their promoters (Fig. 3.3c). To test whether functional IRF2 is needed for TAP2 and ERAP1 mRNA expression, we overexpressed wild-type IRF2 or the IRF2-K78R mutant in the DC3.2 IRF2-KO cells and found that the TAP2 and ERAP1 mRNA levels were increased in the cells expressing wild-type but not mutant IRF2 (Fig. 3.3d).

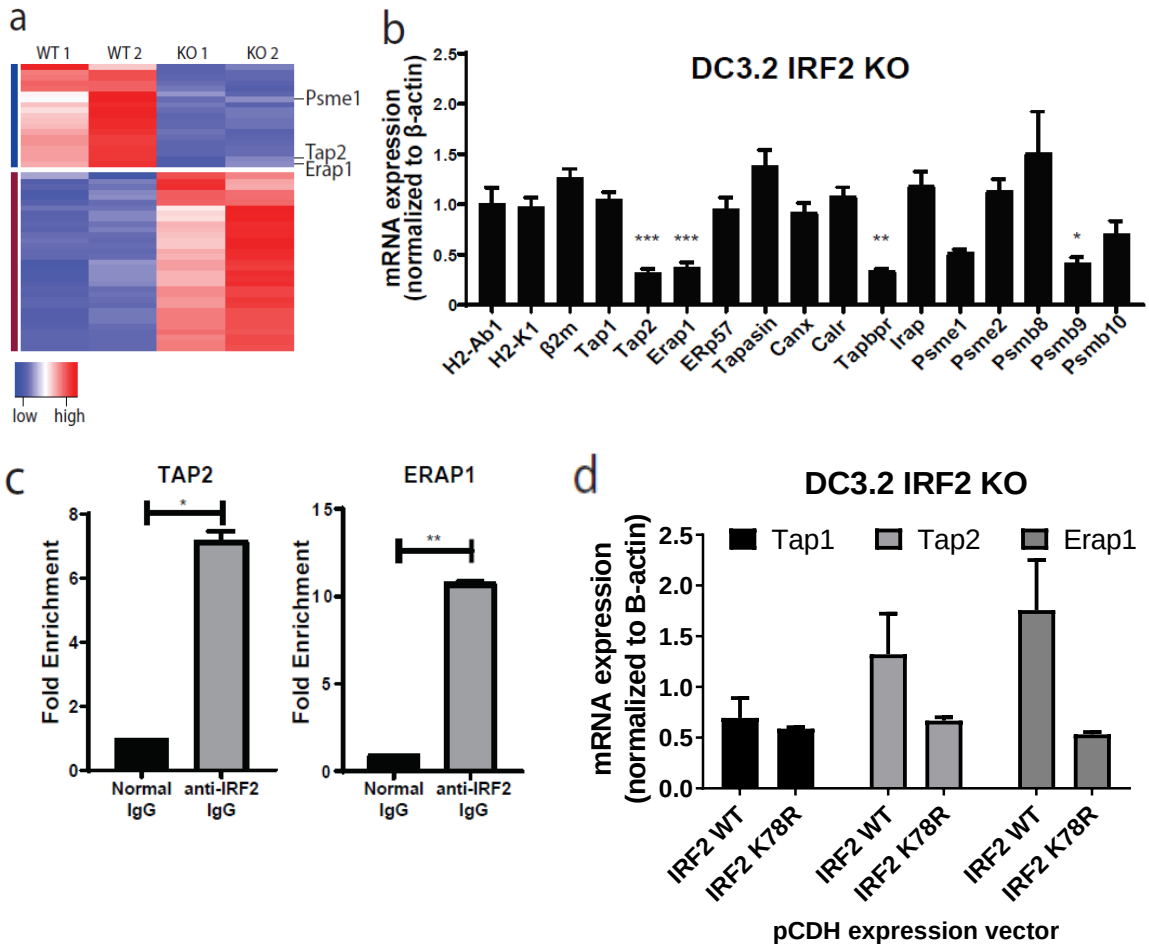

Figure 3.3. IRF2 transcriptionally regulates components of the MHC-I pathway

Figure 3.3. IRF2 transcriptionally regulates components of the MHC-I pathway

(a) Heatmap of genes (52) differentially expressed by >2-fold between the DC3.2 no sgRNA ("WT") and IRF2 sgRNA ("IRF2 KO") lines. Columns represent independent duplicate RNA-seq runs in these two lines. Red → blue indicates high → low expression for a given row (gene). For clarity, only three of the downregulated genes in the KO line (Psme1, Tap2, and Erap1) are shown here and all are listed in Table 3.1; (b) mRNA expression levels by qPCR in DC3.2 IRF2 KO relative to those in DC3.2 WT; normalized to the mRNA expression of mouse β-actin in each sample ($2^{\wedge-\Delta\Delta Ct}$). Values >1 indicate higher expression in DC3.2 IRF2 KO and values<1 indicate lower expression in the DC3.2 IRF2 KO. Bars represent mean + SEM mRNA expression (N≥3). Statistical analysis by two-tailed unpaired t-tests by comparing the expression of a given gene to that of H2-Ab1 (control); (c) ChIP-qPCR in DC3.2 WT for TAP2 (left) or ERAP1 (right) DNA with rabbit anti-IRF2 IgG or normal rabbit IgG (control). Bars represent mean + SEM fold enrichment ($2^{\wedge-\Delta Ct}$) over the normal rabbit IgG control IP (N=2). Statistical analysis by two-tailed ratio paired t-tests; (d) mRNA expression levels by qPCR in DC3.2 IRF2 KO 24hrs after overexpressing pCDH wild-type IRF2 (IRF2 WT) or mutant IRF2 (IRF2 K78R) relative to overexpressing pCDH empty vector; normalized to the mRNA expression of mouse β-actin in each sample ($2^{\wedge-\Delta\Delta Ct}$). Values >1 indicate higher expression than overexpressing empty vector and values<1 indicate lower expression than overexpressing empty vector. Representative experiment shown; bars represent mean + SD of mRNA expression of duplicate technical replicates. *p<0.05, **p<0.01, ***p<0.001, ns=not significant

Table 3.1. RNA-Seq differentially expressed genes in DC3.2 WT vs. IRF2-KO under basal conditions. Genes listed below in the order shown in the heatmap.

Cluster 1 (blue bar)	**Cluster 2 (red bar)**
Isg20	Socs1
Arg1	Ifit1
Acadl	H2-T22
Ddx58	Hck
Thbs1	Igtp
C1qa	Flt1
Psme1	Mx2
Fabp7	Tnfsf13b
Nmi	H2-T9
Arg2	Ly6a
Epsti1	Scimp
Mov10	Tmem140
Il15ra	Cmpk2
Casp7	Gbp5
Gsdmd	Rsad2
Parp14	Gbp2
Ifi27	Gbp6
Tap2	Cd40
Erap1	Gbp11
	Trafd1
	Psmb8
	Irg1
	Cst7
	Tspan13
	Gbp3
	Ifi47
	Gbp8
	Irgm2
	Fgl2
	Tgtp2
	Gbp9
	Gbp4
	Gbp7

To more closely examine the functional effects of IRF2 on peptide transport and trimming, 3T3-K^b IRF2-KO cells were transfected with various pTracer plasmids, each of which contained a GFP reporter and a minigene encoding a peptide that could be processed down to the mature epitope (i.e., SIINFEKL/S8L). The cells were surface stained with the antibody 25-D1.16, which recognizes H2-K^b-S8L complexes [142], and transfected cells (GFP-positive) were analyzed. IRF2-KO cells presented fewer H2-K^b-S8L complexes than wild-type cells when given the TAP-dependent, ERAP1-dependent antigens CD16-OVA (full-length ovalbumin protein) [161], N25-S8L (a S8L precursor extended by 25 amino acids on the N-terminus), or N5-S8L (a S8L precursor extended by 5 amino acids on the N-terminus) (Fig. 3.4a). We also tested the presentation of a version of the precursor peptide with 5 extra N-terminal residues that was targeted into the ER by a co-linear signal sequence (ss-N5-S8L). Since the signal sequence allows this peptide to enter the ER through SEC61 instead of TAP, its presentation is TAP-independent but still dependent on ERAP1 to remove the extra N-terminal residues. IRF2-KO cells also presented fewer H2-K^b-S8L complexes than wild-type cells when transfected with ss-N5-S8L (Fig. 3.4b). However, IRF2-deficient cells were equally capable of presenting H2-K^b-S8L complexes when given a TAP-independent, ERAP1-independent peptide (S8L with no extra N-terminal residues that was targeted into the ER via a co-linear signal sequence; ss-S8L) (Fig 3.4c), demonstrating

that while IRF2 affects the transport and processing of MHC-I epitopes, it does not affect the ability of such peptides to be loaded onto MHC-I.

We also assessed the functional significance of IRF2-mediated changes in TAP2 and ERAP1 expression by measuring the extent to which TAP2 and ERAP1 contribute to the low surface MHC-I phenotype observed in the IRF2-KO cells. The magnitude of the reduction in MHC-I levels on IRF2-KO cells was in between that of the TAP2- and ERAP1-knockout cells (Fig. 3.4d), which is consistent with our findings that IRF2 positively regulates TAP2 and ERAP1 but their expression is not entirely lost in IRF2-KO cells. Lastly, we performed rescue experiments wherein we overexpressed TAP2 and/or ERAP1 in the IRF2-knockout DC3.2 and checked surface MHC-I levels two days after transduction (Fig. 3.4e). Although the double-rescue partially restored MHC-I levels, it was not complete, suggesting that other genes regulated by IRF2 also contribute to surface MHC-I expression.

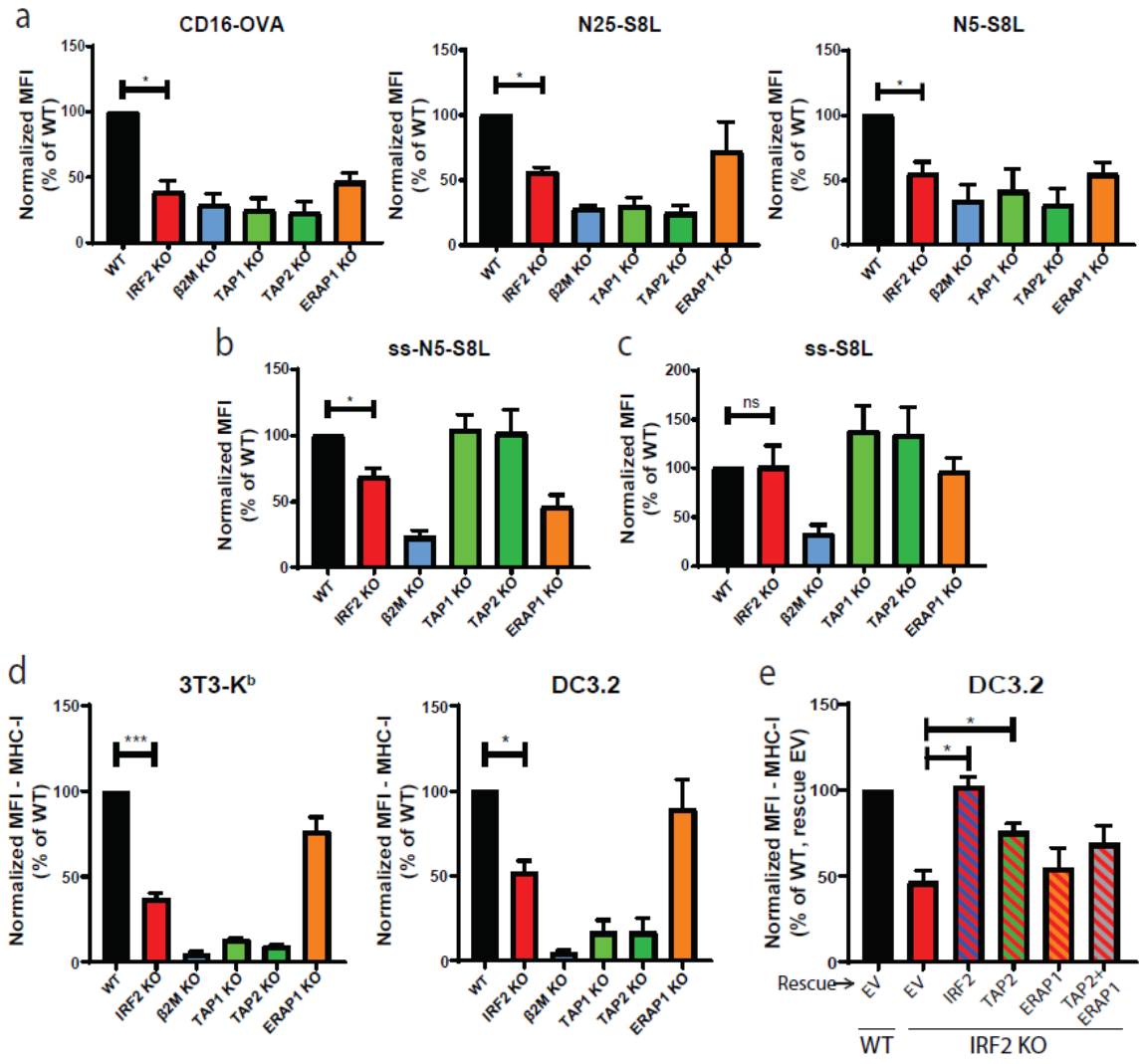

Figure 3.4. IRF2 affects antigen transport and processing

(a-c) H-2K^b presentation of SIINFEKL derived from (a) the TAP-dependent, ERAP1-dependent antigens CD16-OVA (left), N25-S8L (middle), or N5-S8L (right); (b) the TAP-independent, ERAP1-dependent antigen ss-N5-S8L; and (c) the TAP-independent, ERAP1-independent antigen ss-S8L on 3T3-K^b knockout lines. 25-D1.16 staining analyzed on transfected (GFP+) cells; (d) Normalized MFI of surface MHC I levels on 3T3-K^b (left) or DC3.2 (right) knockout lines; (e) Normalized MFI of surface MHC I levels on DC3.2 lines 48hrs after transduction with pCDH expression vectors containing empty vector (EV), IRF2, TAP2, ERAP1, or dual transduction of TAP2 and ERAP1. (a-e) Bars represent the mean + SEM of the normalized MFI from independent experiments (N≥3). Statistical analysis by two-tailed ratio paired t-tests. *p<0.05, ***p<0.001, ns=not significant

Summary

Through a CRISPR-Cas9 screen, we identified IRF2 as a novel positive regulator of MHC-I antigen presentation. Moreover, we found that, under basal conditions, IRF2 is important for both classical MHC-I presentation and cross-presentation. This was demonstrated in a number of human and mouse cell types including both professional and non-professional APCs. IRF2 binds the promoters of TAP2 and ERAP1 and transcriptionally activates their expression. In the absence of IRF2, cells express less TAP2 and ERAP1 and, due to the consequent defects in antigen transport and processing, present fewer peptide-MHC-I complexes at the cell surface. Additionally, IRF2 regulates the expression of other genes, such as immunoproteasome subunits, which likely also influence the MHC-I presentation in IRF2-deficient cells. Given that MHC-I presentation is essential for immune recognition and elimination of tumors by $CD8^+$ T cells and that a loss of IRF2 dramatically reduces MHC-I presentation, we decided to investigate whether some cancers may downregulate IRF2, thereby facilitating their escape from the immune system (Chapter IV).

Chapter IV: IRF2, immune checkpoint, and cancer

Attributions and Copyright Information

The data described in this chapter is part of a manuscript under review. Co-authors of this manuscript include Pranitha Vangala, Benjamin J. Chen, Paul Meraner, Abraham L. Brass, Manuel Garber, and Kenneth L. Rock. All experiments were performed by me (B.A.K.) and analyzed by B.A.K. and K.L.R. P.V. compiled and analyzed the RNA-seq data, which was also examined by M.G. B.J.C. provided the clinical biopsy specimens and checked their PD-L1 expression.

Chapter IV: IRF2, immune checkpoint, and cancer

Introduction

Based on our findings that IRF2-deficient cells have significantly lower MHC-I presentation than IRF2-sufficient cells (Chapter III), we were interested in determining whether IRF2 expression is downregulated in cancers. In addition to the aforementioned effects of immunoediting on MHC-I levels, inhibitory immune checkpoint molecules (e.g., PD-L1) are often upregulated on tumor cells, which facilitate their escape from the immune system. Fortuitously, as we were mining our RNA-seq results for antigen presentation genes, we noticed that the IRF2-KO dendritic cells also had higher expression of PD-L1 than the WT controls and this was of obvious interest to explore further. Additionally, because IRF2 is an interferon regulatory factor and interferon is known to upregulate both MHC-I presentation and PD-L1 expression, we wanted to investigate the effects of interferon stimulation on cells lacking IRF2. Below, we address each of these topics and show that IRF2 downregulation leads to immune evasion.

Results

IRF2 represses PD-L1 expression

One of the upregulated genes in the IRF2-KO RNA-seq dataset was *Cd274* (Fig. 4.1), also known as programmed death-ligand 1 (PD-L1), which is often upregulated in certain cancers (e.g., non-small cell lung cancer) and functions as

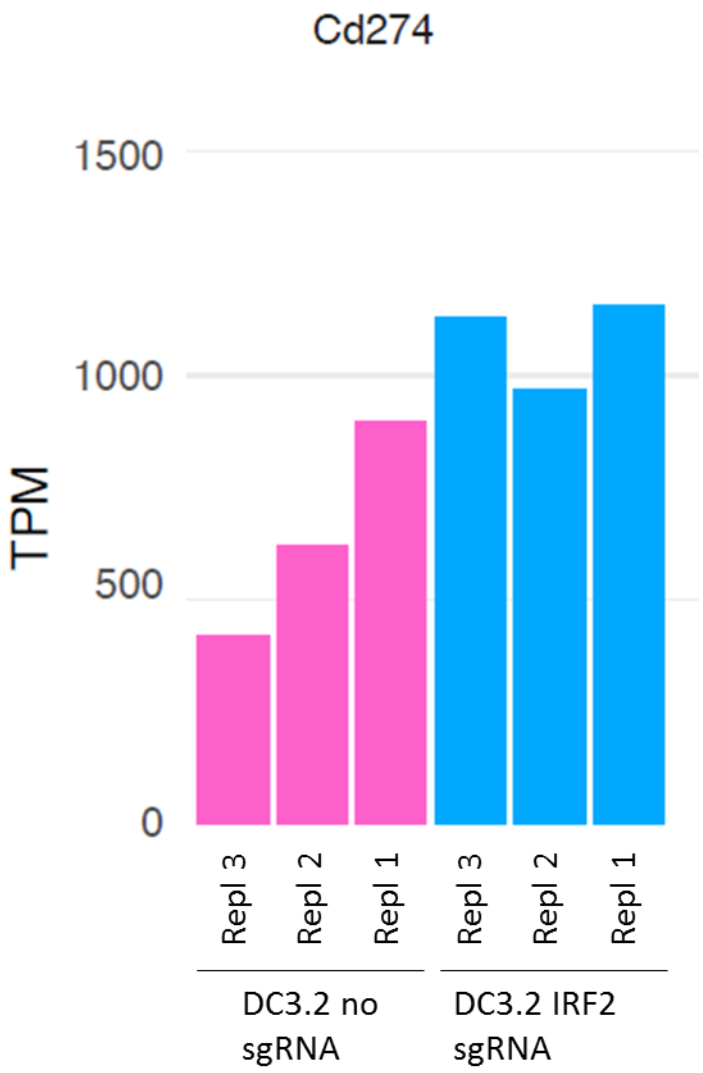

Figure 4.1. PD-L1 (Cd274) mRNA expression in RNA-seq replicates

PD-L1 mRNA expression in the DC3.2 no sgRNA (“WT”) and IRF2 sgRNA (“IRF2 KO”) lines. Bars show TPM from 3 independent RNA-seq replicates.

a checkpoint inhibitor to suppress antigen-specific $CD8^+$ T cell effector function [162, 163]. To validate our RNA-seq finding with an independent technique, we performed qPCR on the IRF2-KO and wild-type DC3.2 lines and found that the IRF2-KO cells expressed approximately twice as much PD-L1 mRNA as the wild-type controls (Fig. 4.2a). Additionally, ChIP-qPCR revealed that IRF2 regulates PD-L1 mRNA expression by directly binding the PD-L1 promoter (Fig. 4.2b). Therefore, IRF2 acts as a transcriptional repressor of PD-L1 in these cells. To evaluate the extent to which a roughly 2-fold increase in PD-L1 mRNA translates to surface PD-L1 expression, we analyzed these cells by flow cytometry (Fig. 4.2c). Interestingly, the surface PD-L1 levels increased by roughly 50% in the IRF2-KO cells (Fig. 4.2d). Taken together, these results demonstrate that IRF2 plays a role in repressing PD-L1 expression under basal conditions.

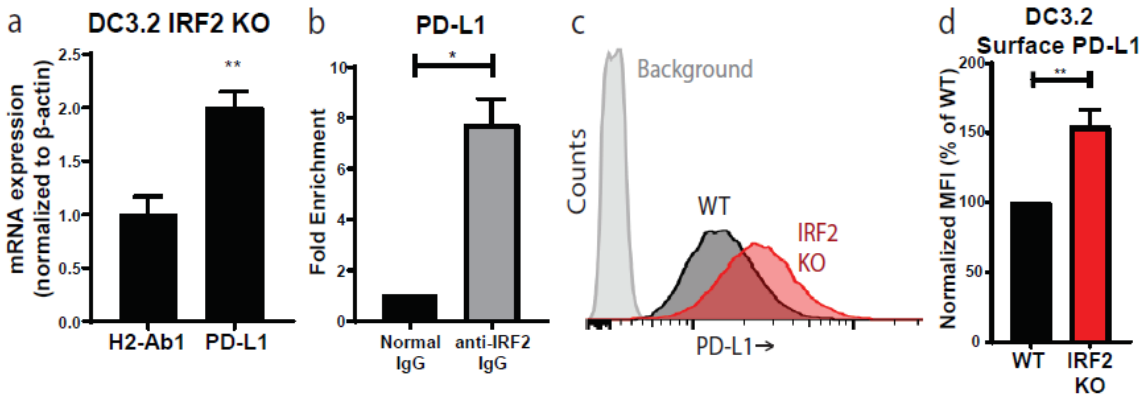

Figure 4.2. IRF2 represses PD-L1 expression under basal conditions

(a) H2-Ab1 and PD-L1 mRNA expression levels by qPCR in DC3.2 IRF2 KO relative to those in DC3.2 WT; normalized to the mRNA expression of mouse β-actin in each sample ($2^{\wedge-\Delta\Delta Ct}$). Values >1 indicate higher expression in DC3.2 IRF2-KO. Bars represent mean + SEM mRNA expression (N=3). Statistical analysis by two-tailed unpaired t-test by comparing the expression of PD-L1 to that of H2-Ab1; (b) ChIP-qPCR of DC3.2 WT for PD-L1 DNA with rabbit anti-IRF2 IgG or normal rabbit IgG (control); bars represent mean + SEM fold enrichment ($2^{\wedge-\Delta Ct}$) over the normal rabbit IgG control IP (N=2). Statistical analysis by two-tailed ratio paired t-test; (c) Representative histograms of surface PD-L1 levels by 10F.9G2 staining in DC3.2 lines stably transduced with the LentiCRISPRv2 constructs; IRF2-KO ("IRF2 sgRNA") or WT control ("No sgRNA"). Background = isotype control staining; (d) Normalized MFI of surface PD-L1 levels on DC3.2 lines; bars represent mean + SEM (N=6). Statistical analysis by two-tailed ratio paired t-test. *$p<0.05$, **$p<0.01$

Contributions of IRF1 vs. IRF2

Because IRF2 is an interferon regulatory transcription factor, we wanted to see how interferon induction would affect IRF2's regulation of the MHC-I pathway and PD-L1 expression. Interestingly, stimulation with either IFNγ or IFNα restored the surface MHC-I expression in the IRF2-KO DC3.2 (Fig. 4.3). This is an important finding because it indicates that impairment of the MHC-I pathway from loss of IRF2 is reversible. IRF1 and IRF2 recognize the same IFN-stimulated response element (ISRE) [82, 84, 164] and, whereas IRF2 is constitutively expressed and minimally affected by interferon induction, IRF1 is significantly upregulated in response to interferon (Fig. 4.3) [88, 165, 166]. Consistent with the literature that IRF1 positively regulates both MHC-I and PD-L1 expression under IFN-stimulated conditions [167-169], we found that knocking out IRF1 decreased both surface MHC-I and PD-L1 levels after IFNγ stimulation (Fig. 4.3). Interestingly, when we examined the dual effects of IRF1 and IRF2 on surface MHC-I and PD-L1 levels using single or double knockout DC3.2 lines (Fig. 4.3), we found that: (1) IRF1/2 double knockouts have a larger reduction in surface MHC-I than is observed in either single knockout; and (2) IRF2-knockouts have a larger effect than the IRF1-knockouts on both MHC-I and PD-L1 expression under basal conditions. This suggested that, although these two IRFs recognize the same ISRE, the subset of genes they each primarily regulate differs and that a cell's dependence on IRF2 vs. IRF1 for any given gene may vary depending on the cues (e.g., interferon) which that cell receives from its environment.

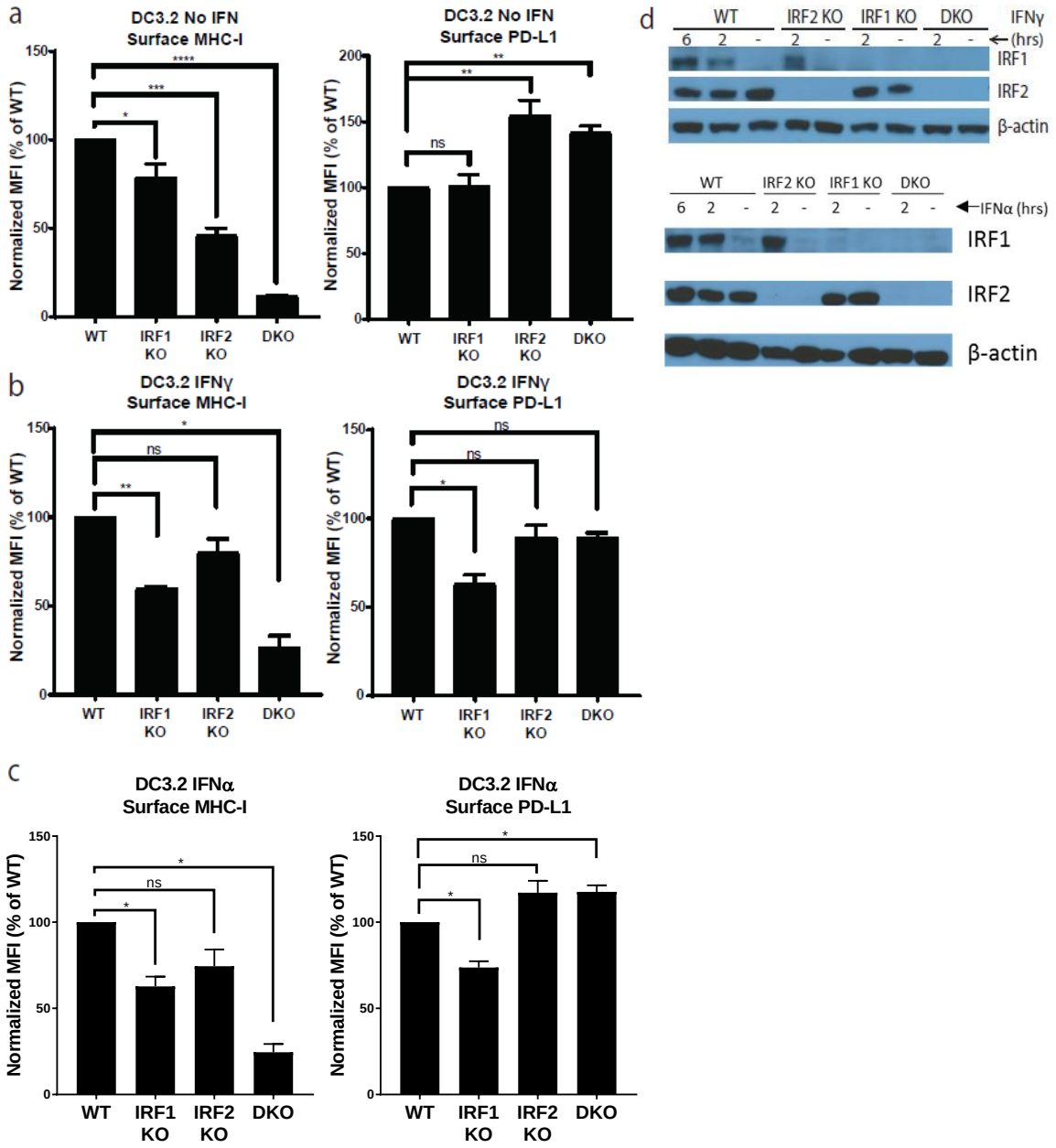

Figure 4.3. Contributions of IRF1 and IRF2 in the presence or absence of IFN

(a-c) Normalized MFI of surface MHC I and PD-L1 levels on DC3.2 stable lines after overnight incubation with (a) media alone, (b) 2ng/mL IFNγ, or (c) 5,000 U/mL IFNα; bars represent mean + SEM (N≥3). Statistical analysis by two-tailed ratio paired t-tests. *p<0.05, **p<0.01, ***p<0.001, ****p<0.0001, ns=not significant. (d) Western blots of IRF1 and IRF2 (and β-actin as loading control) in DC3.2 lines in the absence or presence of 2ng/mL IFNγ (top) or 5,000U/mL IFNα (bottom) for the durations indicated.

To test this, we stimulated the DC3.2 with IFNγ and checked IRF1 and IRF2 binding to the TAP2, ERAP1, and PD-L1 promoters. We found that IFNγ induces IRF1 expression, which causes IRF1 to compete with IRF2 for these promoters, ultimately displacing it from them (Fig. 4.4a). To better characterize the IRF1 vs. IRF2 regulated expression changes more globally, we performed RNA-seq on the single and double knockout DC3.2 lines under basal conditions (Fig. 4.4b, Table 4.1) or after adding IFNγ (Fig. 4.4c, Table 4.2). From this analysis, several genes known to be important for antigen presentation and immune cell function were identified (Tables 4.1 and 4.2). Furthermore, this analysis showed that genes influenced by IRF1 and IRF2 could be grouped into multiple classes. Under basal conditions, there was a subset of antigen presentation-related genes whose expression was activated by IRF2 (e.g., TAP2, ERAP1), others that were repressed by IRF2 and remained so in the double knockouts (e.g., H2-T9), and yet others that were repressed by IRF2 but did not remain so in the double knockouts (e.g., PSMB8, PSMB10) (Fig. 4.4b). After stimulating with IFNγ, some genes were primarily activated by IRF1 (e.g., PSME1, PSME2, PSMB9), others were primarily repressed by IRF2 (e.g., PD-L1), and yet others were activated by both IRF1 and IRF2 (e.g., TAP2, ERAP1) (Fig. 4.4c). Collectively, these studies demonstrate that while some genes are acted on antagonistically by IRF1 and IRF2, other genes are regulated synergistically by these two transcription factors and that the relative contributions of IRF1 vs. IRF2 in mediating these expression changes varies depending on the inflammatory state of the cell.

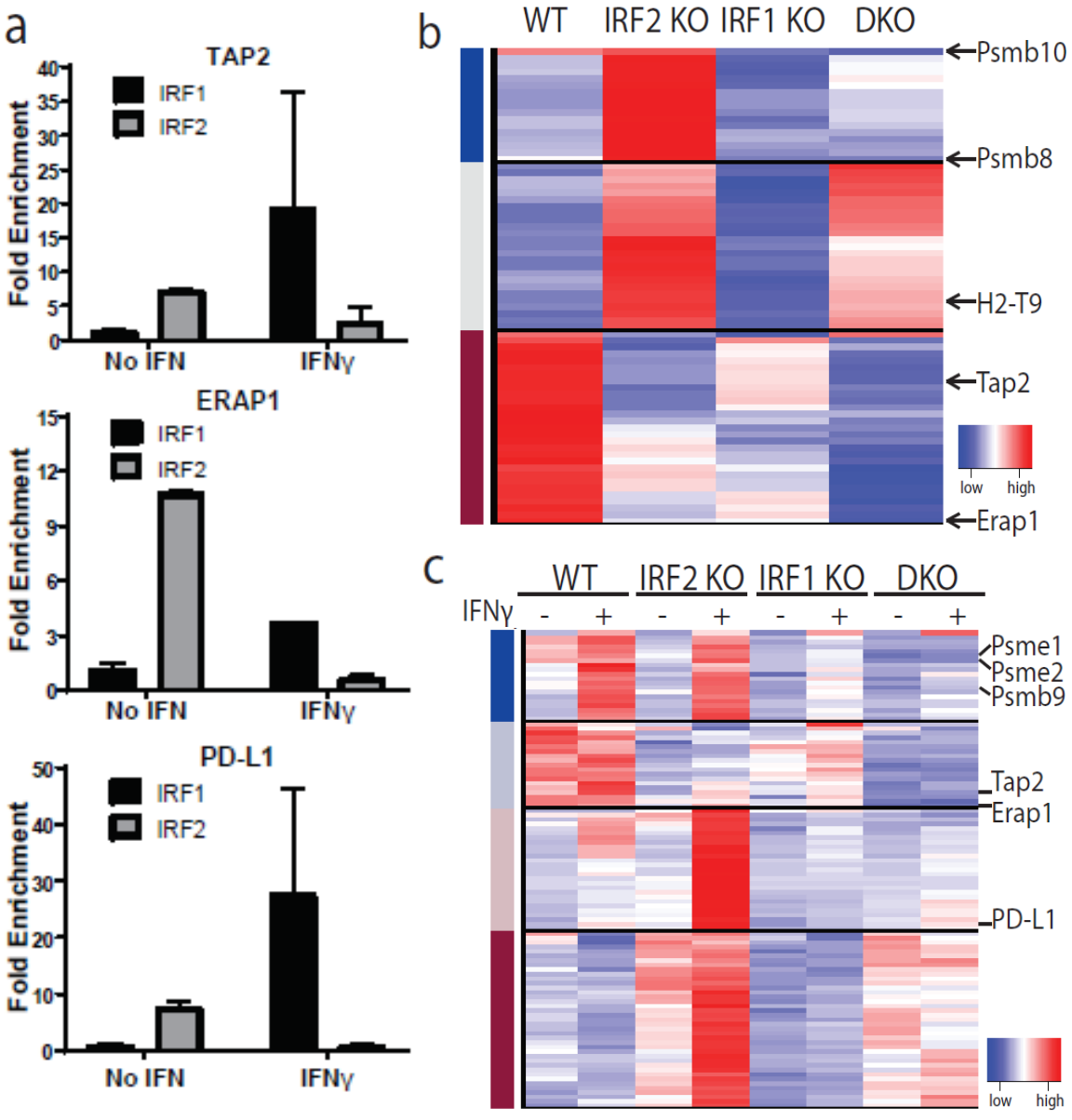

Figure 4.4. IRF1/IRF2-mediated gene regulation in DC3.2

(a) ChIP-qPCR of DC3.2 WT cells stimulated with ± 2ng/mL IFNγ for 2hrs for TAP2 (top), ERAP1 (middle), or PD-L1 (bottom) DNA with rabbit anti-IRF2 IgG, rabbit anti-IRF1 IgG, or normal rabbit IgG (control). Bars represent mean + SEM fold enrichment ($2^{\wedge-\Delta Ct}$) over the normal rabbit IgG control IP (N=2). (b, c) Heatmap of genes differentially expressed between the DC lines (b) at baseline or (c) after stimulation with ± 2ng/mL IFNγ for 2hrs. For clarity, only a few genes are shown, and all are listed in Tables 4.1 and 4.2.

Table 4.1. RNA-Seq differentially expressed genes in DC3.2 WT, IRF1 KO, IRF2 KO, and double KO under basal conditions. Genes listed below in the order shown in the heatmap in Figure 4.4b.

Cluster 1 (Blue)	**Cluster 2 (Grey)**	**Cluster 3 (Red)**
Psmb10	Lepre1	C1qa
Tspan13	Cry1	Arg1
Ly6a	Gmcl1	Arg2
H2−T22	Lrp10	Parp14
Gbp11	Tm6sf1	Casp7
Irg1	Glipr2	Nmi
Gbp6	mmu−mir−155*	Ddx58
Mx2	Socs1	Tap2
Rsad2	Scimp	Epsti1
Ifi47	Tnfsf13b	Acadl
Irgm2	Entpd1	Gsdmd
Trafd1	Tmem140	Thbs1
Tgtp2	Gbp4	Isg20
Ifit1	Cd40	Trim30a
Cmpk2	Gbp5	Isg15
Igtp	Gbp2	Il15ra
Psmb8	Cst7	Ifitm3
	Hck	Psmb9
	Fgl2	Sp110
	Gbp8	Psme2
	H2−T9	Cox6a2
	Flt1	Psme1
	Gbp3	mKIAA1554
	Gbp9	Pla2g2d
	Gbp7	Fabp7
		Ube2l6
		Ifi27
		Mov10
		Erap1

Table 4.2. RNA-Seq differentially expressed genes in DC3.2 WT, IRF1 KO, IRF2 KO, and double KO after ± IFNγ stimulation. Genes listed below in the order shown in the heatmap in Figure 4.4c.

Cluster 1 (Dark blue)	Cluster 2 (Light blue)	Cluster 3 (Light red)	Section 4 (Dark red)
C1qb	Egr2	Mx1	Dusp1
Trim30a	Lpin1	Phf11b	Flrt3
Rab19	Isg20	Usp18	Adora2b
Il15ra	AI427809	Psmb10	Rhof
Sp110	Arg2	Ifi203	Rab15
Psme1	Arg1	Dtx3l	Scimp
Psme2	Acadl	Gbp11	Sla2
Oasl2	Epsti1	Tgtp1	Tuba1a
Parp14	Nmi	Ifi47	Trem1
Samd9l	Mov10	Tgtp2	H2−T9
Ube2l6	Ifi27	Igtp	Cst7
Isg15	Gsdmd	Ifit3	Flt1
Psmb9	Casp7	Ifit1	H2−T22
Mndal	mKIAA1554	Gm14446	Tmem140
Fam26f	Ddx58	Gbp6	Herc6
Gm12250	Tap2	I830012O16Rik	Slc15a3
Iigp1	Slfn9	Cmpk2	Lysmd2
Mnda	Pla2g2d	Rsad2	Lrp10
Gm12185	Erap1	Mx2	Gmcl1
Parp9		Irg1	Tm6sf1
		Nos2	2810408M09Rik
		Gbp5	Lepre1
		Cd40	Cry1
		Gbp4	Pithd1
		Gbp8	Rab22a
		Cd274	Hdac2
		Gbp2	Traf1
			Ptgs2
			Vegfa
			Nfkbie
			Smim3
			Adam8
			Ets2
			mmu−mir−155*
			Tnfsf13b
			Gbp3
			Il1r2
			Gbp9
			Gbp7

IRF2 in cancer

Given that experimentally-induced loss of IRF2 both compromises MHC-I presentation and increases PD-L1 expression, it was of interest to see how often IRF2 is downregulated in primary cancers. We used the TIMER bioinformatics tool [170] to mine publicly available databases for IRF2 expression in primary human cancers. Remarkably, IRF2 was downregulated in several kinds of human cancers and the overall reductions were highly statistically significant (Fig. 4.5). For each of the IRF2-low cancers, which included invasive breast carcinoma, cholangiocarcinoma, colon adenocarcinoma, liver hepatocellular carcinoma, lung adenocarcinoma and squamous cell carcinoma (non-small cell lung cancers; NSCLCs), prostate, rectum and stomach adenocarcinomas, and uterine corpus endometrial carcinoma, a subset of patients had very low levels of IRF2.

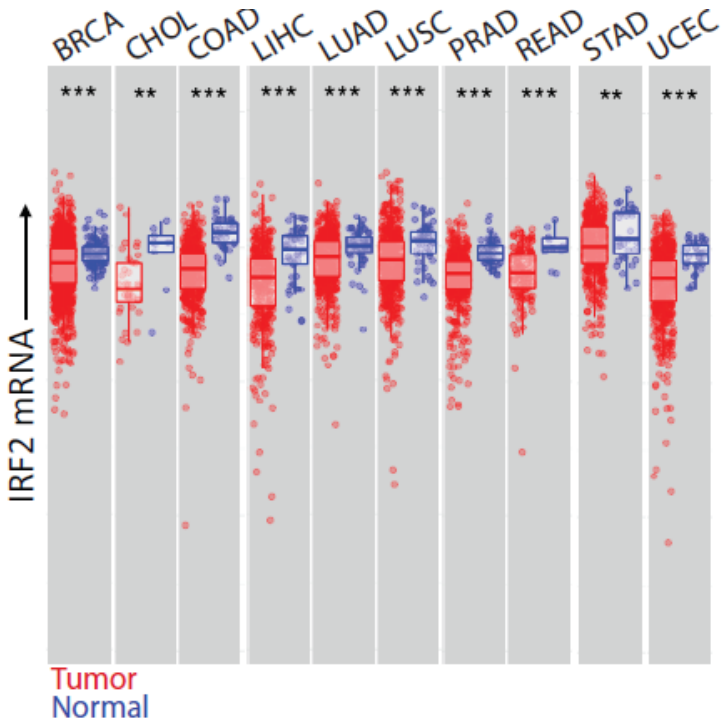

Figure 4.5. IRF2 expression in human tumors vs. normal tissues

Differential IRF2 expression in tumor and normal tissue from patients with the indicated cancer types (TCGA abbreviations), as queried from TIMER [170].

We chose one of the IRF2-low cancers, NSCLC, to determine whether IRF2 levels were functionally limiting in primary cancers. At our institution, NSCLCs are screened for PD-L1 expression by immunohistochemistry (IHC) at the time of diagnosis, which enabled us to randomly select tumors spanning a spectrum of PD-L1 expression. We extracted RNA from archival patient biopsy material and quantified expression of IRF2, TAP2, and ERAP1 by qPCR. In these lung cancers, IRF2 mRNA levels and PD-L1 IHC status were significantly inversely correlated (Fig. 4.6a). Additionally, consistent with our cell line findings, TAP2 and ERAP1 mRNA levels positively and significantly correlated with IRF2 mRNA levels (Fig. 4.6b). To formally test cause and effect for these correlations, we analyzed a human NSCLC cell line, A549, that is IRF2-low relative to other NSCLCs tested in the NCI-60 panel [171]. A549 cells are also MHC-I-low and PD-L1-positive [172, 173]. Eliminating the residual IRF2 in A549 cells by CRISPR-Cas9-mediated knockout further decreased surface MHC-I but did not further increase surface PD-L1 (Fig. 4.7a). In contrast, restoring IRF2 by transfection repressed surface PD-L1 expression and increased surface MHC-I expression (Fig. 4.7a). Stimulation of A549 with IFNγ augments both surface MHC-I and PD-L1 expression, as expected, but transfection of IRF2 still has the same pattern of effects as without IFN (repressing PD-L1 and further increasing MHC-I expression) (Fig. 4.7b). To further generalize these findings, we analyzed two human breast cancers, two mouse sarcomas, and a mouse lymphoma and found similar results (Fig. 4.8).

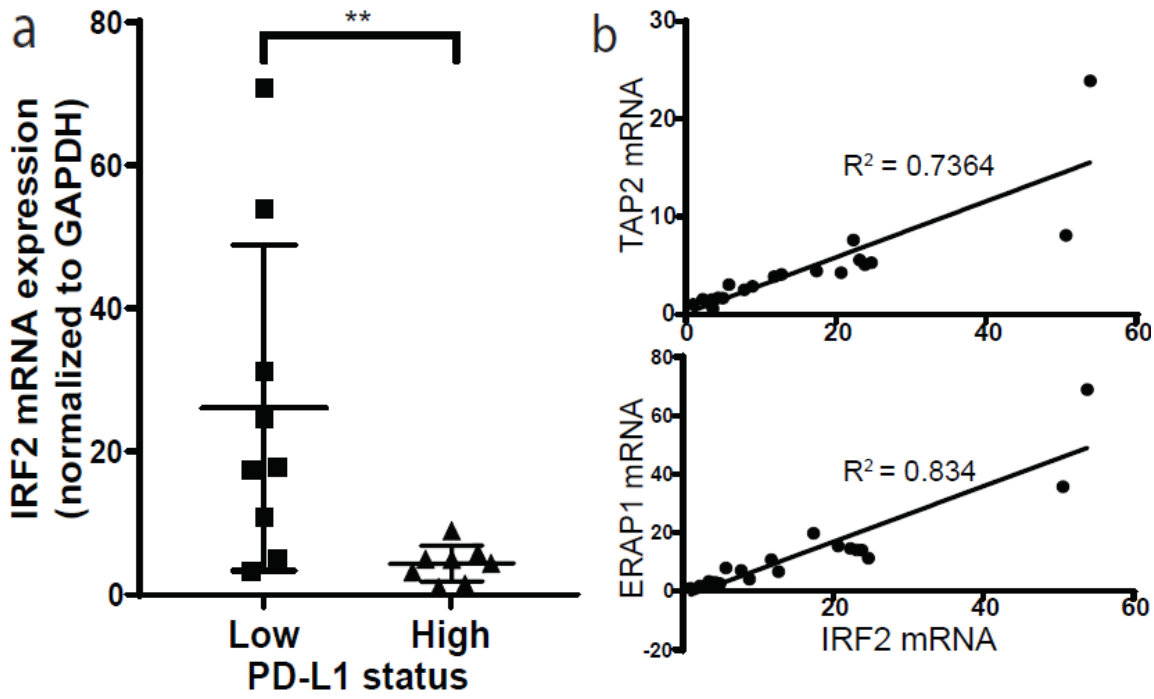

Figure 4.6. IRF2 in human NSCLC biopsies

(a) IRF2 mRNA expression in patient NSCLC specimens scored as PD-L1 low (1-50%) or high (>50%) by immunohistochemistry. IRF2 mRNA expression was normalized to GAPDH mRNA expression in each lung specimen and then IRF2 expression across specimens was compared by calculating fold changes over the lowest IRF2-expressing specimen, which was set as equal to 1. Statistical analysis by Mann-Whitney U test, **p<0.01; (b) TAP2 (top) and ERAP1 (bottom) mRNA correlations with IRF2 mRNA in NSCLC specimens. Linear regression models shown with R^2 for goodness of fit.

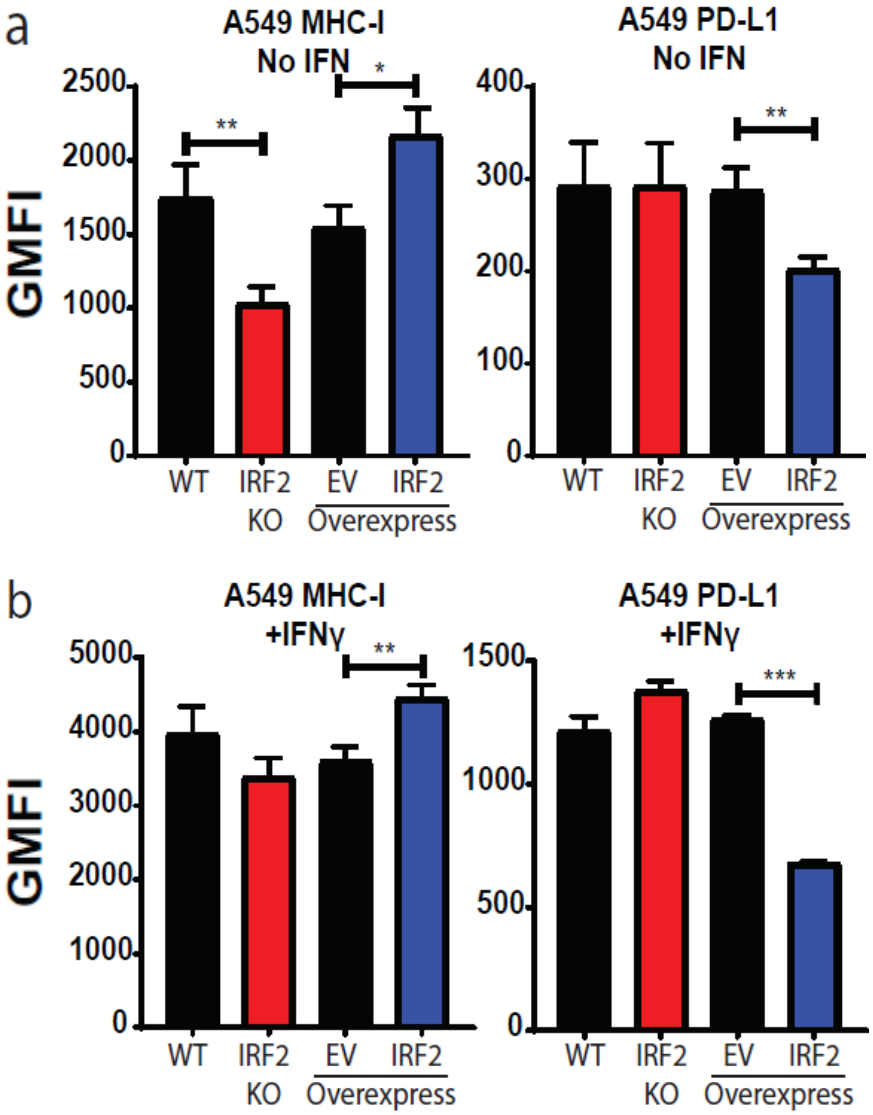

Figure 4.7. Surface MHC-I and PD-L1 expression on A549 lines

(a, b) Geometric MFI of surface MHC I (left) and PD-L1 (right) on (a) unstimulated or (b) overnight IFNγ-stimulated A549 lines knocked out for IRF2 ("IRF2 KO") or control ("WT") or overexpressing IRF2 or empty vector (EV) as control. Bars represent mean + SEM (N=3). Statistical analysis by two-tailed ratio paired t-tests. *p<0.05, **p<0.01, ***p<0.001

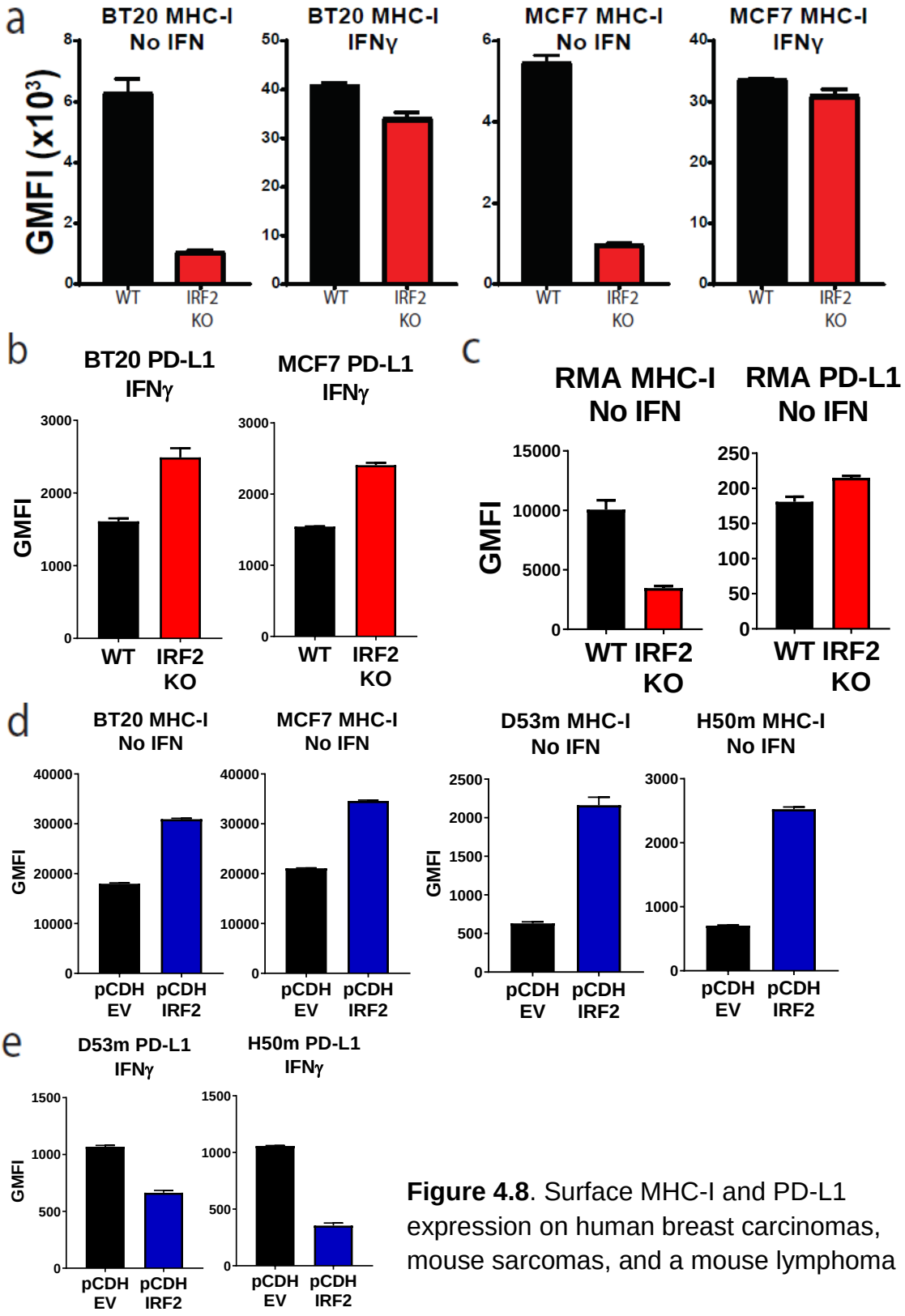

Figure 4.8. Surface MHC-I and PD-L1 expression on human breast carcinomas, mouse sarcomas, and a mouse lymphoma

Figure 4.8. Surface MHC-I and PD-L1 expression on human breast carcinomas, mouse sarcomas, and a mouse lymphoma

(a-e) Geometric MFI of (a) surface MHC-I on unstimulated or overnight IFNγ-stimulated human breast carcinoma (BT20 and MCF7) lines knocked out for IRF2 (“IRF2 KO”) or control (“WT”); (b) surface PD-L1 on IFNγ-stimulated BT20 and MCF7 knockout lines; (c) surface MHC-I (left) or surface PD-L1 (right) on unstimulated RMA lymphoma knockout lines; (d) surface MHC-I on (left) unstimulated BT20 and MCF7 lines or (right) unstimulated D53m and H50m mouse sarcoma lines overexpressing IRF2 (pCDH IRF2) or empty vector control (pCDH EV); and (e) surface PD-L1 on IFNγ-stimulated D53m and H50m overexpression lines. Representative experiments shown, error bars represent staining of technical replicates.

The effects of IRF2 loss on antigen presentation and checkpoint inhibition are predicted to make it harder for $CD8^+$ T cells to kill IRF2-low cells. To test this and quantify the magnitude of the effect, we analyzed mouse wild-type vs. IRF2-KO lymphoma (RMA) cell lines. RMA cells were chosen because they are known to be very good targets for cytotoxic T cell killing assays (and are, therefore, a stringent test) and express H2-K^b, which allows the use of potent $CD8^+$ T cell effectors from the H2-K^b-S8L-specific TCR transgenic OT-I model. Pre-activated OT-I effectors were cultured with pairs of wild-type or IRF2-KO cells that were S8L-pulsed or not and labeled with different amounts of the dye CFSE. After 4 hours, specific killing was quantified by flow cytometry and was found to be significantly lower in the IRF2-KO RMA, as compared to the wild-type RMA (Fig. 4.9), demonstrating that tumor cells lacking IRF2 are harder for $CD8^+$ T cells to eliminate. Taken together, these findings show that IRF2 downregulation leads to immune evasion and that there are several types of human cancers which may use this escape mechanism.

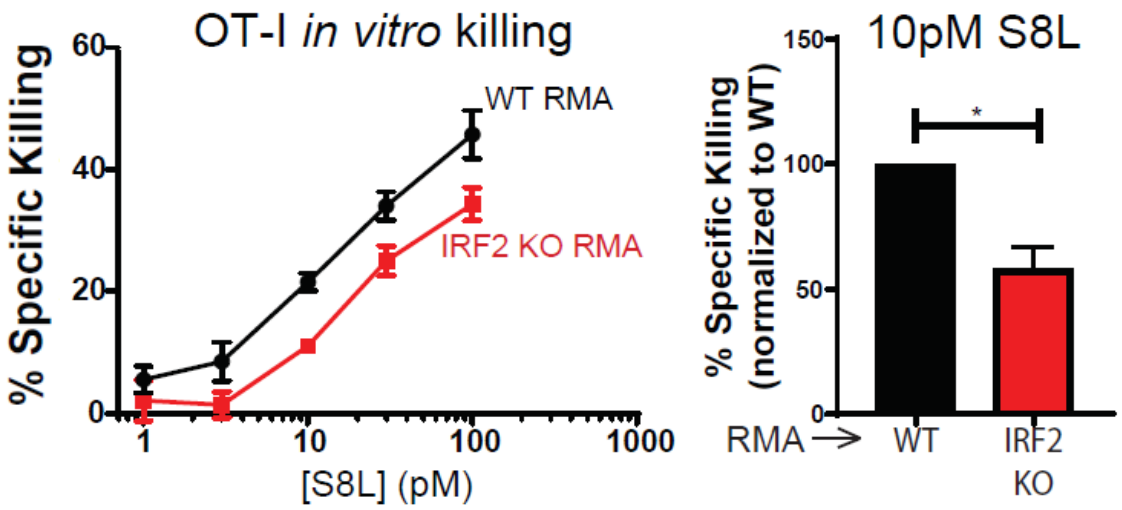

Figure 4.9. OT-I *in vitro* killing of RMA lines

Pre-activated OT-I effectors were cultured with pairs of wild-type ("WT RMA") or IRF2 KO ("IRF2 KO RMA") cells that were S8L-pulsed or not and labeled with different amounts of the dye CFSE. After 4 hours, specific killing was quantified by flow cytometry. (Left) % specific killing dose-titration curve for one representative experiment using an effector to target ratio of 1:2 and [S8L] indicated, points show mean ± SD of technical triplicates; (Right) % specific killing of IRF2 KO RMA relative to that of WT RMA at 10pM S8L; bars show mean + SEM (N=4). Statistical analysis by two-tailed ratio paired t-test, *p<0.05.

Summary

Here, we found that many cancers of diverse origins (NSCLC, breast, colorectal, liver, stomach, prostate, uterine) downregulate IRF2 expression, which is not essential for viability in fully differentiated cells. As a result of losing IRF2, tumor cells not only decrease their surface MHC-I expression, but also increase their surface PD-L1 expression. Thus, loss of a single gene can generate a “double whammy” for the immune system as it enables tumor cells lacking IRF2 to become both harder to identify (loss of MHC-I antigen presentation) and better able to suppress T cell-mediated elimination (increased checkpoint inhibition). As shown in our *in vitro* cytotoxicity assay, the loss of IRF2 renders such tumor cells more difficult for $CD8^+$ T cells to kill. These findings have implications for cancer progression and immunotherapy, which will be discussed further in Chapter VI.

Chapter V: Other novel genes from MHC-I screens

Attributions and Copyright Information

The data described in Chapter V are unpublished. The cross-presentation siRNA screen was conducted by Freidrich Cruz. Subsequent validation of gene hits and all other experiments described in this chapter were performed by me (B.A.K.) and analyzed with Kenneth L. Rock.

Chapter V: Other novel genes from MHC-I screens

Introduction

Prior to my time in the Rock Lab, a forward-genetic screen was conducted in mouse dendritic cells to identify novel genes affecting cross-presentation [174]. As detailed above, cross-presentation and classical MHC-I presentation share much of the same machinery, particularly if antigen is processed via the phagosome-to-cytosol pathway. Because I was interested in identifying new genes important for both cross-presentation and classical MHC-I presentation, I analyzed the results of this screen to select genes that, based on their expression in various tissues and what was already known in the literature about their subcellular localizations and functions, might also impact the classical MHC-I pathway. Among these genes were a couple co-chaperones that were of particular interest to me because of the unresolved role of chaperones in classical MHC-I presentation.

As mentioned in Chapter I, the heat-shock protein (HSP) chaperone Hsp70 has been reported to affect cross-presentation but the mechanisms by which it may facilitate classical MHC-I presentation are not well understood. Hsp70 never works alone – its ability to bind and release client proteins is regulated by two groups of co-factors, J proteins (co-chaperones also known as DnaJs or Hsp40s) and nucleotide exchange factors (NEFs) [175-177]. J proteins stimulate Hsp70's ATPase activity, thereby promoting client capture; NEFs stimulate dissociation of

ADP, thereby facilitating client release from Hsp70 [178]. J proteins are widely believed to drive the multi-functionality of Hsp70, in part because of the large structural diversity among J proteins [178]. Humans have 41 different J proteins, but outside of the J domain (the part of the J protein that interacts with Hsp70), any two randomly selected J proteins may be quite dissimilar. Historically, the J proteins have been divided into three classes – A, B, and C [179, 180]. Class A proteins have an N-terminal J domain, a glycine/phenylalanine-rich region, a zinc finger-like region (ZFLR), and a C-terminal extension that can bind client proteins [181]. The major distinctions among the classes are that class B proteins lack the ZFLR found in class A and that class C proteins do not fit into either class A or class B. Despite this classification, J proteins within each class have tremendous diversity in both structure and function, including their ability (or lack thereof) to bind client proteins. It is possible, therefore, that Hsp70's function in antigen presentation may be driven, in part, by one or more J proteins. It is also possible that, since some J proteins have functions that are Hsp70-independent [182], the J proteins identified in this cross-presentation screen may exert their functions in an Hsp70-independent manner.

For the cytosolic co-chaperone "hit," Dnajb4, we were interested in addressing the question of whether chaperones preferentially protect proteasome-generated peptides containing MHC-I epitopes. The majority of peptides made by the proteasome are rapidly destroyed by cytosolic peptidases [183] yet some peptides manage to avoid the peptidases and translocate into the

ER via TAP. It is unknown whether this “survival” is a selective process whereby chaperones protect peptides and shuttle them to TAP or whether it is purely stochastic. For the ER-localized co-chaperone “hit,” Dnajc10, which is known to play a role in ER-associated degradation (ERAD) [184], we wondered whether it may translocate peptide precursors through the ERAD pathway and/or whether it may be involved in folding members of the peptide-loading complex. Below, I will document our preliminary findings on these two J proteins.

Results

J proteins and MHC-I antigen presentation

In our lab’s genome-wide DC3.2 cross-presentation screen [174], each mouse gene was silenced for 48 hours with a pool of four mouse siRNAs. After silencing, the cells were incubated with OVA-coated iron-oxide beads and OVA-peptide-specific $CD8^+$ T cells or $CD4^+$ T cells overnight to assess cross-presentation or MHC-II presentation, respectively. siRNAs targeting β2m or $I\text{-}A^b$ were used as positive or negative controls of cross-presentation, respectively, and as negative or positive controls of MHC-II presentation, respectively. This setup allowed us to identify genes which uniquely regulate the MHC-I pathway (and not those which are simply necessary for cell viability). In the screen, silencing Dnajb4 or Dnajc10 decreased cross-presentation by 77% or 55%, respectively (and did not decrease MHC-II presentation). To validate these results, we repeated the DC3.2 cross-presentation assay and found similar

results (Fig. 5.1a). Additionally, when we tested each of the four siRNAs from the siRNA pools individually, we found that multiple independent siRNAs targeting Dnajb4 (Fig. 5.1b) or Dnajc10 (Fig. 5.1c) produced the same effects.

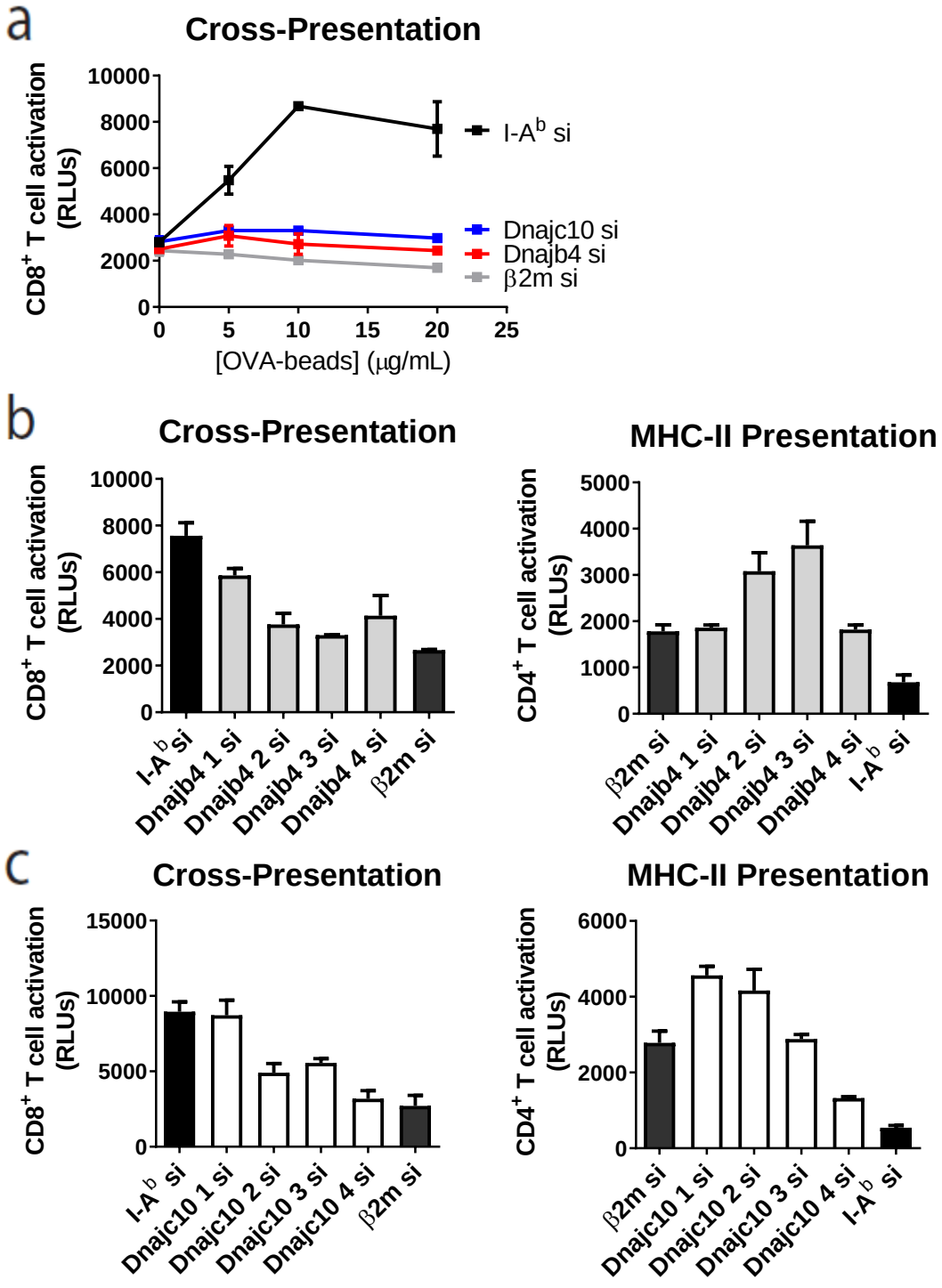

Figure 5.1. Knockdown of Dnajb4 or Dnajc10 reduces cross-presentation

Figure 5.1. Knockdown of Dnajb4 or Dnajc10 reduces cross-presentation

(a) $CD8^+$ T cell activation (relative luciferase units; RLUs) following addition of OVA-beads at the indicated concentrations and $CD8^+$ T cells to the DC3.2 silenced for 48 hours with siRNA pools targeting Dnajb4, Dnajc10, β2m (positive control) or $I\text{-}A^b$ (negative control); (b-c) T cell activation (RLUs) following the addition of 20µg/mL OVA-beads and $CD8^+$ T cells (left) or 2µg/mL OVA-beads and $CD4^+$ T cells (right) to the DC3.2 silenced for 48 hours with individual siRNAs targeting β2m or $I\text{-}A^b$ (controls) or (b) Dnajb4 or (c) Dnajc10. Representative experiments shown, error bars represent SD of technical replicates.

Next, we wanted to examine whether Dnajb4 or Dnajc10 could also affect classical MHC-I presentation. To test whether these J proteins act downstream of phagosome-to-cytosol antigen translocation, we used DC3.2 cells that express non-secretable OVA (NS-OVA) under a doxycycline-inducible promoter, which allows the OVA antigen to be made in the cytosol instead of requiring the internalization step necessary for the OVA-beads. As expected given the subcellular localizations of these J proteins, siRNA targeting either Dnajb4 or Dnajc10 reduced SIINFEKL-H2-K^b presentation on these cells (Fig. 5.2a). Next, to test whether Dnajb4 and Dnajc10 act upstream or downstream of the proteasome, we used a DC3.2 line that expresses ubiquitin-SIINFEKL (Ub-S8L) in the cytosol upon doxycycline induction. Unlike ovalbumin, Ub-S8L does not require any proteasomal processing; ubiquitin cleavage by a deubiquitinating enzyme can generate the mature MHC-I epitope. In these cells, silencing Dnajb4 or Dnajc10 reduced SIINFEKL-H2-K^b presentation (Fig. 5.2b), indicating that both J proteins act on the MHC-I pathway downstream of the proteasome.

To further evaluate the contributions of these genes to the classical MHC-I pathway, we checked surface MHC-I levels on DC3.2 (Fig. 5.2c) and 3T3-K^b fibroblasts (Fig. 5.2d) after siRNA treatment. Knocking down Dnajb4 or Dnajc10 decreased surface MHC-I levels but did not decrease surface expression of MHC-II (Fig. 5.2c) or CD71 (Fig. 5.2d), again showing selectivity in the effects of these J proteins. We also tested the effects of silencing Dnajb4 or Dnajc10 on 3T3-K^b presentation of SIINFEKL-H2-K^b complexes following transient OVA

transfection (Fig. 5.2e), constitutive NS-OVA expression (Fig. 5.2f), or induced expression of Ub-S8L (Fig. 5.2g). As opposed to dendritic cells, these fibroblasts are not professional APCs but still require and perform classical MHC-I presentation. Surprisingly, although silencing Dnajc10 strongly reduced MHC-I presentation in all three systems, silencing Dnajb4 only minimally affected it (Fig. 5.2e-g), suggesting that the requirement of Dnajb4 for controlling MHC-I presentation may be cell-type dependent.

We also acquired Dnajc10-knockout mouse embryonic fibroblasts (MEFs) (Fig. 5.2h) [185] and found that they too have impaired surface MHC-I expression (Fig. 5.2i) and MHC-I presentation of cytosolic OVA (Fig. 5.2j) as compared to the control MEFs, thus confirming the Dnajc10 phenotype observed in the siRNA studies. Overall, our results demonstrated that Dnajb4 and Dnajc10 affect both cross-presentation and classical MHC-I presentation. However, because the Dnajc10 findings were more robust, we decided to focus our additional characterization studies solely on Dnajc10.

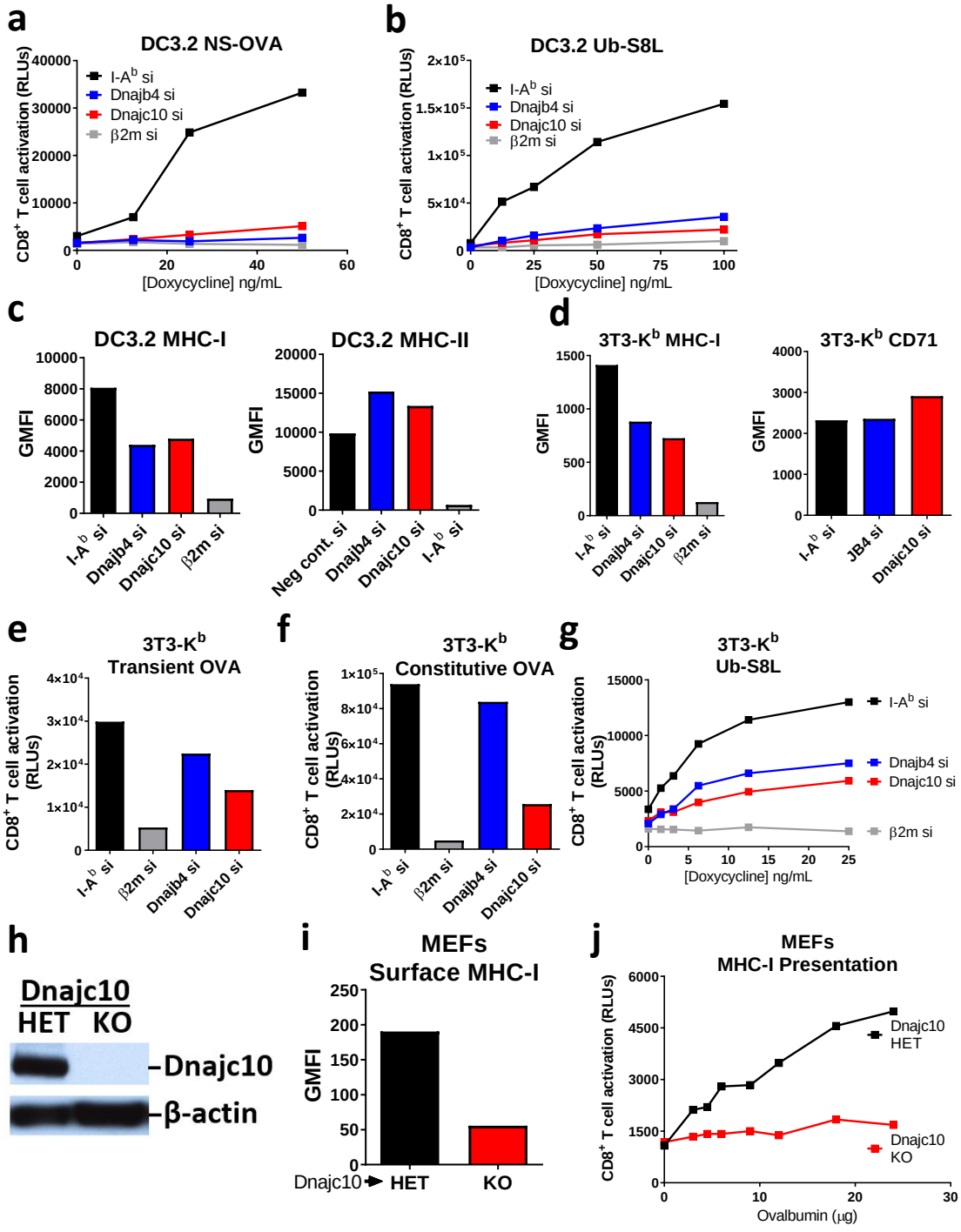

Figure 5.2. Dnajb4 and Dnajc10 affect classical MHC-I presentation

Figure 5.2. Dnajb4 and Dnajc10 affect classical MHC-I presentation

(a-b) $CD8^+$ T cell activation (relative luciferase units; RLUs) following endogenous expression (via 2 hours of doxycycline induction) of (a) non-secretable OVA (NS-OVA) or (b) ubiquitin-SIINFEKL (Ub-S8L) in DC3.2 cells after 48 hour siRNA knockdown of Dnajb4, Dnajc10, β2m (positive control) or I-A^b (negative control); (c) Geometric MFI of surface MHC-I (left) or MHC-II (right) on DC3.2 cells 48 hours after siRNA knockdown; (d) Geometric MFI of surface MHC-I (left) or CD71 (right) on 3T3-K^b after siRNA knockdown; (e-g) $CD8^+$ T cell activation (RLUs) following (e) 24 hour transient transfection of CD16-OVA in 3T3-K^b cells silenced for 48 hours, (f) 48 hour siRNA knockdowns in a stable 3T3-K^b line constitutively expressing non-secretable OVA, or (g) endogenous expression (via 2 hours of doxycycline induction) of Ub-S8L in 3T3-K^b cells after 48 hour siRNA knockdowns; (h) Western blot of Dnajc10 or β-actin (as loading control) in the mouse embryonic fibroblasts (MEFs) derived from Dnajc10 heterozygous (HET) or knockout (KO) mice; (i) Geometric MFI of surface MHC-I on Dnajc10 HET or KO MEFs; and (j) $CD8^+$ T cell activation (RLUs) following cytosolic loading of the indicated concentrations of OVA (using PULSin [186]) into Dnajc10 HET or KO MEFs. (a-j) Representative experiments are shown.

Dnajc10 and its binding partners

Given the pronounced phenotype observed in the Dnajc10-deficient cells, we wanted to examine this ER-resident co-chaperone further and identify how and to which client proteins it binds. The Dnajc10 protein sequence encodes for an N-terminal ER signal peptide followed by a J domain, four thioredoxin-like (Trx) motifs, and a C-terminal ER-retention (KDEL) motif. Within the J domain lies a histidine-proline-aspartic acid (HPD) motif which is essential for functional interaction between the J protein and Hsp70 [187]. To test whether Dnajc10 exerts its effects in an Hsp70-dependent manner, we created a mutant Dnajc10 construct which possesses a histidine to glutamine point mutation at its 63rd residue (H63Q), thereby abrogating its interaction with the ER-resident Hsp70, BiP [185, 187]. When we induced the expression of either wild-type (WT) Dnajc10 or the H63Q Dnajc10 mutant in Dnajc10-KO MEFs (Fig. 5.3a), surface MHC-I levels increased (Fig. 5.3b), indicating that Dnajc10 can affect surface MHC-I expression in a BiP-independent manner.

To determine whether Dnajc10 affects MHC-I presentation by reducing another protein in the ER, we mutated its Trx motifs. Each of these Trx motifs (C-XX-C) contains an N-terminal cysteine which forms a mixed disulfide with its substrate and a C-terminal cysteine which releases the substrate by attacking the intermolecular disulfide bond [188]. To this end, we created two new Dnajc10 constructs, one where all four Trx motifs were changed from C-XX-C to A-XX-A (4X-AA), thereby preventing Dnajc10 from reducing its substrate, and one where

all four Trx motifs were changed from C-XX-C to C-XX-A (4X-CA), thereby keeping Dnajc10 bound to its substrate [185]. Overexpression of the 4X-AA construct only slightly increased surface MHC-I levels, as compared to overexpression of the 4X-CA construct (Fig. 5.3c), suggesting that Dnajc10 mediates its effects on MHC-I presentation by reducing another protein in the ER. We also made a number of other Dnajc10 constructs (Table 5.1) to pinpoint which specific Trx motif(s) were responsible for binding client proteins in the context of MHC-I presentation, in the hopes that we could then use these constructs to identify Dnajc10's redox partners. Unfortunately, despite several approaches to increase the signal to noise ratio of our assay (e.g., acid-stripping, ± IFNγ, time/dose titrations of doxycycline-induction, switching constructs to constitutive expression vectors, changing cell lines, and examining SIINFEKL-H2-K^b rather than all H2-K^b), we were unable to get sufficient resolution to be able to draw conclusions about which Dnajc10 Trx motifs are contributory to MHC-I presentation.

In order to probe whether Dnajc10 physically interacts with known members of the MHC-I peptide-loading complex, we overexpressed Dnajc10 in the Dnajc10-KO MEFs. We then immunoprecipitated Dnajc10 and blotted for some known MHC-I pathway components. Blotting for Dnajc10 and BiP (positive controls) revealed that both were present in the immunoprecipitated eluate whereas β-actin (negative control) did not associate with the ER-resident Dnajc10 (Fig. 5.3d). One limitation of these studies was the quality of antibodies

at our disposal, but we could clearly see that β2m does not associate with Dnajc10 (Fig. 5.3d). Of the other proteins tested (MHC-I heavy chain, TAP1, ERp57, and calreticulin), we did not observe any apparent interactions with Dnajc10.

Table 5.1. Dnajc10 constructs

Name	HPD	Trx1	Trx2	Trx3	Trx4
WT	HPD	CXXC	CXXC	CXXC	CXXC
H63Q	QPD	CXXC	CXXC	CXXC	CXXC
4X-CA	HPD	CXXA	CXXA	CXXA	CXXA
4X-AA	HPD	AXXA	AXXA	AXXA	AXXA
AA1	HPD	AXXA	CXXC	CXXC	CXXC
AA2	HPD	CXXC	AXXA	CXXC	CXXC
AA3	HPD	CXXC	CXXC	AXXA	CXXC
AA4	HPD	CXXC	CXXC	CXXC	AXXA
CA1	HPD	CXXA	AXXA	AXXA	AXXA
CA2	HPD	AXXA	CXXA	AXXA	AXXA
CA3	HPD	AXXA	AXXA	CXXA	AXXA
CA4	HPD	AXXA	AXXA	AXXA	CXXA
CC1	HPD	CXXC	AXXA	AXXA	AXXA
CC2	HPD	AXXA	CXXC	AXXA	AXXA
CC3	HPD	AXXA	AXXA	CXXC	AXXA
CC4	HPD	AXXA	AXXA	AXXA	CXXC

The HPD motif is part of Dnajc10's J domain and is necessary for functional Hsp70-Dnajc10 interaction. The four thioredoxin-like (Trx) motifs consist of two cysteines (C) flanking two other amino acids (X). When both cysteines are mutated to alanines (A), the Trx motif cannot reduce its substrate. When only the second cysteine is mutated to alanine, the client protein remains trapped by a disulfide linkage to Dnajc10 at that Trx motif.

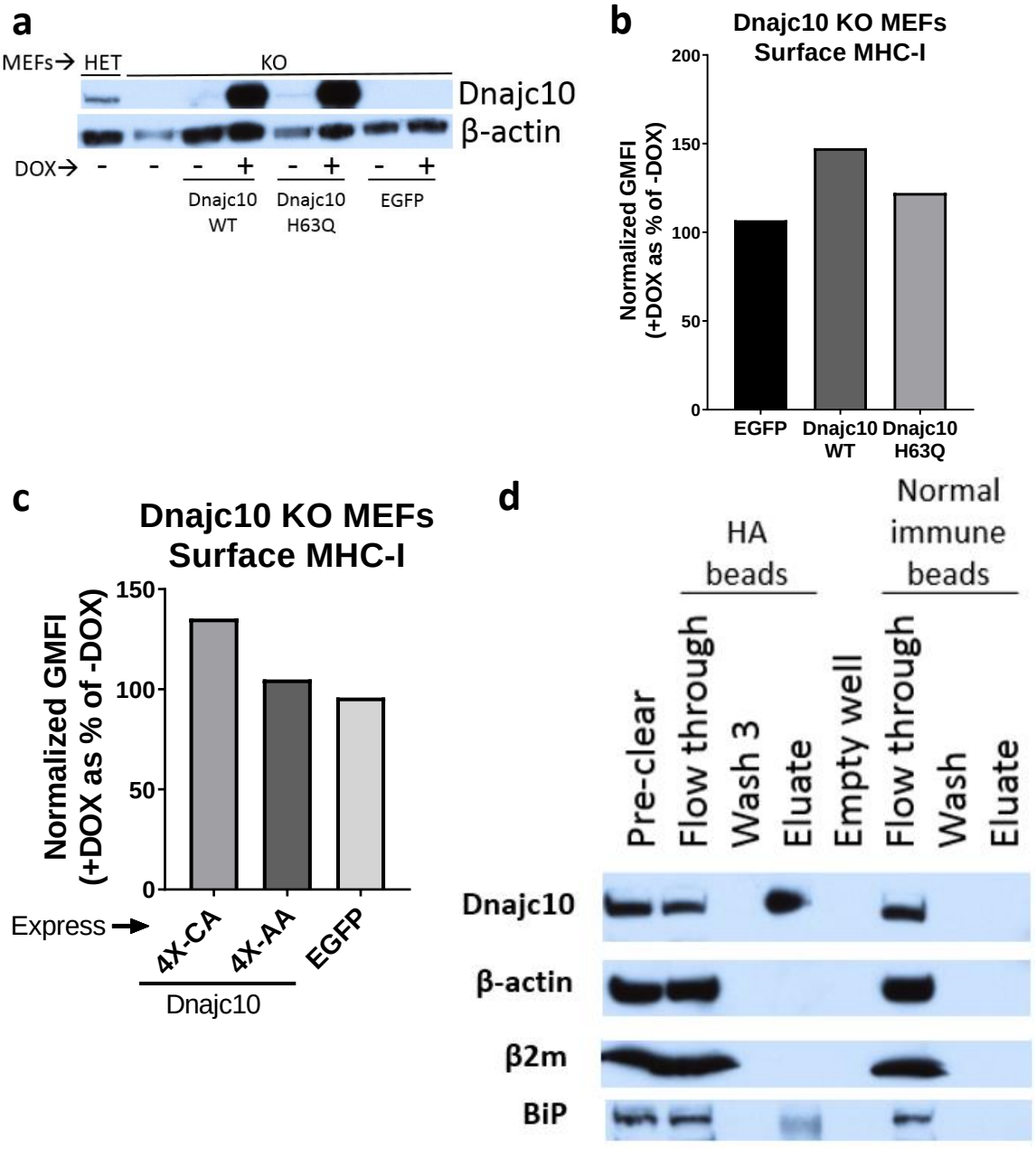

Figure 5.3. Dnajc10's thioredoxin-like motifs mediate its effects on MHC-I presentation

Figure 5.3. Dnajc10's thioredoxin-like motifs mediate its effects on MHC-I presentation

(a) Western blot of Dnajc10 KO MEFs ± doxycycline (DOX)-inducible overexpression of Dnajc10 WT, Dnajc10 H63Q, or EGFP for Dnajc10 protein expression and β-actin as control. Untransduced Dnajc10 heterozygous (HET) and knockout (KO) MEFs were run in parallel as controls; (b-c) Normalized MFI of surface MHC-I on Dnajc10 KO MEFs ± DOX-inducible overexpression of (b) Dnajc10 WT, Dnajc10 H63Q, or EGFP, or (c) Dnajc10 4X-CA, Dnajc10 4X-AA, or EGFP; (d) Immunoprecipitation of HA-tagged Dnajc10 by anti-HA or normal immune IgG followed by blotting with anti-Dnajc10, anti-β-actin, anti-β2m, or anti-BiP. Representative experiments are shown.

Dnajc10 in primary cells

We also acquired Dnajc10-knockout mice [137] in order to evaluate the biological significance of this co-chaperone on MHC-I presentation in primary cells. Surprisingly, despite our cell line data showing a low MHC-I phenotype in both Dnajc10-knockdown and knockout cells and a high MHC-I phenotype upon Dnajc10 overexpression, we did not observe any MHC-I deficits in the mice constitutively lacking Dnajc10. We examined surface MHC-I and MHC-II expression (Fig. 5.4a) and cross-presentation (Fig. 5.4b) on bone marrow-derived dendritic cells as well as surface MHC-I and MHC-II expression on splenocytes (Fig. 5.4c) and found no significant differences between the Dnajc10-knockouts and the wild-type controls. Because Dnajc10 does not appear to have a significant effect on MHC-I presentation in primary cells, we were swayed from pursuing this gene any further.

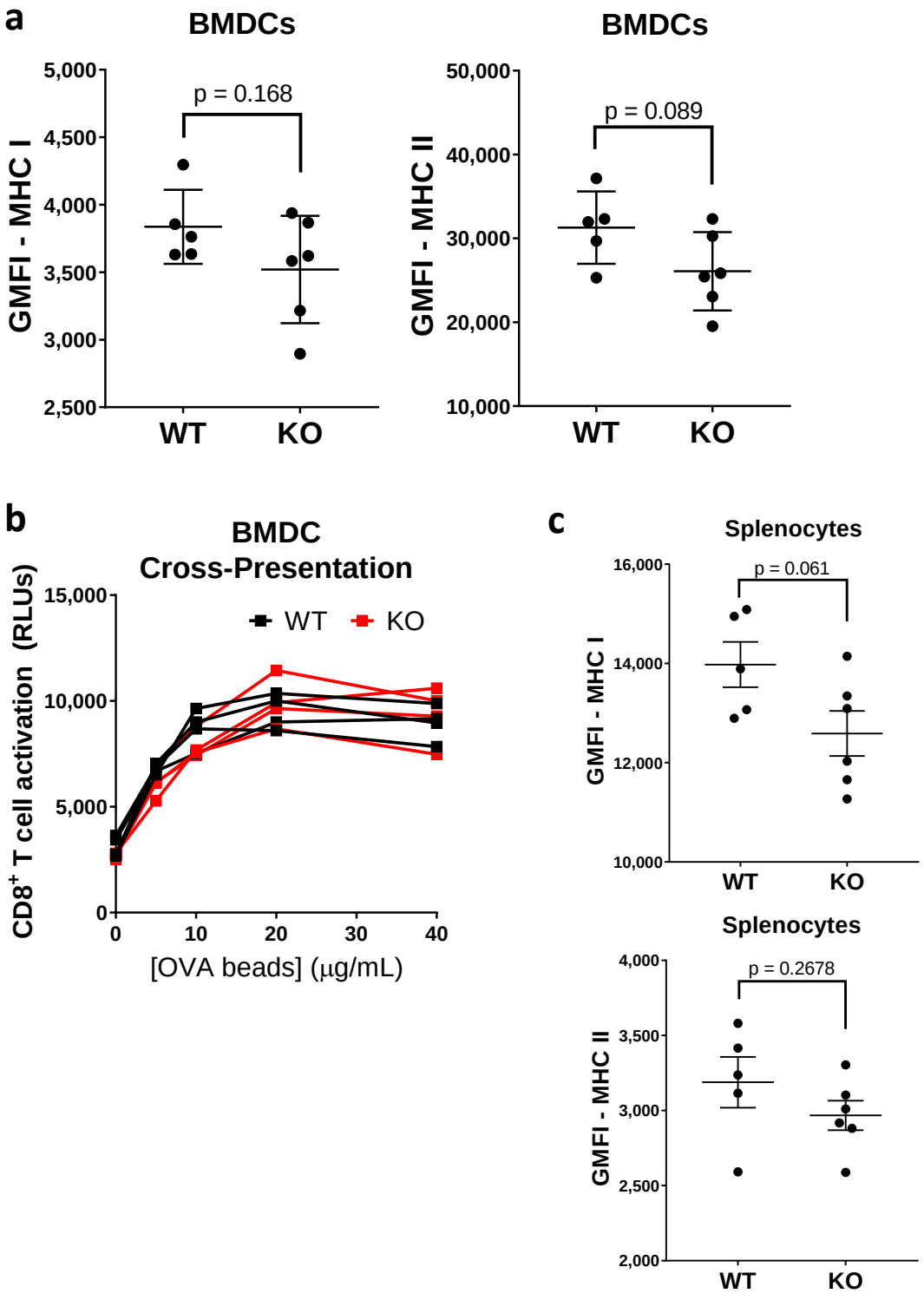

Figure 5.4. Dnajc10 *ex vivo* studies

Figure 5.4. Dnajc10 *ex vivo* studies

(a) Geometric MFI of surface MHC-I (left) or surface MHC-II (right) on wild-type (WT) or Dnajc10 knockout (KO) bone marrow-derived dendritic cells (BMDCs); (b) $CD8^+$ T cell activation (RLUs) following addition of OVA-beads at the indicated concentrations and $CD8^+$ T cells to WT or KO BMDCs. Lines represent independent mice; (c) Geometric MFI of surface MHC-I (top) or surface MHC-II (bottom) on wild-type (WT) or Dnajc10 knockout (KO) splenocytes. (a-c) Dots represent independent mice, statistical analysis by two-sided unpaired t-tests.

Summary

From our lab's forward-genetic screen, we identified two co-chaperones, Dnajb4 and Dnajc10, that strongly affect cross-presentation and classical MHC-I presentation, but not MHC-II presentation, in mouse dendritic cells. The effects of Dnajc10 on classical MHC-I presentation also extended to non-professional APCs (e.g., fibroblasts). Dnajc10's thioredoxin-like motifs mediate its effects on surface MHC-I levels by reducing a yet unidentified substrate. Moreover, in the absence of any functional interaction with BiP, Dnajc10 can still regulate MHC-I presentation. Where examined, primary cells lacking Dnajc10 do not have as strong of an MHC-I phenotype as was observed in the siRNA-treated cell lines; this will be discussed in greater detail in Chapter VI.

Chapter VI: Discussion

Chapter VI: Discussion

Transcriptional control of MHC-I presentation and PD-L1 expression by IRF2

The transcriptional control of many MHC-I pathway components, particularly under basal conditions, has not been well defined. In Chapter III, we identified IRF2 as a novel positive regulator of MHC-I antigen presentation and found that, under basal conditions, it is important for both classical MHC-I presentation and cross-presentation. Mechanistically, this is achieved by IRF2 binding the promoters of TAP2 and ERAP1 and transcriptionally activating their expression. In the absence of IRF2, cells express less TAP2 and ERAP1 and, due to the consequent defects in antigen transport and processing, present fewer peptide-MHC-I complexes at the cell surface. Additionally, IRF2 regulates the expression of other genes, such as immunoproteasome subunits, which likely also influence the MHC-I presentation in IRF2-deficient cells [189].

Analysis of IRF2-knockout cells also revealed that PD-L1 was highly upregulated under basal conditions. It is well-established that IRF1 can promote IFNγ-inducible activation of PD-L1 [168, 169] but the role of IRF2 on PD-L1 expression had not been thoroughly explored. Recently, Dorand et al. found that hyperphosphorylation of IRF2BP2 (an IRF2-binding protein) could lead to decreased PD-L1 expression after IFNγ stimulation [190]. Additionally, Wu et al. recently discovered that a loss of IRF2BP2 can lead to enhanced IRF2 binding to the PD-L1 promoter and that IFNγ stimulation releases IRF2 from the PD-L1

promoter [191]. In accordance with these findings, our ChIP-qPCR data shows that IFNγ stimulation leads to both increased IRF1 binding and decreased IRF2 binding to the PD-L1 promoter. Moreover, we found for the first time that in IFNγ-stimulated tumor cells, overexpression of IRF2 decreases surface PD-L1 levels. In addition, we discovered that under basal conditions, a loss of IRF2 significantly increases PD-L1 mRNA and surface expression and IRF2 overexpression produces the opposite effects. Collectively, these results establish the repressive role of IRF2 on PD-L1 expression in the absence and presence of IFNγ and reveal that unstimulated cells can upregulate PD-L1 expression if upstream regulatory factors, such as IRF2, are defective/absent.

IRF2 and immune evasion

Our findings that IRF2 both positively regulates the MHC class I pathway and negatively regulates PD-L1 expression have implications for cancer progression and immunotherapy. Cancers need to evade the immune system and, if they are immunogenic, require editing to escape and progress [157]. One of the ways that murine tumors can evade immune elimination is by downregulating the MHC-I pathway [154]. Similar immunoediting of this pathway occurs in humans as it has been found that tumors, which were predominantly MHC-I positive at early stages, subsequently become homogeneously MHC-I deficient [69, 72] and progressing cancers are frequently MHC-I deficient [192, 193]. Another way in which tumors can evade immune elimination is by expressing inhibitory

checkpoint molecules. Indeed, many human cancers upregulate PD-L1 and those that do tend to be more aggressive and have fewer T cells present in the tumor [194]. Blocking PD-L1 or its receptor (PD-1) can lead to tumor rejection in both mice and humans, proving that this is an important immune evasion mechanism [117, 195]. The molecular mechanisms whereby cancers exploit these immune evasion strategies are incompletely understood but are important to know for understanding pathogenesis, how they affect prognosis and immunotherapy, and how they might be reversed to improve therapy. Our studies revealed that the loss of a single gene, IRF2, can generate a “double whammy” for the immune system as it enables tumor cells lacking IRF2 to become both harder to identify (through a loss of MHC-I antigen presentation) and better able to suppress T cell-mediated elimination (through increased checkpoint inhibition) (Figure 6.1). As shown in our *in vitro* cytotoxicity assay, this makes IRF2-deficient tumor cells more difficult to kill.

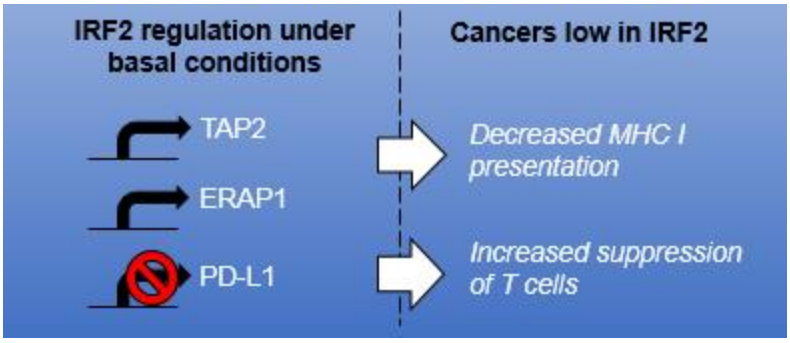

Figure 6.1. Model of cancer immune evasion by loss of IRF2

Under basal conditions, IRF2 acts as a transcriptional activator of both TAP2 and ERAP1 and as a transcriptional repressor of PD-L1. When IRF2 expression is downregulated (e.g., in cancers), TAP2 and ERAP1 expression are decreased thereby resulting in MHC-I presentation defects and PD-L1 expression is increased thereby resulting in increased suppression of T cell effector function. The reduction in TAP2 expression has a profound effect on surface MHC-I levels as the inability to transport peptides into the ER reduces the availability of peptides to bind MHC-I in the ER, thus preventing MHC-I egress. The reduction in ERAP1 expression does not have as large of an effect on surface MHC-I levels but significantly alters the antigenic peptide repertoire presented on MHC-I [196].

IRF2-IRF1 interplay

In the DC line where we focused most of our studies and in other cell lines described in the literature, IRF2 is constitutively expressed, relatively stable with a half-life of 8 hours, and minimally affected by IFN [88, 165, 166]. However, in these same sets of cells, IRF1 is minimally expressed under basal conditions but strongly induced in the presence of IFN and more short-lived than IRF2, with a half-life of only 0.5 hours [165]. Due to these differences between IRF2 and IRF1, even though they both recognize and bind to the same ISRE [82, 84, 164], we hypothesized that the relative contributions of IRF2 and IRF1 to certain signaling pathways varies depending on the inflammatory state of the cell. Although IRF1 and IRF2 were originally characterized as an activator and repressor of IFN-α/β expression, respectively [84], several reports since then have highlighted that IRF1 and IRF2 do not always act as such [86-88]. Yet, there have been no global differential expression analyses in IRF1- and/or IRF2-lacking cells of the same cell type to better understand the synergistic vs. antagonistic roles these transcription factors perform. Consequently, we conducted RNA-seq on IRF1- and/or IRF2-knockout DCs in the absence or presence of IFN to help fill this void. Globally, we found that the expression profile of the double knockout DCs differed from that of either IRF single knockout and that the relative contributions of IRF1 vs. IRF2, in terms of their ability to positively or negatively regulate certain genes, varied depending on the inflammatory state of the cell. Not only do these studies provide insight into the contributions of IRF1 and IRF2 on antigen

presentation and immune function, but they also firmly establish that, although IRF2 may compete with IRF1 for a given DNA binding site, it does not necessarily antagonize the transcriptional effects mediated by IRF1.

Additionally, our RNA-seq analysis revealed a number of differentially expressed genes in the IRF2-knockout DCs that may also contribute to the immune evasion phenotype proposed for IRF2-low cancers. These include Arg1, Arg2, Casp7, and Gsdmd, which were all downregulated and H2-T9, H2-T22, and Fgl2, which were all upregulated in the IRF2-knockout DCs under basal conditions. Arg1 and Arg2 are involved in establishing macrophage polarization (M1 vs. M2) [197] and an imbalance of these two arginases likely affects the tumor microenvironment. Casp7 induces apoptosis [198] and reduced expression of this caspase would, therefore, likely result in increased cell survival. Gsdmd controls pyroptosis and it was recently shown that downregulation of gasdermin D can promote gastric cancer proliferation [199]. The upregulation of non-classical MHC-I proteins by IRF2-low cells, which are deficient in their surface expression of classical MHC-I proteins, may serve to inhibit NK cell-mediated killing. Lastly, secreted Fgl2 negatively regulates the immune response [200] and this may also promote the growth of IRF2-deficient cells, which have high Fgl2 expression.

It is worth stating that the transcriptional control of genes can be highly cell-type dependent and therefore, it is possible that in other cells, the contribution of IRF2 on surface MHC-I and PD-L1 expression may vary. However, our

concordant observations in multiple mouse and human cell lines and primary tumors suggest that the number of cell types in which IRF2 regulates these genes in this manner is quite large.

IRF2 as a potential cancer biomarker and/or therapeutic target

Immune evasion due to tumor PD-L1 upregulation can be reversed by blocking the PD-L1/PD-1 interaction, which is the basis of targeted checkpoint blockade immunotherapy. However, any natural or invigorated (from checkpoint blockade) $CD8^+$ T cell response to kill tumors that have downregulated their MHC-I expression will continue to be impaired. In this context, it is of considerable interest and potential importance that the downregulation of the MHC-I pathway from the loss of IRF2 is reversible. When IRF2-deficient cells were treated with IFN, MHC-I levels were restored, likely because of induction of IRF1 and possibly some other transcriptional activators. These findings suggest that interferons (which are FDA-approved for other indications) or interferon-inducing agents could be used to restore MHC-I antigen presentation in IRF2-low tumors. This would be predicted to enhance the effects of immunotherapies, such as checkpoint blockade, that are ultimately dependent on T cell receptor recognition of tumor MHC-I presentation. Currently, checkpoint therapy is effective in only some patients [201, 202] and, based on the mechanisms we have uncovered, it is conceivable that reversing the IRF2 defects might increase the number of patients that can benefit. In addition, because checkpoint blockade

is an extremely expensive therapy and one that can have serious side effects, there is a need for good biomarkers to identify those patients that would be more likely to benefit from this type of therapy. Therefore, it will be of interest to examine in future studies whether expression of IRF2 and its downstream target genes (e.g., TAP2 and ERAP1) could be used as biomarkers to help identify checkpoint blockade-responsive patients.

Future studies examining the role of IRF2 on cancer immunosurveillance

Given our findings that several cancer types downregulate IRF2 expression and that IRF2-deficient tumor cells are more difficult to kill *in vitro*, we are interested in determining whether a loss of IRF2 impairs cancer immunosurveillance *in vivo*. To examine this, we plan to try a couple different approaches, which I will briefly describe below.

First, we will test cancer growth and immune evasion using the methylcholanthrene (MCA)-induced tumor model established by Bob Schreiber's group [152]. Classical experiments carried out in this model revealed the importance of adaptive immunity in preventing cancer as immunodeficient animals, such as those lacking IFNγ, perforin, or RAG-2, were found to have a higher rate of mutagen-induced tumors [152-154]. For this reason, we hypothesize that if we use MCA to induce sarcomas in WT or IRF2-knockout mice, the IRF2-knockout animals will develop tumors at a greater frequency. Additionally, similar to other experiments performed by Schreiber's group

wherein MCA-induced sarcomas derived from immunodeficient animals were found to progress when transplanted into other immunodeficient hosts but were rejected when placed into immunocompetent hosts (in contrast to the findings that tumors arising in immunocompetent animals progressed when transplanted into other immunocompetent hosts) [154-156], we plan to transplant tumors derived from IRF2-knockout mice into other mice. We hypothesize that tumors originating in an IRF2-knockout mouse will possess an intrinsic advantage in terms of their ability to escape immune elimination and should, therefore, grow when transplanted into either immunodeficient or immunocompetent mice. If we were to transfect IRF2 into the IRF2-knockout tumor, we would expect that the IRF2-reconstituted tumors would be rejected or grow more slowly in the immunocompetent hosts, as compared to the growth rates of the IRF2-deficient tumors.

Second, we will test the growth of human cancers *in vivo* which differ in their IRF2 status. To do this, we will transplant either an IRF2-knockout or an IRF2-transfected human cancer of the same origin (lung, breast, etc.) into highly immunodeficient mice (non-obese diabetic-*scid Il2rg*$^{-/-}$ (NSG)), a model system in which human cancers have been shown to grow [203]. Given that we observed very strong effects on MHC-I and PD-L1 levels in the human NSCLC line, A549, as well as in the human breast cancers, BT20 (triple negative for estrogen, progesterone, and HER-2 receptors) and MCF7 (estrogen receptor-positive), we will start off by testing these tumors. Importantly, we will also evaluate tumor

growth in NSG mice reconstituted with human hematopoietic stem cells wherein the consequences of immunoediting resulting in the loss of IRF2 can be directly probed. Additionally, because some patient NSCLCs can be treated with anti-PD-1 (pembrolizumab) immunotherapy [128], we will also perform some studies in the presence or absence of pembrolizumab administration, which has been shown to inhibit tumor growth in the humanized mice [204].

MHC-I presentation and the roles of co-chaperones

The role of chaperones in MHC-I antigen presentation has been a topic of interest for a quite some time. Beyond the requirements of the ER-resident co-chaperones calnexin and calreticulin in preserving the stability of newly synthesized MHC-I and the integrity of the peptide-loading complex [11, 12], HSP family members have also been reported to regulate a number of steps in the MHC-I pathway [47, 48]. We hoped to advance our knowledge in this field by studying two co-chaperones, Dnajb4 (cytosolic) and Dnajc10 (ER-localized), that were identified through a forward-genetic screen in dendritic cells [174]. We found that transiently knocking down either J protein with siRNA reduces cross-presentation and classical MHC-I presentation in mouse dendritic cells. The effects of Dnajc10 on classical MHC-I presentation were more robust as deficits were also observed in mouse fibroblasts lacking Dnajc10.

Mechanistically, we determined that Dnajc10 mediates its effects on the MHC-I pathway likely through its ability to reduce client proteins via its Trx motifs.

To better discern how Dnajc10 acts on the MHC-I pathway, we wished to identify the proteins to which Dnajc10 binds in this context. Unfortunately, due to the technical limitations of our main functional assay (checking for surface MHC-I expression) where the low signal-to-noise ratio could not be overcome, we were unable to identify which of Dnajc10's four Trx motifs mediate these effects, which would have been helpful for subsequent experiments in order to trap only the relevant substrates. As an alternate technique, we tried to identify which known members of the MHC-I pathway physically associate with Dnajc10 by immunoprecipitating HA-tagged Dnajc10. Unfortunately, in this assay, we did not identify Dnajc10-specific interactions with any of the ER-resident proteins we selected other than BiP, the ER-localized Hsp70 to which Dnajc10 is known to interact [185]. One caveat of these results is that some of the antibodies used were of poor quality and perhaps, with better reagents and a broader array of possible substrate targets, one could identify which protein clients are bound by Dnajc10 in the context of MHC-I presentation. An alternative approach would be to perform mass spectrometry on all Dnajc10-immunoprecipitated proteins. The downside of this is that the list of proteins bound to Dnajc10 may be quite extensive as it is known to recognize aggregation-prone sequences [205]. However, one could design immunoprecipitation-mass spectrometry studies in which the Dnajc10 Trx mutants (4X-CA and 4X-AA) are utilized with the hopes that this could filter out proteins that are not specific for the MHC-I pathway (i.e., those which bind the 4X-AA mutant).

We were surprised by the findings that primary BMDCs and splenocytes constitutively lacking Dnajc10 do not display significant deficits in MHC-I presentation as this conflicted with our cell line data, which strongly supports a role for Dnajc10 in this pathway. However, there are some caveats between these two systems which I would like to briefly discuss.

First, as opposed to siRNA studies which transiently knock down a gene's mRNA expression, a knockout animal constitutively lacks the gene of interest. In order to develop and carry out cellular functions properly, the knockout animal may acquire compensatory mechanisms to minimize the loss of that gene, especially in instances where there is functional redundancy. There are multiple ER J proteins [205] and it is possible that, if given enough time, cells may acclimate to the loss of Dnajc10 by having a different ER J protein take over Dnajc10's responsibilities. Moreover, if compensatory mechanisms do exist for Dnajc10 and its effects on MHC-I presentation, then in short-term studies where cells do not have time to adapt to the loss of Dnajc10, such as those where Dnajc10 is transiently knocked down by siRNA, the cells will display a pronounced MHC-I phenotype.

Second, despite the aforementioned benefit of using siRNA to query a gene's role in a pathway, there are limitations to siRNA studies, one of which is off-target effects. Although it is fairly straightforward to assess the knockdown efficiency of a given gene after siRNA treatment (by qPCR and/or western blot), it is not as easy to determine whether the siRNA is also targeting other genes. One can

search whether the siRNA sequence being used is homologous or nearly identical to other regions of the transcriptome but this, on its own, will not confirm which off-target gene(s) are actually affected and what types of effects they may have on a given assay. Furthermore, we and others have found that some siRNAs induce a strong type I IFN response [206], which could confound results probing the MHC-I pathway as IFN upregulates surface MHC-I expression. It is therefore important to conduct rescue experiments, such as those described in Chapter III, in which cells lacking a gene are reconstituted with that gene. In the event that reconstitution completely restores the phenotype (as in Fig. 3.2), one can infer that the observed effects are due to the gene being targeted. However, if the levels are not completely restored, one may question whether other off-target genes are contributory. Although we were able to increase surface MHC-I expression by overexpressing Dnajc10 in the Dnajc10-knockout MEFs, thus reversing the phenotype caused by loss of Dnajc10, the degree to which MHC-I levels were upregulated upon Dnajc10 overexpression was not as large as the degree to which MHC-I levels were downregulated by Dnajc10 knockdown. Not only did this limit our ability to obtain useful data in the Trx binding partner studies, but it also made us question whether the siRNA used to target Dnajc10 was having undesirable off-target effects.

We tried to address this issue by reconstituting Dnajc10 expression in Dnajc10-knockdown cells either by (1) creating stable cell lines in which Dnajc10 (harboring six synonymous mutations in the siRNA target site) expression could

be induced by doxycycline before or after siRNA knockdown, or (2) transiently overexpressing Dnajc10 (harboring six synonymous mutations in the siRNA target site) in cells post-siRNA treatment. In both approaches, the phenotype was not restored upon Dnajc10 overexpression; however, when we tried the same things with β2m siRNA and β2m overexpression, we were also unable to rescue the phenotype. This was particularly disconcerting because β2m has a well-established role in the MHC-I pathway and, if our positive control cannot rescue the phenotype, there is little expectation that other genes would be able to do so. Therefore, it is worth noting that, at least for some studies examining the MHC-I pathway, phenotypes observed upon siRNA knockdown cannot be totally restored upon overexpression of that gene.

Concluding remarks

Upon joining the Rock Lab, I decided to devote my thesis research to investigating novel genes in the MHC-I antigen presentation pathway. From the screens conducted by myself and others in the lab, I selected over two dozen gene candidates. After working up these hits and deciding which ones were most appealing, I focused most of my efforts on IRF2, Dnajb4, and Dnajc10, as described in this dissertation. The IRF2 studies, which ended up being particularly fruitful, reinforce the need for these types of screens in identifying novel yet highly important components of the MHC-I pathway. Our findings not only contribute to our understanding of the transcriptional machinery involved in

antigen presentation and cancer immune evasion, but they also have substantial implications for cancer immunotherapy.

Bibliography

1. Cruz, F.M., et al., *The Biology and Underlying Mechanisms of Cross-Presentation of Exogenous Antigens on MHC-I Molecules.* Annu Rev Immunol, 2017. **35**: p. 149-176.
2. Kovacsovics-Bankowski, M., et al., *Efficient major histocompatibility complex class I presentation of exogenous antigen upon phagocytosis by macrophages.* Proc Natl Acad Sci U S A, 1993. **90**(11): p. 4942-6.
3. Rock, K.L., et al., *Characterization of antigen-presenting cells that present exogenous antigens in association with class I MHC molecules.* J Immunol, 1993. **150**(2): p. 438-46.
4. Shen, Z., et al., *Cloned dendritic cells can present exogenous antigens on both MHC class I and class II molecules.* J Immunol, 1997. **158**(6): p. 2723-30.
5. Rock, K.L., S. Gamble, and L. Rothstein, *Presentation of exogenous antigen with class I major histocompatibility complex molecules.* Science, 1990. **249**(4971): p. 918-21.
6. Lenschow, D.J., T.L. Walunas, and J.A. Bluestone, *CD28/B7 system of T cell costimulation.* Annu Rev Immunol, 1996. **14**: p. 233-58.
7. Rock, K.L., et al., *Inhibitors of the proteasome block the degradation of most cell proteins and the generation of peptides presented on MHC class I molecules.* Cell, 1994. **78**(5): p. 761-71.
8. Abele, R. and R. Tampe, *The ABCs of immunology: structure and function of TAP, the transporter associated with antigen processing.* Physiology (Bethesda), 2004. **19**: p. 216-24.
9. Saric, T., et al., *An IFN-gamma-induced aminopeptidase in the ER, ERAP1, trims precursors to MHC class I-presented peptides.* Nat Immunol, 2002. **3**(12): p. 1169-76.
10. Serwold, T., et al., *ERAAP customizes peptides for MHC class I molecules in the endoplasmic reticulum.* Nature, 2002. **419**(6906): p. 480-3.
11. Hebert, D.N., S.C. Garman, and M. Molinari, *The glycan code of the endoplasmic reticulum: asparagine-linked carbohydrates as protein maturation and quality-control tags.* Trends Cell Biol, 2005. **15**(7): p. 364-70.
12. Sadasivan, B., et al., *Roles for calreticulin and a novel glycoprotein, tapasin, in the interaction of MHC class I molecules with TAP.* Immunity, 1996. **5**(2): p. 103-14.
13. Dick, T.P., et al., *Disulfide bond isomerization and the assembly of MHC class I-peptide complexes.* Immunity, 2002. **16**(1): p. 87-98.
14. Dong, G., et al., *Insights into MHC class I peptide loading from the structure of the tapasin-ERp57 thiol oxidoreductase heterodimer.* Immunity, 2009. **30**(1): p. 21-32.
15. Grandea, A.G., 3rd, et al., *Impaired assembly yet normal trafficking of MHC class I molecules in Tapasin mutant mice.* Immunity, 2000. **13**(2): p. 213-22.
16. Gao, B., et al., *Assembly and antigen-presenting function of MHC class I molecules in cells lacking the ER chaperone calreticulin.* Immunity, 2002. **16**(1): p. 99-109.
17. Garbi, N., et al., *Impaired assembly of the major histocompatibility complex class I peptide-loading complex in mice deficient in the oxidoreductase ERp57.* Nat Immunol, 2006. **7**(1): p. 93-102.
18. Norbury, C.C., et al., *Class I MHC presentation of exogenous soluble antigen via macropinocytosis in bone marrow macrophages.* Immunity, 1995. **3**(6): p. 783-91.

19. Pfeifer, J.D., et al., *Phagocytic processing of bacterial antigens for class I MHC presentation to T cells.* Nature, 1993. **361**(6410): p. 359-62.
20. Burgdorf, S., V. Lukacs-Kornek, and C. Kurts, *The mannose receptor mediates uptake of soluble but not of cell-associated antigen for cross-presentation.* J Immunol, 2006. **176**(11): p. 6770-6.
21. Kamphorst, A.O., et al., *Route of antigen uptake differentially impacts presentation by dendritic cells and activated monocytes.* J Immunol, 2010. **185**(6): p. 3426-35.
22. Kovacsovics-Bankowski, M. and K.L. Rock, *A phagosome-to-cytosol pathway for exogenous antigens presented on MHC class I molecules.* Science, 1995. **267**(5195): p. 243-6.
23. Shen, L., et al., *Important role of cathepsin S in generating peptides for TAP-independent MHC class I crosspresentation in vivo.* Immunity, 2004. **21**(2): p. 155-65.
24. Gobin, S.J., et al., *The role of enhancer A in the locus-specific transactivation of classical and nonclassical HLA class I genes by nuclear factor kappa B.* J Immunol, 1998. **161**(5): p. 2276-83.
25. Chang, C.H., et al., *The activation of major histocompatibility complex class I genes by interferon regulatory factor-1 (IRF-1).* Immunogenetics, 1992. **35**(6): p. 378-84.
26. Ludigs, K., et al., *NLRC5 exclusively transactivates MHC class I and related genes through a distinctive SXY module.* PLoS Genet, 2015. **11**(3): p. e1005088.
27. Meissner, T.B., et al., *NLRC5 cooperates with the RFX transcription factor complex to induce MHC class I gene expression.* J Immunol, 2012. **188**(10): p. 4951-8.
28. Neerincx, A., et al., *NLRC5 controls basal MHC class I gene expression in an MHC enhanceosome-dependent manner.* J Immunol, 2012. **188**(10): p. 4940-50.
29. Biswas, A., et al., *Cutting edge: impaired MHC class I expression in mice deficient for Nlrc5/class I transactivator.* J Immunol, 2012. **189**(2): p. 516-20.
30. Staehli, F., et al., *NLRC5 deficiency selectively impairs MHC class I- dependent lymphocyte killing by cytotoxic T cells.* J Immunol, 2012. **188**(8): p. 3820-8.
31. Meissner, T.B., et al., *NLR family member NLRC5 is a transcriptional regulator of MHC class I genes.* Proc Natl Acad Sci U S A, 2010. **107**(31): p. 13794-9.
32. Jongsma, M.L.M., G. Guarda, and R.M. Spaapen, *The regulatory network behind MHC class I expression.* Mol Immunol, 2017.
33. Strehl, B., et al., *Interferon-gamma, the functional plasticity of the ubiquitin-proteasome system, and MHC class I antigen processing.* Immunol Rev, 2005. **207**: p. 19-30.
34. Doody, G.M., et al., *PRDM1/BLIMP-1 modulates IFN-gamma-dependent control of the MHC class I antigen-processing and peptide-loading pathway.* J Immunol, 2007. **179**(11): p. 7614-23.
35. Samie, M. and P. Cresswell, *The transcription factor TFEB acts as a molecular switch that regulates exogenous antigen-presentation pathways.* Nat Immunol, 2015. **16**(7): p. 729-36.
36. Bertholet, S., et al., *Leishmania antigens are presented to CD8+ T cells by a transporter associated with antigen processing-independent pathway in vitro and in vivo.* J Immunol, 2006. **177**(6): p. 3525-33.
37. Hornung, V., et al., *Silica crystals and aluminum salts activate the NALP3 inflammasome through phagosomal destabilization.* Nat Immunol, 2008. **9**(8): p. 847-56.

38. Savina, A., et al., *NOX2 controls phagosomal pH to regulate antigen processing during crosspresentation by dendritic cells.* Cell, 2006. **126**(1): p. 205-18.
39. Houde, M., et al., *Phagosomes are competent organelles for antigen cross-presentation.* Nature, 2003. **425**(6956): p. 402-6.
40. Campbell-Valois, F.X., et al., *Quantitative proteomics reveals that only a subset of the endoplasmic reticulum contributes to the phagosome.* Mol Cell Proteomics, 2012. **11**(7): p. M111 016378.
41. Ye, Y., H.H. Meyer, and T.A. Rapoport, *The AAA ATPase Cdc48/p97 and its partners transport proteins from the ER into the cytosol.* Nature, 2001. **414**(6864): p. 652-6.
42. Ruggiano, A., O. Foresti, and P. Carvalho, *Quality control: ER-associated degradation: protein quality control and beyond.* J Cell Biol, 2014. **204**(6): p. 869-79.
43. Mehnert, M., T. Sommer, and E. Jarosch, *Der1 promotes movement of misfolded proteins through the endoplasmic reticulum membrane.* Nat Cell Biol, 2014. **16**(1): p. 77-86.
44. Ackerman, A.L., A. Giodini, and P. Cresswell, *A role for the endoplasmic reticulum protein retrotranslocation machinery during crosspresentation by dendritic cells.* Immunity, 2006. **25**(4): p. 607-17.
45. Zehner, M., et al., *Mannose receptor polyubiquitination regulates endosomal recruitment of p97 and cytosolic antigen translocation for cross-presentation.* Proc Natl Acad Sci U S A, 2011. **108**(24): p. 9933-8.
46. Menager, J., et al., *Cross-presentation of synthetic long peptides by human dendritic cells: a process dependent on ERAD component p97/VCP but Not sec61 and/or Derlin-1.* PLoS One, 2014. **9**(2): p. e89897.
47. Imai, T., et al., *Heat shock protein 90 (HSP90) contributes to cytosolic translocation of extracellular antigen for cross-presentation by dendritic cells.* Proc Natl Acad Sci U S A, 2011. **108**(39): p. 16363-8.
48. Udono, H. and P.K. Srivastava, *Heat shock protein 70-associated peptides elicit specific cancer immunity.* J Exp Med, 1993. **178**(4): p. 1391-6.
49. Blachere, N.E., et al., *Heat shock protein-peptide complexes, reconstituted in vitro, elicit peptide-specific cytotoxic T lymphocyte response and tumor immunity.* J Exp Med, 1997. **186**(8): p. 1315-22.
50. Basu, S., et al., *Necrotic but not apoptotic cell death releases heat shock proteins, which deliver a partial maturation signal to dendritic cells and activate the NF-kappa B pathway.* Int Immunol, 2000. **12**(11): p. 1539-46.
51. Basu, S., et al., *CD91 is a common receptor for heat shock proteins gp96, hsp90, hsp70, and calreticulin.* Immunity, 2001. **14**(3): p. 303-13.
52. Binder, R.J. and P.K. Srivastava, *Essential role of CD91 in re-presentation of gp96-chaperoned peptides.* Proc Natl Acad Sci U S A, 2004. **101**(16): p. 6128-33.
53. Binder, R.J., et al., *CD91-Dependent Modulation of Immune Responses by Heat Shock Proteins: A Role in Autoimmunity.* Autoimmune Dis, 2012. **2012**: p. 863041.
54. Breloer, M., et al., *Isolation of processed, H-2Kb-binding ovalbumin-derived peptides associated with the stress proteins HSP70 and gp96.* Eur J Immunol, 1998. **28**(3): p. 1016-21.

55. Stocki, P., et al., *Identification of potential HLA class I and class II epitope precursors associated with heat shock protein 70 (HSPA).* Cell Stress Chaperones, 2010. **15**(5): p. 729-41.
56. Kamiguchi, K., et al., *Disruption of the association of 73 kDa heat shock cognate protein with transporters associated with antigen processing (TAP) decreases TAP-dependent translocation of antigenic peptides into the endoplasmic reticulum.* Microbiol Immunol, 2008. **52**(2): p. 94-106.
57. Levitskaya, J., et al., *Inhibition of antigen processing by the internal repeat region of the Epstein-Barr virus nuclear antigen-1.* Nature, 1995. **375**(6533): p. 685-8.
58. Daskalogianni, C., et al., *Gly-Ala repeats induce position- and substrate-specific regulation of 26 S proteasome-dependent partial processing.* J Biol Chem, 2008. **283**(44): p. 30090-100.
59. Masucci, M.G., *Epstein-Barr virus oncogenesis and the ubiquitin-proteasome system.* Oncogene, 2004. **23**(11): p. 2107-15.
60. Fruh, K., et al., *A viral inhibitor of peptide transporters for antigen presentation.* Nature, 1995. **375**(6530): p. 415-8.
61. Ahn, K., et al., *The ER-luminal domain of the HCMV glycoprotein US6 inhibits peptide translocation by TAP.* Immunity, 1997. **6**(5): p. 613-21.
62. Koppers-Lalic, D., et al., *Varicelloviruses avoid T cell recognition by UL49.5-mediated inactivation of the transporter associated with antigen processing.* Proc Natl Acad Sci U S A, 2005. **102**(14): p. 5144-9.
63. Horst, D., et al., *Specific targeting of the EBV lytic phase protein BNLF2a to the transporter associated with antigen processing results in impairment of HLA class I-restricted antigen presentation.* J Immunol, 2009. **182**(4): p. 2313-24.
64. Lee, S., et al., *Structural and functional dissection of human cytomegalovirus US3 in binding major histocompatibility complex class I molecules.* J Virol, 2000. **74**(23): p. 11262-9.
65. Bennett, E.M., et al., *Cutting edge: adenovirus E19 has two mechanisms for affecting class I MHC expression.* J Immunol, 1999. **162**(9): p. 5049-52.
66. Wiertz, E.J., et al., *Sec61-mediated transfer of a membrane protein from the endoplasmic reticulum to the proteasome for destruction.* Nature, 1996. **384**(6608): p. 432-8.
67. Wiertz, E.J., et al., *The human cytomegalovirus US11 gene product dislocates MHC class I heavy chains from the endoplasmic reticulum to the cytosol.* Cell, 1996. **84**(5): p. 769-79.
68. Boname, J.M. and P.G. Stevenson, *MHC class I ubiquitination by a viral PHD/LAP finger protein.* Immunity, 2001. **15**(4): p. 627-36.
69. Carretero, R., et al., *Analysis of HLA class I expression in progressing and regressing metastatic melanoma lesions after immunotherapy.* Immunogenetics, 2008. **60**(8): p. 439-47.
70. Garrido, F., et al., *Natural history of HLA expression during tumour development.* Immunol Today, 1993. **14**(10): p. 491-9.
71. Garcia-Lora, A., et al., *Immunoselection by T lymphocytes generates repeated MHC class I-deficient metastatic tumor variants.* Int J Cancer, 2001. **91**(1): p. 109-19.
72. del Campo, A.B., et al., *Immune escape of cancer cells with beta2-microglobulin loss over the course of metastatic melanoma.* Int J Cancer, 2014. **134**(1): p. 102-13.

73. Henle, A.M., et al., *Downregulation of TAP1 and TAP2 in early stage breast cancer.* PLoS One, 2017. **12**(11): p. e0187323.
74. Garcia-Lora, A., et al., *MHC class I-deficient metastatic tumor variants immunoselected by T lymphocytes originate from the coordinated downregulation of APM components.* Int J Cancer, 2003. **106**(4): p. 521-7.
75. Karre, K., *Natural killer cell recognition of missing self.* Nat Immunol, 2008. **9**(5): p. 477-80.
76. Zhang, J., F. Basher, and J.D. Wu, *NKG2D Ligands in Tumor Immunity: Two Sides of a Coin.* Front Immunol, 2015. **6**: p. 97.
77. Groh, V., et al., *Costimulation of CD8alphabeta T cells by NKG2D via engagement by MIC induced on virus-infected cells.* Nat Immunol, 2001. **2**(3): p. 255-60.
78. Pende, D., et al., *Major histocompatibility complex class I-related chain A and UL16-binding protein expression on tumor cell lines of different histotypes: analysis of tumor susceptibility to NKG2D-dependent natural killer cell cytotoxicity.* Cancer Res, 2002. **62**(21): p. 6178-86.
79. Ishido, S., et al., *Downregulation of major histocompatibility complex class I molecules by Kaposi's sarcoma-associated herpesvirus K3 and K5 proteins.* J Virol, 2000. **74**(11): p. 5300-9.
80. Thomas, M., et al., *Down-regulation of NKG2D and NKp80 ligands by Kaposi's sarcoma-associated herpesvirus K5 protects against NK cell cytotoxicity.* Proc Natl Acad Sci U S A, 2008. **105**(5): p. 1656-61.
81. Bach, E.A., M. Aguet, and R.D. Schreiber, *The IFN gamma receptor: a paradigm for cytokine receptor signaling.* Annu Rev Immunol, 1997. **15**: p. 563-91.
82. Darnell, J.E., Jr., I.M. Kerr, and G.R. Stark, *Jak-STAT pathways and transcriptional activation in response to IFNs and other extracellular signaling proteins.* Science, 1994. **264**(5164): p. 1415-21.
83. Miyamoto, M., et al., *Regulated expression of a gene encoding a nuclear factor, IRF-1, that specifically binds to IFN-beta gene regulatory elements.* Cell, 1988. **54**(6): p. 903-13.
84. Harada, H., et al., *Structurally similar but functionally distinct factors, IRF-1 and IRF-2, bind to the same regulatory elements of IFN and IFN-inducible genes.* Cell, 1989. **58**(4): p. 729-39.
85. Tamura, T., et al., *The IRF family transcription factors in immunity and oncogenesis.* Annu Rev Immunol, 2008. **26**: p. 535-84.
86. Jesse, T.L., et al., *Interferon regulatory factor-2 is a transcriptional activator in muscle where It regulates expression of vascular cell adhesion molecule-1.* J Cell Biol, 1998. **140**(5): p. 1265-76.
87. Vaughan, P.S., et al., *Activation of a cell-cycle-regulated histone gene by the oncogenic transcription factor IRF-2.* Nature, 1995. **377**(6547): p. 362-5.
88. Ren, G., et al., *Division of labor between IRF1 and IRF2 in regulating different stages of transcriptional activation in cellular antiviral activities.* Cell Biosci, 2015. **5**: p. 17.
89. Palombella, V.J. and T. Maniatis, *Inducible processing of interferon regulatory factor-2.* Mol Cell Biol, 1992. **12**(8): p. 3325-36.
90. Cohen, L. and J. Hiscott, *Characterization of TH3, an induction-specific protein interacting with the interferon beta promoter.* Virology, 1992. **191**(2): p. 589-99.

91. Whiteside, S.T., P. King, and S. Goodbourn, *A truncated form of the IRF-2 transcription factor has the properties of a postinduction repressor of interferon-beta gene expression.* J Biol Chem, 1994. **269**(43): p. 27059-65.
92. Yamamoto, H., et al., *The oncogenic transcription factor IRF-2 possesses a transcriptional repression and a latent activation domain.* Oncogene, 1994. **9**(5): p. 1423-8.
93. Birnbaum, M.J., et al., *Phosphorylation of the oncogenic transcription factor interferon regulatory factor 2 (IRF2) in vitro and in vivo.* J Cell Biochem, 1997. **66**(2): p. 175-83.
94. Duncan, G.S., et al., *The transcription factor interferon regulatory factor-1 is essential for natural killer cell function in vivo.* J Exp Med, 1996. **184**(5): p. 2043-8.
95. Lohoff, M., et al., *Deficiency in the transcription factor interferon regulatory factor (IRF)-2 leads to severely compromised development of natural killer and T helper type 1 cells.* J Exp Med, 2000. **192**(3): p. 325-36.
96. Lohoff, M., et al., *Interferon regulatory factor-1 is required for a T helper 1 immune response in vivo.* Immunity, 1997. **6**(6): p. 681-9.
97. Elser, B., et al., *IFN-gamma represses IL-4 expression via IRF-1 and IRF-2.* Immunity, 2002. **17**(6): p. 703-12.
98. Penninger, J.M., et al., *The interferon regulatory transcription factor IRF-1 controls positive and negative selection of CD8+ thymocytes.* Immunity, 1997. **7**(2): p. 243-54.
99. Ichikawa, E., et al., *Defective development of splenic and epidermal CD4+ dendritic cells in mice deficient for IFN regulatory factor-2.* Proc Natl Acad Sci U S A, 2004. **101**(11): p. 3909-14.
100. Tanaka, N., et al., *Cellular commitment to oncogene-induced transformation or apoptosis is dependent on the transcription factor IRF-1.* Cell, 1994. **77**(6): p. 829-39.
101. Tamura, T., et al., *An IRF-1-dependent pathway of DNA damage-induced apoptosis in mitogen-activated T lymphocytes.* Nature, 1995. **376**(6541): p. 596-9.
102. Tan, R.S., T. Taniguchi, and H. Harada, *Identification of the lysyl oxidase gene as target of the antioncogenic transcription factor, IRF-1, and its possible role in tumor suppression.* Cancer Res, 1996. **56**(10): p. 2417-21.
103. Harada, H., et al., *Anti-oncogenic and oncogenic potentials of interferon regulatory factors-1 and -2.* Science, 1993. **259**(5097): p. 971-4.
104. Tada, Y., et al., *Reduced incidence and severity of antigen-induced autoimmune diseases in mice lacking interferon regulatory factor-1.* J Exp Med, 1997. **185**(2): p. 231-8.
105. Hida, S., et al., *CD8(+) T cell-mediated skin disease in mice lacking IRF-2, the transcriptional attenuator of interferon-alpha/beta signaling.* Immunity, 2000. **13**(5): p. 643-55.
106. Marie, I., J.E. Durbin, and D.E. Levy, *Differential viral induction of distinct interferon-alpha genes by positive feedback through interferon regulatory factor-7.* EMBO J, 1998. **17**(22): p. 6660-9.
107. Sato, M., et al., *Distinct and essential roles of transcription factors IRF-3 and IRF-7 in response to viruses for IFN-alpha/beta gene induction.* Immunity, 2000. **13**(4): p. 539-48.
108. Sato, M., et al., *Positive feedback regulation of type I IFN genes by the IFN-inducible transcription factor IRF-7.* FEBS Lett, 1998. **441**(1): p. 106-10.
109. Nayar, R., et al., *TCR signaling via Tec kinase ITK and interferon regulatory factor 4 (IRF4) regulates CD8+ T-cell differentiation.* Proc Natl Acad Sci U S A, 2012. **109**(41): p. E2794-802.

110. Nayar, R., et al., *Graded levels of IRF4 regulate CD8+ T cell differentiation and expansion, but not attrition, in response to acute virus infection.* J Immunol, 2014. **192**(12): p. 5881-93.
111. Takaoka, A., et al., *Integral role of IRF-5 in the gene induction programme activated by Toll-like receptors.* Nature, 2005. **434**(7030): p. 243-9.
112. Richardson, R.J., et al., *Irf6 is a key determinant of the keratinocyte proliferation-differentiation switch.* Nat Genet, 2006. **38**(11): p. 1329-34.
113. Schiavoni, G., et al., *ICSBP is essential for the development of mouse type I interferon-producing cells and for the generation and activation of CD8alpha(+) dendritic cells.* J Exp Med, 2002. **196**(11): p. 1415-25.
114. Aliberti, J., et al., *Essential role for ICSBP in the in vivo development of murine CD8alpha + dendritic cells.* Blood, 2003. **101**(1): p. 305-10.
115. Driggers, P.H., et al., *An interferon gamma-regulated protein that binds the interferon-inducible enhancer element of major histocompatibility complex class I genes.* Proc Natl Acad Sci U S A, 1990. **87**(10): p. 3743-7.
116. Levy, D.E., et al., *Cytoplasmic activation of ISGF3, the positive regulator of interferon-alpha-stimulated transcription, reconstituted in vitro.* Genes Dev, 1989. **3**(9): p. 1362-71.
117. Pardoll, D.M., *The blockade of immune checkpoints in cancer immunotherapy.* Nat Rev Cancer, 2012. **12**(4): p. 252-64.
118. Yan, Y., et al., *Combining Immune Checkpoint Inhibitors With Conventional Cancer Therapy.* Front Immunol, 2018. **9**: p. 1739.
119. Linsley, P.S., et al., *Human B7-1 (CD80) and B7-2 (CD86) bind with similar avidities but distinct kinetics to CD28 and CTLA-4 receptors.* Immunity, 1994. **1**(9): p. 793-801.
120. Qureshi, O.S., et al., *Trans-endocytosis of CD80 and CD86: a molecular basis for the cell-extrinsic function of CTLA-4.* Science, 2011. **332**(6029): p. 600-3.
121. Lee, K.M., et al., *Molecular basis of T cell inactivation by CTLA-4.* Science, 1998. **282**(5397): p. 2263-6.
122. Parry, R.V., et al., *CTLA-4 and PD-1 receptors inhibit T-cell activation by distinct mechanisms.* Mol Cell Biol, 2005. **25**(21): p. 9543-53.
123. Hodi, F.S., et al., *Improved survival with ipilimumab in patients with metastatic melanoma.* N Engl J Med, 2010. **363**(8): p. 711-23.
124. Leach, D.R., M.F. Krummel, and J.P. Allison, *Enhancement of antitumor immunity by CTLA-4 blockade.* Science, 1996. **271**(5256): p. 1734-6.
125. Freeman, G.J., et al., *Engagement of the PD-1 immunoinhibitory receptor by a novel B7 family member leads to negative regulation of lymphocyte activation.* J Exp Med, 2000. **192**(7): p. 1027-34.
126. Terme, M., et al., *IL-18 induces PD-1-dependent immunosuppression in cancer.* Cancer Res, 2011. **71**(16): p. 5393-9.
127. Velu, V., et al., *Enhancing SIV-specific immunity in vivo by PD-1 blockade.* Nature, 2009. **458**(7235): p. 206-10.
128. Brahmer, J.R., et al., *Phase I study of single-agent anti-programmed death-1 (MDX-1106) in refractory solid tumors: safety, clinical activity, pharmacodynamics, and immunologic correlates.* J Clin Oncol, 2010. **28**(19): p. 3167-75.
129. Garon, E.B., et al., *Pembrolizumab for the treatment of non-small-cell lung cancer.* N Engl J Med, 2015. **372**(21): p. 2018-28.

130. Reck, M., et al., *Pembrolizumab versus Chemotherapy for PD-L1-Positive Non-Small-Cell Lung Cancer.* N Engl J Med, 2016. **375**(19): p. 1823-1833.
131. Kluger, H.M., et al., *PD-L1 Studies Across Tumor Types, Its Differential Expression and Predictive Value in Patients Treated with Immune Checkpoint Inhibitors.* Clin Cancer Res, 2017. **23**(15): p. 4270-4279.
132. Le, D.T., et al., *PD-1 Blockade in Tumors with Mismatch-Repair Deficiency.* N Engl J Med, 2015. **372**(26): p. 2509-20.
133. Anagnostou, V., et al., *Evolution of Neoantigen Landscape during Immune Checkpoint Blockade in Non-Small Cell Lung Cancer.* Cancer Discov, 2017. **7**(3): p. 264-276.
134. Zaretsky, J.M., et al., *Mutations Associated with Acquired Resistance to PD-1 Blockade in Melanoma.* N Engl J Med, 2016. **375**(9): p. 819-29.
135. Gettinger, S., et al., *Impaired HLA Class I Antigen Processing and Presentation as a Mechanism of Acquired Resistance to Immune Checkpoint Inhibitors in Lung Cancer.* Cancer Discov, 2017. **7**(12): p. 1420-1435.
136. Rock, K.L., L. Rothstein, and S. Gamble, *Generation of class I MHC-restricted T-T hybridomas.* J Immunol, 1990. **145**(3): p. 804-11.
137. Hosoda, A., et al., *Positive contribution of ERdj5/JPDI to endoplasmic reticulum protein quality control in the salivary gland.* Biochem J, 2009. **425**(1): p. 117-25.
138. Sanjana, N.E., O. Shalem, and F. Zhang, *Improved vectors and genome-wide libraries for CRISPR screening.* Nat Methods, 2014. **11**(8): p. 783-784.
139. Shalem, O., et al., *Genome-scale CRISPR-Cas9 knockout screening in human cells.* Science, 2014. **343**(6166): p. 84-87.
140. Brinkman, E.K., et al., *Easy quantitative assessment of genome editing by sequence trace decomposition.* Nucleic Acids Res, 2014. **42**(22): p. e168.
141. Hearn, A., I.A. York, and K.L. Rock, *The specificity of trimming of MHC class I-presented peptides in the endoplasmic reticulum.* J Immunol, 2009. **183**(9): p. 5526-36.
142. Porgador, A., et al., *Localization, quantitation, and in situ detection of specific peptide-MHC class I complexes using a monoclonal antibody.* Immunity, 1997. **6**(6): p. 715-26.
143. Bolger, A.M., M. Lohse, and B. Usadel, *Trimmomatic: a flexible trimmer for Illumina sequence data.* Bioinformatics, 2014. **30**(15): p. 2114-20.
144. Li, B. and C.N. Dewey, *RSEM: accurate transcript quantification from RNA-Seq data with or without a reference genome.* BMC Bioinformatics, 2011. **12**: p. 323.
145. Pruitt, K.D., et al., *NCBI Reference Sequences (RefSeq): current status, new features and genome annotation policy.* Nucleic Acids Res, 2012. **40**(Database issue): p. D130-5.
146. Johnson, W.E., C. Li, and A. Rabinovic, *Adjusting batch effects in microarray expression data using empirical Bayes methods.* Biostatistics, 2007. **8**(1): p. 118-127.
147. Leek, J.T., et al., *The sva package for removing batch effects and other unwanted variation in high-throughput experiments.* Bioinformatics, 2012. **28**(6): p. 882-3.
148. Love, M.I., W. Huber, and S. Anders, *Moderated estimation of fold change and dispersion for RNA-seq data with DESeq2.* Genome Biol, 2014. **15**(12): p. 550.
149. Mould, A.W., et al., *Blimp1/Prdm1 Functions in Opposition to Irf1 to Maintain Neonatal Tolerance during Postnatal Intestinal Maturation.* PLoS Genet, 2015. **11**(7): p. e1005375.
150. Lu, C., et al., *The expression profiles and regulation of PD-L1 in tumor-induced myeloid-derived suppressor cells.* Oncoimmunology, 2016. **5**(12): p. e1247135.

151. Munro, S. and H.R. Pelham, *A C-terminal signal prevents secretion of luminal ER proteins.* Cell, 1987. **48**(5): p. 899-907.
152. Kaplan, D.H., et al., *Demonstration of an interferon gamma-dependent tumor surveillance system in immunocompetent mice.* Proc Natl Acad Sci U S A, 1998. **95**(13): p. 7556-61.
153. Street, S.E., E. Cretney, and M.J. Smyth, *Perforin and interferon-gamma activities independently control tumor initiation, growth, and metastasis.* Blood, 2001. **97**(1): p. 192-7.
154. Shankaran, V., et al., *IFNgamma and lymphocytes prevent primary tumour development and shape tumour immunogenicity.* Nature, 2001. **410**(6832): p. 1107-11.
155. Svane, I.M., et al., *Chemically induced sarcomas from nude mice are more immunogenic than similar sarcomas from congenic normal mice.* Eur J Immunol, 1996. **26**(8): p. 1844-50.
156. Engel, A.M., et al., *MCA sarcomas induced in scid mice are more immunogenic than MCA sarcomas induced in congenic, immunocompetent mice.* Scand J Immunol, 1997. **45**(5): p. 463-70.
157. Mittal, D., et al., *New insights into cancer immunoediting and its three component phases--elimination, equilibrium and escape.* Curr Opin Immunol, 2014. **27**: p. 16-25.
158. Sabbatino, F., et al., *PD-L1 and HLA Class I Antigen Expression and Clinical Course of the Disease in Intrahepatic Cholangiocarcinoma.* Clin Cancer Res, 2016. **22**(2): p. 470-8.
159. Zamora, A.E., J.C. Crawford, and P.G. Thomas, *Hitting the Target: How T Cells Detect and Eliminate Tumors.* J Immunol, 2018. **200**(2): p. 392-399.
160. Masumi, A., et al., *Interferon regulatory factor-2 regulates cell growth through its acetylation.* J Biol Chem, 2003. **278**(28): p. 25401-7.
161. Fernandes, D.M., L. Vidard, and K.L. Rock, *Characterization of MHC class II-presented peptides generated from an antigen targeted to different endocytic compartments.* Eur J Immunol, 2000. **30**(8): p. 2333-43.
162. Dong, H., et al., *Tumor-associated B7-H1 promotes T-cell apoptosis: a potential mechanism of immune evasion.* Nat Med, 2002. **8**(8): p. 793-800.
163. Yu, H., et al., *PD-L1 Expression in Lung Cancer.* J Thorac Oncol, 2016. **11**(7): p. 964-75.
164. Tanaka, N., T. Kawakami, and T. Taniguchi, *Recognition DNA sequences of interferon regulatory factor 1 (IRF-1) and IRF-2, regulators of cell growth and the interferon system.* Mol Cell Biol, 1993. **13**(8): p. 4531-8.
165. Watanabe, N., et al., *Activation of IFN-beta element by IRF-1 requires a posttranslational event in addition to IRF-1 synthesis.* Nucleic Acids Res, 1991. **19**(16): p. 4421-8.
166. Oshima, S., et al., *Interferon regulatory factor 1 (IRF-1) and IRF-2 distinctively up-regulate gene expression and production of interleukin-7 in human intestinal epithelial cells.* Mol Cell Biol, 2004. **24**(14): p. 6298-310.
167. Hobart, M., et al., *IFN regulatory factor-1 plays a central role in the regulation of the expression of class I and II MHC genes in vivo.* J Immunol, 1997. **158**(9): p. 4260-9.
168. Lee, S.J., et al., *Interferon regulatory factor-1 is prerequisite to the constitutive expression and IFN-gamma-induced upregulation of B7-H1 (CD274).* FEBS Lett, 2006. **580**(3): p. 755-62.
169. Garcia-Diaz, A., et al., *Interferon Receptor Signaling Pathways Regulating PD-L1 and PD-L2 Expression.* Cell Rep, 2017. **19**(6): p. 1189-1201.

170. Li, B., et al., *Comprehensive analyses of tumor immunity: implications for cancer immunotherapy.* Genome Biol, 2016. **17**(1): p. 174.
171. Rajapakse, V.N., et al., *CellMinerCDB for Integrative Cross-Database Genomics and Pharmacogenomics Analyses of Cancer Cell Lines.* iScience, 2018. **10**: p. 247-264.
172. Teo, J., et al., *A preliminary study for the assessment of PD-L1 and PD-L2 on circulating tumor cells by microfluidic-based chipcytometry.* Future Sci OA, 2017. **3**(4): p. FSO244.
173. Redondo, M., et al., *Altered HLA class I expression in non-small cell lung cancer is independent of c-myc activation.* Cancer Res, 1991. **51**(9): p. 2463-8.
174. Cruz, F., *Identification and Characterization of Rab39a and Its Role in Cross-Presentation: A Dissertation.* UMass GSBS Dissertations and Theses, 2017.
175. Laufen, T., et al., *Mechanism of regulation of hsp70 chaperones by DnaJ cochaperones.* Proc Natl Acad Sci U S A, 1999. **96**(10): p. 5452-7.
176. McCarty, J.S., et al., *The role of ATP in the functional cycle of the DnaK chaperone system.* J Mol Biol, 1995. **249**(1): p. 126-37.
177. Szabo, A., et al., *The ATP hydrolysis-dependent reaction cycle of the Escherichia coli Hsp70 system DnaK, DnaJ, and GrpE.* Proc Natl Acad Sci U S A, 1994. **91**(22): p. 10345-9.
178. Kampinga, H.H. and E.A. Craig, *The HSP70 chaperone machinery: J proteins as drivers of functional specificity.* Nat Rev Mol Cell Biol, 2010. **11**(8): p. 579-92.
179. Cheetham, M.E. and A.J. Caplan, *Structure, function and evolution of DnaJ: conservation and adaptation of chaperone function.* Cell Stress Chaperones, 1998. **3**(1): p. 28-36.
180. Ohtsuka, K. and M. Hata, *Mammalian HSP40/DNAJ homologs: cloning of novel cDNAs and a proposal for their classification and nomenclature.* Cell Stress Chaperones, 2000. **5**(2): p. 98-112.
181. Lu, Z. and D.M. Cyr, *The conserved carboxyl terminus and zinc finger-like domain of the co-chaperone Ydj1 assist Hsp70 in protein folding.* J Biol Chem, 1998. **273**(10): p. 5970-8.
182. Hageman, J., et al., *A DNAJB chaperone subfamily with HDAC-dependent activities suppresses toxic protein aggregation.* Mol Cell, 2010. **37**(3): p. 355-69.
183. Reits, E., et al., *Peptide diffusion, protection, and degradation in nuclear and cytoplasmic compartments before antigen presentation by MHC class I.* Immunity, 2003. **18**(1): p. 97-108.
184. Ushioda, R., J. Hoseki, and K. Nagata, *Glycosylation-independent ERAD pathway serves as a backup system under ER stress.* Mol Biol Cell, 2013. **24**(20): p. 3155-63.
185. Ushioda, R., et al., *Redox-assisted regulation of Ca2+ homeostasis in the endoplasmic reticulum by disulfide reductase ERdj5.* Proc Natl Acad Sci U S A, 2016. **113**(41): p. E6055-E6063.
186. Colbert, J.D., D.J. Farfan-Arribas, and K.L. Rock, *Substrate-induced protein stabilization reveals a predominant contribution from mature proteins to peptides presented on MHC class I.* J Immunol, 2013. **191**(11): p. 5410-9.
187. Tsai, J. and M.G. Douglas, *A conserved HPD sequence of the J-domain is necessary for YDJ1 stimulation of Hsp70 ATPase activity at a site distinct from substrate binding.* J Biol Chem, 1996. **271**(16): p. 9347-54.
188. Sevier, C.S. and C.A. Kaiser, *Formation and transfer of disulphide bonds in living cells.* Nat Rev Mol Cell Biol, 2002. **3**(11): p. 836-47.
189. Kincaid, E.Z., et al., *Mice completely lacking immunoproteasomes show major changes in antigen presentation.* Nat Immunol, 2011. **13**(2): p. 129-35.

190. Dorand, R.D., et al., *Cdk5 disruption attenuates tumor PD-L1 expression and promotes antitumor immunity.* Science, 2016. **353**(6297): p. 399-403.
191. Wu, A., et al., *Loss of VGLL4 suppresses tumor PD-L1 expression and immune evasion.* EMBO J, 2019. **38**(1).
192. Marincola, F.M., et al., *Escape of human solid tumors from T-cell recognition: molecular mechanisms and functional significance.* Adv Immunol, 2000. **74**: p. 181-273.
193. Hicklin, D.J., F.M. Marincola, and S. Ferrone, *HLA class I antigen downregulation in human cancers: T-cell immunotherapy revives an old story.* Mol Med Today, 1999. **5**(4): p. 178-86.
194. Zou, W. and L. Chen, *Inhibitory B7-family molecules in the tumour microenvironment.* Nat Rev Immunol, 2008. **8**(6): p. 467-77.
195. Wang, X., et al., *Effectiveness and safety of PD-1/PD-L1 inhibitors in the treatment of solid tumors: a systematic review and meta-analysis.* Oncotarget, 2017. **8**(35): p. 59901-59914.
196. Stratikos, E., *Modulating antigen processing for cancer immunotherapy.* Oncoimmunology, 2014. **3**(1): p. e27568.
197. Yang, Z. and X.F. Ming, *Functions of arginase isoforms in macrophage inflammatory responses: impact on cardiovascular diseases and metabolic disorders.* Front Immunol, 2014. **5**: p. 533.
198. Brentnall, M., et al., *Caspase-9, caspase-3 and caspase-7 have distinct roles during intrinsic apoptosis.* BMC Cell Biol, 2013. **14**: p. 32.
199. Wang, W.J., et al., *Downregulation of gasdermin D promotes gastric cancer proliferation by regulating cell cycle-related proteins.* J Dig Dis, 2018. **19**(2): p. 74-83.
200. Yan, J., et al., *FGL2 as a Multimodality Regulator of Tumor-Mediated Immune Suppression and Therapeutic Target in Gliomas.* J Natl Cancer Inst, 2015. **107**(8).
201. Chen, Q., T. Li, and W. Yue, *Drug response to PD-1/PD-L1 blockade: based on biomarkers.* Onco Targets Ther, 2018. **11**: p. 4673-4683.
202. Ribas, A. and J.D. Wolchok, *Cancer immunotherapy using checkpoint blockade.* Science, 2018. **359**(6382): p. 1350-1355.
203. Kanaji, N., et al., *Higher susceptibility of NOD/LtSz-scid Il2rg (-/-) NSG mice to xenotransplanted lung cancer cell lines.* Cancer Manag Res, 2014. **6**: p. 431-6.
204. Wang, M., et al., *Humanized mice in studying efficacy and mechanisms of PD-1-targeted cancer immunotherapy.* FASEB J, 2018. **32**(3): p. 1537-1549.
205. Behnke, J., et al., *Members of the Hsp70 Family Recognize Distinct Types of Sequences to Execute ER Quality Control.* Mol Cell, 2016. **63**(5): p. 739-52.
206. Reynolds, A., et al., *Induction of the interferon response by siRNA is cell type- and duplex length-dependent.* RNA, 2006. **12**(6): p. 988-93.